PEOPLE'S DEMOCRATIC REPUBLIC OF ALGERIA
MINSTRY OF HIGHER EDUCATION AND RESEARCH SCIENTIST

**UNIVERSITY Dr. YAHIA FARES of MEDEA**



**Technology Faculty**

# Graduation Project Presented for Graduation

# From master

Specialty: Mechanic Engineering
Option: Renewable Energy

---

# Analyze and Simulation of a Photovoltaic System

---

Realized by:

**Mr. TAKDENTI Osama**

Directed by:

**Pr. ABUDURA SALAM**

**June 2019**

REPUBLIQUE ALGERIENNE DEMOCRATIQUE ET POPULAIRE
MINISTERE DE L'ENSEIGNEMENT SUPERIEUR ET DE LA RECHERCHE SCIENTIFIQUE

**UNIVERSITE YAHIA FARES DE MEDEA**



**F**aculté de **T**echnologie

# Mémoire de fin d'études de Master

Filière : Génie Mécanique
Spécialité : Energie renouvelable en mécanique

---

# Analyse et Simulation d'un system photovoltaïque

---

Présenté par

**Mr. TAKDENTI Oussama**

Proposé et Dirigé par

**Pr. ABUDURA SALAM**

**Promotion 2019**

## ABSTRACT

Solar energy is an abundant renewable source, which is expected to play an increasing role in the grid's future infrastructure for distributed generation. The research described in the thesis focuses on the analysis of integrating multi-megawatt photo-voltaic systems with battery energy storage into the existing grid and on the theory supporting the electrical operation of components and systems. The PV system is divided into several sections, each having its own DC-DC converter for maximum power point tracking and a two-level grid connected inverter with different control strategies. The functions of the battery are explored by connecting it to the system in order to prevent possible voltage fluctuations and as a buffer storage in order to eliminate the power mismatch between PV array generation and load demand. Computer models of the system are developed Software.


**Keywords:** photovoltaics, battery, inverter, off grid



## RÉSUMÉ

L'énergie solaire est une source renouvelable abondante qui devrait jouer un rôle croissant dans l'infrastructure future du réseau pour la production décentralisée. La recherche décrite dans le mémoire porte sur l'analyse de l'intégration de systèmes photovoltaïques multi-mégawatts avec stockage d'énergie par batterie dans le réseau existant et sur la théorie prenant en charge le fonctionnement électrique des composants et des systèmes. Le système PV est divisé en plusieurs sections, chacune ayant son propre convertisseur CC-CC pour une poursuite maximale du point de puissance et un onduleur connecté au réseau au deux niveaux avec différentes stratégies de contrôle. Les fonctions de la batterie sont explorées en la connectant au système afin d'éviter toute fluctuation de tension et en tant que mémoire tampon afin d'éliminer l'inadéquation de la puissance entre la génération du générateur photovoltaïque et la demande de charge. Des modèles informatiques du système sont logiciels développés


**Mots-clés :** photovoltaïque, batterie, onduleur, autonome

**ملخص**

تعتبر الطاقة الشمسية مصدرًا وفيرًا ومتجددًا ، ومن المتوقع أن تلعب دورًا متزايدًا في البنية التحتية المستقبلية للشبكة لتوليد الكهرباء. يركز البحث الموضح في الأطروحة على تحليل دمج أنظمة الفولتية الضوئية متعددة ميجاوات مع إلى تخزين طاقة البطارية في الشبكة الحالية وعلى النظرية الداعمة للتشغيل الكهربائي للمكونات والأنظمة. ينقسم نظام خاص به لتتبع نقطة القدرة القصوى وعاكس متصل محول جهد مستمر عدة أقسام ، ولكل منها محول طاقة شمسية بشبكة من مستويين مع استراتيجيات تحكم مختلفة. يتم استكشاف وظائف البطارية عن طريق توصيلها بالنظام من أجل منع تقلبات الجهد المحتملة وكوحدة تخزين أفضل من أجل القضاء على عدم تطابق الطاقة بين توليد طاقة شمسية. والطلب على الحمل. تم تطوير نماذج الكمبيوتر للنظام

**كلمات مفتاحيه**: الخلايا الكهروضوئية ، البطارية ، العاكس ، خارج الشبكة

# *Thanks*

First of All, we must thank « ALLAH », the merciful for giving us the strength and courage to carry out this modest work.

To my Supervisor Mister **Pr.ABUDURA Salam** for having accepted to supervise me, and for his precious advices and his patient to realize this work.

I also thank all the jury members especially **Dr.MORSLI Abdelkader** for having done them the honor to review this thesis. They find here an expression of our deep respect.

# *Dedication*

Due all my respect and honor, I'd love to dedicate this modest work to:

- The most precious person to me my mother, wish god to give you a good health.
- to my dear father with all his great support during my study life.
- to my sisters
- I don't forget Huda for her helps
- And all who contribute helping me

Osama

**General Introduction ……..…….. 01**

**Chapter I: General Statement of Renewable Energy…..……..... 04**

I.1 Radiant energy ……..……...… 06

I.1.1 Definition …….…….……..... 06

I.2.2 The Solar Constant …….……..……. 07

I.1.3 Spectral Distribution of Extraterrestrial Radiation ……..... 09

I.1.4 Variation Of Extraterrestrial ……..…..….. 11

I.1.5 Direction of Beam Radiation ……..…….…. 14

I.1.6 Angles For Tracking Surfaces……...……..... 19

I.1.7 Ratio of Beam Radiation on Tilted Surface to That on Horizontal Surface . 21

I.1.8 Shading ……...…...……. 22

I.1.9 Extraterrestrial Radiation On A Horizontal Surface …….. 23

**Chapter II: Operating Principle……. …….……..…….. 24**

II.1 Reminds On The Photovoltaic Effect …….……..…...…. 26

II.1.1 Photovoltaic Effect ……..…..……..……..... 26

II.2.2 Photovoltaic history ……..…….. 26

II.1.3.1 Basic Semiconductor Physics ……...…..……..……... 27

II.1.3.2 Doping ……...…..... 30

II.1.3.3 Intrinsic semiconductors ……..... 31

II.1.3.4 Doped semiconductors ……...……...…. 34

II.1.3.5 Transport Properties …….……. 36

II.1.3.6 Drift …….…….. ……. 36

II.1.3.7 Diffusion ……..... 37

II.1.3.8 Continuity Equations ……...…….. …….. 38

II.1.4 Semiconductor Junctions ……..….... ……..... 39

II.1.4.1 formation of a space-charge region in P-N junction ……..... 40

II.1.4.2 The P-N junction under equilibrium ……. 42

**Chapter III: Solar cell parameters & equivalent Circuit …..…….....** **48**

III.1 Electrodynamic basics …… 50

III.2 Electromagnetic waves ……..…..... 51

III.3 External solar cell parameters ……...……..…. ……. 54

III.4 Short-circuit current density …….……. 54

III.5 Open-circuit voltage ……... 55

III.6 Fill Factor ……..... 55

III.7 Conversion efficiency ……..... 56

III.8 The External Quantum efficiency ……... 57

III.9 The Equivalent Circuit ……..... 59

**Chapter IV : PV Systems……** **73**

IV.1 External solar cell parameters …….…… 64

IV.2- Types of PV systems …….……..... 64

IV.2.1 Stand-alone systems ……..……...……..... 65

IV.2.2 Grid-connected systems …….……..... 65

IV.2.3 Hybrid systems …….… 66

IV. 3 Components of a PV system» ……..…… 67

IV. 3.1 PV modules ……..…….. 68

IV.3.2 Monocrystalline, Polycrystalline, Amorphous PV Panels …… 69

IV. 3.3 Series and parallel connections in PV modules:…… …….. 71

IV.3.4 Partial shading and bypass diodes …….…..... 74

IV.3.5- Lifetime testing of PV Modules …….……. 75

IV.3.6 Maximum power point tracking …… 77

IV.3.7 Indirect MPPT…… 79

IV.3.7.1 Fixed voltage method ……..…..…….…… 79

IV.3.7.2 Direct MPPT ……...…… 80

IV.3.7.2.1 Photovoltaic Converters…….. 83

IV.3.7.3- System configurations…….. 83

IV.3.8- Batteries.. ……..… 88

IV.3.8.1 Types of batteries ……. 89

IV.3.9 Charge controllers ……...……..... 94

IV.3.10- Cables ……..…..……..…… 96

IV.3.11- A simple approach for designing off-grid systems …… 97

**Chapter V :Simulating of PV Systems…… 102**

V.1 External solar cell parameters ……..…… 104

V.2 Matlab Code For Pv Array …….……..... 106

V.3 Interfacing Of The Pv Array With Boost Converter ……..... 108

V.4 Parameters Used In The Matlab Code …….……..……..... 110

V.5 Output Waveforms Of The Pv Array …… 111

V.6 Simulink Model ……..…… 114

V. 7 Simulink Results ……..……... 116

V.8 Conclusion ……..……. 117

**General Conclusion……..... 109**

**References……..…... 112**

# FIGURES Table


| | | |
|---|---|---|
| Fig I.1: | Sun & Earth Relationship ……... | 9 |
| Fig I.2: | Sun Radiation to Earth ……..…….. | 9 |
| Fig I.3: | Standard spectral irradiance curve at mean earth-sun distance ….…… | 10 |
| Fig I.4: | Variation of extraterrestrial solar radiation …… | 11 |
| Fig I.5: | The Eqs of time E in minutes as a function of time of year …..…….. | 14 |
| Fig I.6: | Zenith angle…….……..... | 15 |
| Fig I.7: | Nomogram to determine time of sunset and day length. ...……...…..... | 18 |
| Fig I.8: | The solar altitude angle αs ……...….. | 18 |
| Fig I.9: | Extraterrestrial solar radiation …… | 19 |
| Fig I.10: | Nomogram to determine time of sunset and day length… …….. | 21 |
| Fig I.11: | Beam radiation on horizontal ……...……...…… | 22 |
| Fig I.12: | Solar position plot ……..…… | 22 |
| Fig II.1: | diamond lattice unit cell …….…… | 28 |
| Fig II.2: | The bonding model for c-Si …….. | 30 |
| Fig II.3: | The doping process illustrated using the bonding model ……... | 30 |
| Fig II.4: | The range of doping levels used in c-Si …….…….. | 31 |
| Fig II.5: | The basic energy band diagram ……..……..…….. | 32 |
| Fig II.6: | The Fermi-Dirac distribution function)…… …… | 33 |
| Fig II.7: | shift of the position of the Fermi energy …… | 35 |
| Fig II.8: | Visualization of (a) the direction of carrier fluxes …….…… | 37 |
| Fig II.9: | Visualization of electron diffusion ……..……... | 39 |
| Fig II.10: | Schematic representation of an isolated n-type and p-type……. | 41 |
| Fig II.11: | Formation of a space-charge region ……..……. | 41 |
| Fig II.12: | Energy-band diagram of the p-n junction …….. | 43 |
| Fig II.13: | Concentrations profile of mobile charge …… | 43 |
| Fig III.1: | Scheme of light, reflected and refracted ……... | 52 |
| Fig III.2: | J-V characteristics of a p-n junction …….. | 54 |
| Fig III.3: | The FF as a function of Voc……...…… | 56 |
| Fig III.4: | The external quantum efficiency of a high-quality crystalline……... | 57 |
| Fig III.5: | The equivalent circuit for ideal solar cell ……...…… | 59 |
| Fig III.6: | Effect of the (a) series resistance and (b) parallel resistance …….. | 60 |
| Fig III.7: | The equivalent circuit of a solar cell based on the two-diode model. | 60 |

| | | |
|---|---|---|
| Fig IV.1: | Schematic representation of a simple DC PV system to power….. | 64 |
| Fig IV.2: | Schematic representation of a grid-connected PV system ……..….. | 65 |
| Fig IV.3: | The 25.7 MWp Lauingen Energy Park in Bavarian ……..…...…… | 66 |
| Fig IV.4: | Schematic representation of a hybrid PV system…….. | 67 |
| Fig IV.5: | A schematic of the different components of a PV system…….. | 68 |
| Fig IV.6: | Different types of Panels……. | 70 |
| Fig IV.7: | Illustrating a solar cella PV module a solar panel……... | 71 |
| Fig IV.8: | Illustrating (a) a series connection of three solar…… | 72 |
| Fig IV.9: | Illustrating a PV module consisting…… | 73 |
| Fig IV.10: | Illustrating (a) string of six solar cells…… | 75 |
| Fig IV.11: | Effect of increased temperature T or irradiance GM on the I-V curve……. | 77 |
| Fig IV.12: | generic I-V curve and the associated P-V……... | 78 |
| Fig IV.13: | The perturb&observe algorithm struggles from rapidly changing illumination conditions…….. | 80 |
| Fig IV.14: | A summary of the possible options in the P&O algorithm……. | 80 |
| Fig IV.15: | The perturb observe algorithm ……... | 81 |
| Fig IV.16: | conceptual flowchart of the incremental conductance algorithm…… | 82 |
| Fig IV.17: | Different system architectures employed in PV systems…… | 85 |
| Fig IV.18: | The team concept of inverters…… | 87 |
| Fig IV.19: | Ragone chart of different energy storage methods……... | 88 |
| Fig IV.20: | Schematic on a vanadium redox-flow battery that employs vanadium ions…….. | 89 |
| Fig IV.21: | Schematic of a lead-acid battery…….. | 90 |
| Fig IV.22: | Qualitative illustration of the cycle lifetime…….. | 93 |
| Fig IV.23: | Illustrating the position of the charge controller in a generic PVsystem with batteries……. | 94 |
| Fig IV.24: | Basic wiring scheme of a series and a shunt charge controller….. | 96 |
| Fig IV.25: | The average global horizontal insolation of the World……. | 98 |
| Fig IV.26: | The average global horizontal insolation of the Netherlands…… | 99 |

| | | |
|---|---|---|
| Fig IV.27: | Illustrating a simple off-grid PV system with AC and DC loads…. | 100 |
| Fig IV.28: | Worksheet for designing a simple off-grid PV system based on rough assumptions…… | 101 |
| Fig V.1: | Equivalent circuit of a PV cell ……...……..… | 104 |
| Fig V.2: | characteristic of a solar array for a fixed temperature but varying irradiance……. | 105 |
| Fig V.3: | characteristic of a solar array for a fixed temperature but varying irradiance…… | 105 |
| Fig V.4: | Characteristic of a PV array under a fixed irradiance but varying temperatures…… | 106 |
| Fig V.5: | Characteristic of a PV array under a fixed irradiance but varying temperatures.Power…… | 106 |
| Fig V.6: | The complete simulink circuit model showing the coupling of PV array with the boost……. | 108 |
| Fig V.7: | panel block diagram …….. | 109 |
| Fig V.8: | Detailed internal circuit diagram of PV array in Simulink..…… | 109 |
| Fig V.9: | curves obtained at 28° C for various irradiance levels …….. | 112 |
| Fig V.10: | -V curves obtained at 28° C for various irradiance levels …… | 112 |
| Fig V.11: | P-I curves obtained at 28° C for various irradiance levels …… | 113 |
| Fig V.12: | curves obtained at an irradiance of 100 mW /cm² for various temperatures …… | 113 |
| Fig V.13: | P-I curves obtained at an irradiance of 100 mW/cm² for various temperatures ……. | 114 |
| Fig V.14: | P-V curves obtained at an irradiance of 100 mW/cm² various temperatures…… | 114 |
| Fig V.15: | The complete simulation model of the PV energy conversion system…….. | 115 |
| Fig V.16: | Circuit diagram for PWM signal generation …….. | 115 |

Fig V.17: Simulation diagram showing the generation of the PWM signal…. 116

Fig V.18: The current output of the system…….. 116

Fig V.19: The voltage output across the load resistance of the boost converter. 117

# LISTE OF TABLES


| | | |
|---|---|---|
| Tab I.1 : | Extraterrestrial Solar Irradiance (WRC Spectrum) in Increments of Wavelength ……... | 10 |
| Tab I.2 : | Recommended Average Days for Months and Values of n by Months……...…… | 16 |
| Tableau V.1 : | Value of dev on matlab …… | 111 |

# Symbols

| Symbol | Quantity | Unit |
|---|---|---|
| c | Specific heat | J $kg^{-1}$ $K^{-1}$ |
| K | Thermal conductivity | W m-l K-i |
| K | Extinction coefficient’ | $m^{-1}$ |
| n | Index of refraction | |
| α | Absorptance | |
| α | Thermal diffusivity | $M^2$ $S^{-1}$ |
| γ | Specific heat ratio | |
| ϵ | Emittance | |
| ρ | Reflectance | |
| ρ | Density | Kg $m^{-3}$ |
| τ | Transmittance | |
| α | Altitude | 0 to ± 90° |
| β | Surface tilt | 0 to ± 90° towards the equator is +ive |
| γ | Azimuth (of surface) | 0 to ± 360° clockwise from North is +ive |
| δ | Declination | 0 to ± 23.45° |
| Θ, i | Incidence (on surface) | 0 to ± 90° |
| Θz | Zenith angle | 0 to ± 90° |
| φ | Latitude | 0 to ± 90° ; North is + ive |
| ω | Hour angle | - 180° to + 180”; solar noon is 0, afternoon |

| | | |
|---|---|---|
| | | is +ive |
| r | Reflection | 0 to +90° |
| Q | Radiant energy | J |
| φ | Radiant flux | W |
| φ | Radiant flux density | $W\ m^{-2}$ |
| E, H | Irradiance | $W\ m^{-2}$ |
| M, J | Radiosity or Radiant exitance | $W\ m^{-2}$ |
| Ms. E | Radiant emissive power (radiant self-exitance) | $W\ m^{-2}$ |
| L | Radiant intensity (radiance) | $W\ m^{-2}\ sr^{-1}$ |
| H | Irradiation or radiant exposure | $J\ m^{-2}$ |
| G | Global irradiance or solar flux density | $W\ m^{-2}$ |
| Gb | Beam irradiance | $W\ m^{-2}$ |
| Gd | Diffuse irradianoe | $W\ m^{-2}$ |
| H | Global irradiation | $J\ m^{-2}$ |
| Hb | Beam irradiation | $J\ m^{-2}$ |
| Hd | Diffuse irradiation | $J\ m^{-2}$ |
| φ ↓ | Irradiation | $W\ m^{-2}$ |
| φ↥ | Radiosity | $W\ m^{-2}$ |
| φN | Exchange | $W\ m^{-2}$ |
| A | Area | $M^2$ |
| h | Heat transfer coefficient | $W\ m\text{-}^2\ K^{-1}$ |
| M | System mass | Kg |
| M | Air mass (or air mass factor) | |
| ṁ | Mass flow rate | $Kg\ S^{-1}$ |

| | | |
|---|---|---|
| Q | Heat | J |
| $\dot{Q}$ | Heat flow rate | W |
| q | Heat flux | W m-2 |
| U | Overall heat transfer coefficient | |
| λ | Wavelength | M |
| ν | Frequency | s-1 |
| σ | Stefan-Boltzmann constant | W $m^{-2}$ $K^{-4}$ |
| T τ θ | Time | s |
| $I_{mpp}$ | current at maximum power | A |
| $I_{sc}$ | short circuit current | A |
| $U_{oc}$ | open circuit voltage | V |
| $U_{mpp}$ | oltage at maximum power | V |
| $E_{ma}$ | mean annual solar radiation | $kWh/m^2$ |
| $E_p$ | imated peak energy delivered | kWh |
| $kW_p$ | nominal peak energy | kW |
| $n$ | number of modules | |
| $\eta_t$ | temperature derating factor | |
| $P_{max}$ | maximum power | W |
| $T_c$ | temperature of the PV cell | K |
| $T_{stc}$ | temperature of STC | 25 °C, K |
| $W_p$ | peak energy of a single module | W |
| $\eta$ | efficiency of system | |
| $\Upsilon$ | power temperature coefficient | $°C^{-1}$ |
| $I$ | current through load | A |

| | | |
|---|---|---|
| $I_d$ | current through diode | A |
| $I_{pv}$ | current generated of PV | A |
| $I_{sh}$ | current through the shunt resistor | A |
| $R_s$ | equivalent circuit series resistance | Ω |
| $R_{sh}$ | equivalent circuit shunt resistance | Ω |
| $U$ | voltage applied to the load | V |
| $U_{sh}$ | shunt voltage | V |
| $I_o$ | reverse saturation current | V |
| $k$ | Boltzmann's constant ==$(1.3806488\times10^{-23}$ | $J.K^{-1}$ |
| $n$ | linearity factor (1 for ideal diode) | |
| $q$ | elementary charge = $(1.602176565\times10^{-19})$ | C |
| $T$ – p-n | junction absolute temperature | K |
| $V_T$ | thermal voltage | V |

# General Introduction

Much of the energy consumed by humanity is in the form of heat (heating, industrial processes ...). This energy is mainly obtained by the transformation of electricity from nuclear gas or oil. There are ways to replace these conventional sources with renewable sources.

A source of energy is renewable if the fact of consuming it does not limit its future use. This is the case of the energy of the sun, the wind, the rivers, the earth and generally the wet or dry biomass, at the scale of the life span of humanity. This is not the case for fossil and nuclear fuels.

The use of renewable energies is not new. These are by man since the beginning of time. In the past, watermills, windmills, firewood, animal traction and sailing boats have made a major contribution to the development of humanity. They were an economic activity in their own right. Especially in rural areas where they were as important and diversified as food production.

Solar energy is the most promising and most powerful energy source among renewable energies. Photovoltaic electricity (PV) is obtained by direct transformation of sunlight into electricity, by means of PV cells. The goal of this work is to develop PV contact cells interdigital backs.

**Objectives of my work**

The main objectives of this thesis, is to give a general and a main vision of new technology of using Renewable energies, especially the solar energy “photovoltaic” and how to use it with best and optimal and proper way, well I tried to make the most essential of PV technology and how to make it out, by using MATLAB’s Simulink, and I’ll talk about sizing in my presentation

# Chapter I

# General Statement of RE

**Introduction :**

In the coming years, there will not be a single source of electricity, but multiple sources of renewable or non-renewable electricity that will be combined to meet the electrification needs of the planet. Photovoltaic solar origin is one of them.

Photovoltaic systems use the best distributed energy in the world: thousands of photovoltaic systems produce electricity for applications such as electrification of sites isolated, water treatment, tele transmissions, public facilities and now the power supply of the electrical network.

We wish you good weather with the sun and especially good time with the exercises, to discover the facets of its radiant energy when it becomes electricity.

**I. what's Renewable Energy ? :**

Renewable energy is a source of energy that renews itself quickly enough to be considered inexhaustible on a human scale. Renewable energies come from regular or constant natural phenomena caused by the stars, mainly the sun (radiation), but also the moon (tide) and the earth (geothermal energy). Today, we often equate renewable energies with clean energies.

## I.1 Radiant energy:

### I.1.1 Definition:

The sun is a sphere of intensely hot gaseous matter with a diameter of $1.39 \times 10^9$ m and is, on the average, $1.5 \times 10^{11}$ m from the earth. As seen from the earth, the sun rotates on its axis about once every 4 weeks.

However, it does not rotate as a solid body; the equator takes about 27 days and the polar regions take about 30 days for each rotation.

The sun has an effective blackbody temperature of 5777 °K.1 The temperature in the central interior regions is variously estimated at $8 \times 10^6$ to $40 \times 10^6$ °K and the density is estimated to be about 100 times that of water.

The sun is, in effect, a continuous fusion reactor with its constituent gases as the ''containing vessel'' retained by gravitational forces. Several fusion reactions have been suggested to supply the energy radiated by the sun. The one considered the most important is a process in which hydrogen (i.e., four protons) combines to form helium (i.e., one helium nucleus); the mass of the helium nucleus is less than that of the four protons, mass

having been lost in the reaction and converted to energy. The energy produced in the interior of the solar sphere at temperatures of many millions of degrees must be transferred out to the surface and then into space.

A succession of radiative and convective processes occur with successive emission, absorption, and eradiation; the radiation in the sun's core is in the x-ray and gamma-ray parts of the spectrum, with the wavelengths of the radiation increasing as the temperature drops at larger radial distances.. It is estimated that 90% of the energy is generated in the region of 0 to 0.23R (where R is the radius of the sun), which contains 40% of the mass of the sun. At a distance 0.7R from the center, the temperature has dropped to about 130,000 K and the density has dropped to 70 $kg/m^3$; here convection processes begin to become important, and the zone from 0.7 to 1.0 R is known as the convective zone. Within this zone the temperature drops to about 5000 K and the densityto about $10^{-5}\,kg/m^3$ .

The sun's surface appears to be composed of granules (irregular convection cells), with dimensions from 1000 to 3000 km and with cell lifetime of a few minutes. Other features of the solar surface are small dark areas called pores, which are of the same order of magnitude as the convective cells, and larger dark areas called sunspots, which vary in size. The outer layer of the convective zone is called the photosphere.

The edge of thephotosphere is sharply defined, even though it is of low density (about $10^{-4}$ that of air at sea level). It is essentially opaque, as the gases of which it is composed are strongly.

## I.1.2 The Solar Constant:

The eccentricity of the earth's orbit is such that the distance between the sun and the earth variesby 1.7%. At a distance of one astronomical unit, $1.495 \times 10^{11}$ m, the mean earth-sun distance, the sun subtends an angle of 32° .

The radiation emitted by the sun and its spatial relationship to the earth result in a nearly fixed intensity of solar radiation outside of the earth's atmosphere. The solar constant Gsc is the energy from the sun per unit time received on a unit area of surface perpendicular to the direction of propagation of the radiation at mean earth-sun distance outside the atmosphere.

Before rockets and spacecraft, estimates of the solar constant had to be made from ground-based measurements of solar radiation after it had been transmitted through the atmosphere and thus in part absorbed and scattered by components of the atmosphere.

Extrapolations from the terrestrial measurements made from high mountains were based on estimates of atmospheric transmission in various portions of the solar spectrum. Pioneering studies were done by C. G. Abbot and his colleagues at the Smithsonian Institution.

These studies and later measurements from rockets were summarized by Johnson (1954); Abbot's value of the solar constant of 1322 W /m² was revised upward by Johnson to 1395 W / m².

The availability of very high altitude aircraft, balloons, and spacecraft has permitted direct measurements of solar radiation outside most or all of the earth's atmosphere. These measurements were made with a variety of instruments in nine separate experimental programs. They resulted in a value of the solar constant Gsc of 1353 W / m² with an estimated error of ± 1.5%. [23]

For discussions of these experiments, see Thekaekara (1976) or Thekaekara and Drummond (1971). This standard value was accepted by NASA (1971) and by the American Society of Testing and Materials (2006). The data on which the 1353-W / m² value was based have been reexamined by Frohlich (1977) and reduced to a new pyrheliometric scale2 based on comparisons of theinstruments with absolute radiometers.

Data from Nimbus and Mariner satellites have alsobeen included in the analysis, and as of 1978, Frohlich recommends a new value of the solar constant Gscof 1373 W / m², with a probable error of 1 to 2%. This was 1.5% higherthan the earlier value and 1.2% higher than the best available determination of the solarconstant by integration of spectral measurements. Additional spacecraft measurementshave been made with Hickey et al. (1982) reporting 1373 W / m² and Willson et al.(1981) reporting 1368 W / m².

Measurements from three rocket flights reported by Duncanet al. (1982) were 1367, 1372, and 1374 W / m². The World Radiation Center (WRC) hasadopted a value of 1367 W / m², with an uncertainty of the order of 1%. uncertainties in most terrestrial solar radiation measurements are an orderof magnitude larger than those in Gsc1367 W / m² [1]

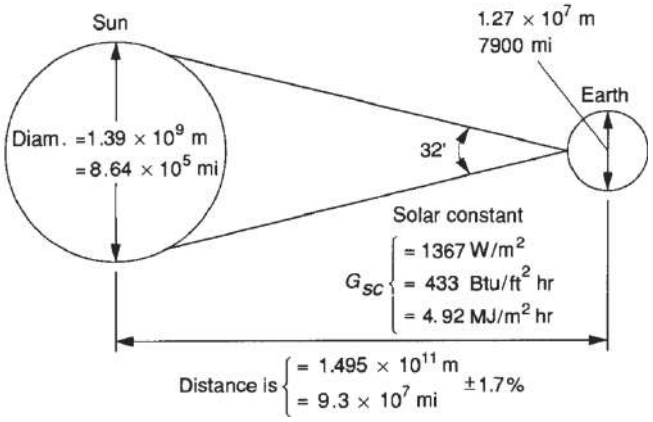



**Fig 1.1** Sun & Earth Relationship

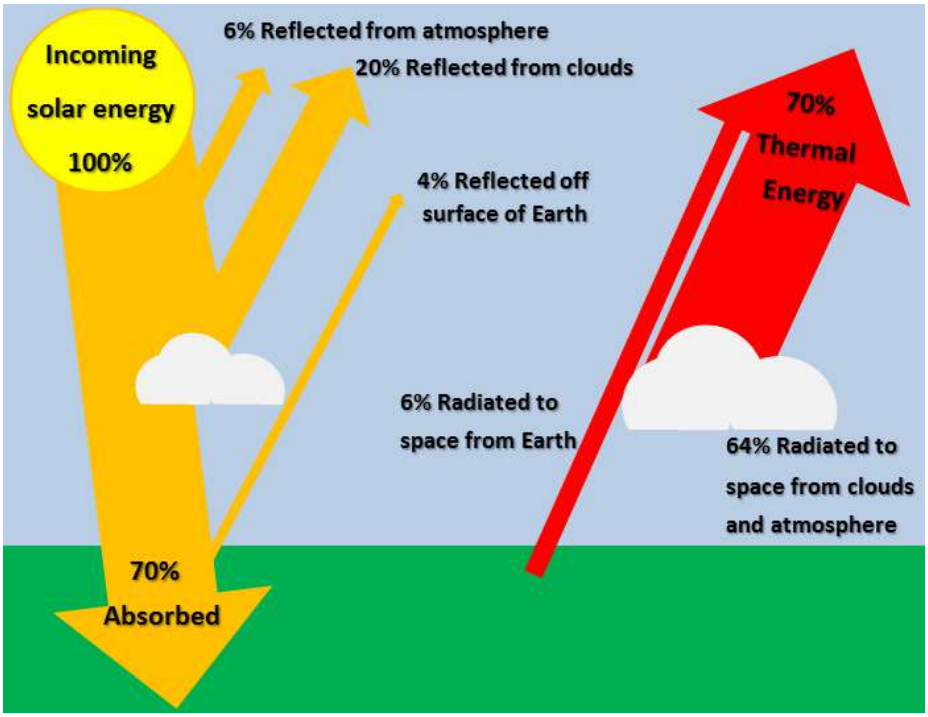



**Fig 1.2** Sun Radiation to Earth [2]

## I.1.3 Spectral Distribution of Extraterrestrial Radiation:

In addition to the total energy in the solar spectrum (i.e., the solar constant), it is useful to know the spectral distribution of the extraterrestrial radiation, that is, the radiation that would be received in the absence of the atmosphere. A standard spectral irradiance curve has been compiled based on high-altitude and space measurements.

The WRC standard is shown in Fig Table below provides the same information on the WRC spectrum in numerical form. The average energy G sc, λ (in W / m² μ m) over small bandwidths centered at wavelength λ is given in the second column. The fraction $f_{0-\lambda}$ of the total energy in the spectrum that is between wavelengths zero and λ is given in the

third column. The table is in two parts, the first at regular intervals of wavelength and the second at even fractions $f_{0-\lambda}$. This is a condensed table; more detailed tables are available elsewhere.

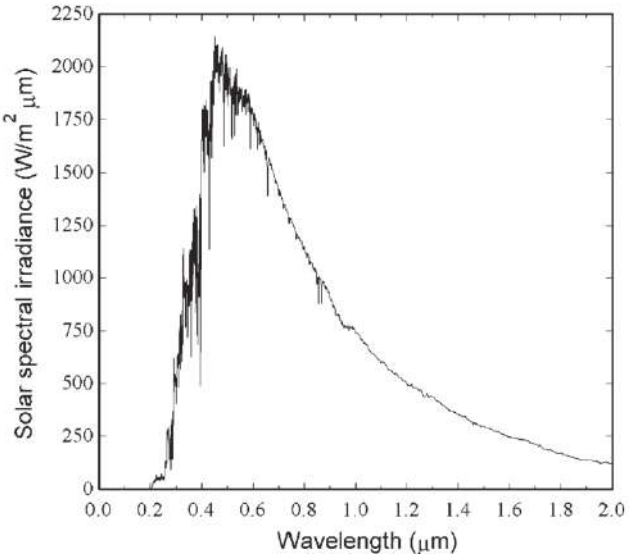



**Fig 1.3** Standard spectral irradiance curve at mean earth-sun distance [3]

| $\lambda$ ($\mu$m) | $G_{sc,\lambda}$ (W/m$^2$ $\mu$m) | $f_{0-\lambda}$ (−) | $\lambda$ ($\mu$m) | $G_{sc,\lambda}$ (W/m$^2$ $\mu$m) | $f_{0-\lambda}$ (−) | $\lambda$ ($\mu$m) | $G_{sc,\lambda}$ (W/m$^2$ $\mu$m) | $f_{0-\lambda}$ (−) |
|---|---|---|---|---|---|---|---|---|
| 0.250 | 81.2 | 0.001 | 0.520 | 1849.7 | 0.243 | 0.880 | 955.0 | 0.622 |
| 0.275 | 265.0 | 0.004 | 0.530 | 1882.8 | 0.257 | 0.900 | 908.9 | 0.636 |
| 0.300 | 499.4 | 0.011 | 0.540 | 1877.8 | 0.271 | 0.920 | 847.5 | 0.648 |
| 0.325 | 760.2 | 0.023 | 0.550 | 1860.0 | 0.284 | 0.940 | 799.8 | 0.660 |
| 0.340 | 955.5 | 0.033 | 0.560 | 1847.5 | 0.298 | 0.960 | 771.1 | 0.672 |
| 0.350 | 955.6 | 0.040 | 0.570 | 1842.5 | 0.312 | 0.980 | 799.1 | 0.683 |
| 0.360 | 1053.1 | 0.047 | 0.580 | 1826.9 | 0.325 | 1.000 | 753.2 | 0.695 |
| 0.370 | 1116.2 | 0.056 | 0.590 | 1797.5 | 0.338 | 1.050 | 672.4 | 0.721 |
| 0.380 | 1051.6 | 0.064 | 0.600 | 1748.8 | 0.351 | 1.100 | 574.9 | 0.744 |
| 0.390 | 1077.5 | 0.071 | 0.620 | 1738.8 | 0.377 | 1.200 | 507.5 | 0.785 |
| 0.400 | 1422.8 | 0.080 | 0.640 | 1658.7 | 0.402 | 1.300 | 427.5 | 0.819 |
| 0.410 | 1710.0 | 0.092 | 0.660 | 1550.0 | 0.425 | 1.400 | 355.0 | 0.847 |
| 0.420 | 1687.2 | 0.105 | 0.680 | 1490.2 | 0.448 | 1.500 | 297.8 | 0.871 |
| 0.430 | 1667.5 | 0.116 | 0.700 | 1413.8 | 0.469 | 1.600 | 231.7 | 0.891 |
| 0.440 | 1825.0 | 0.129 | 0.720 | 1348.6 | 0.489 | 1.800 | 173.8 | 0.921 |
| 0.450 | 1992.8 | 0.143 | 0.740 | 1292.7 | 0.508 | 2.000 | 91.6 | 0.942 |
| 0.460 | 2022.8 | 0.158 | 0.760 | 1235.0 | 0.527 | 2.500 | 54.3 | 0.968 |
| 0.470 | 2015.0 | 0.173 | 0.780 | 1182.3 | 0.544 | 3.000 | 26.5 | 0.981 |
| 0.480 | 1975.6 | 0.188 | 0.800 | 1133.6 | 0.561 | 3.500 | 15.0 | 0.988 |
| 0.490 | 1940.6 | 0.202 | 0.820 | 1085.0 | 0.578 | 4.000 | 7.7 | 0.992 |
| 0.500 | 1932.2 | 0.216 | 0.840 | 1027.7 | 0.593 | 5.000 | 2.5 | 0.996 |
| 0.510 | 1869.1 | 0.230 | 0.860 | 980.0 | 0.608 | 8.000 | 1.0 | 0.999 |

[a] $G_{sc,\lambda}$ is the average solar irradiance over the interval from the middle of the preceding wavelength interval to the middle of the following wavelength interval. For example, at 0.600 $\mu$m. 1748.8 W/m$^2$ $\mu$m is the average value between 0.595 and 0.610 $\mu$m.

**Tab 1.1** Extraterrestrial Solar Irradiance (WRC Spectrum) in Increments of Wavelength [3]

Ultraviolet 0.20 <λ<0.38μm 6.4%

Visible 0.38 <λ<0.78μm 48.0%

Infrared 0.78 <λ <10 . μm 45.6%

μm = micrometer: 1 μm = $10^{-6}$ m, 1 000 μm = 1 mm

nm = nanometer: 1 nm = $10^{-9}$ mm, 1 000 nm = 1 μm

Å = angström: 1 Å = $10^{-10}$ m, 10 000 Å = 1 μm Hz = hertz: 1 Hz = 1/1 s = $s^{-1}$

## I.1.4Variation Of Extraterrestrial:

Two sources of variation in extraterrestrial radiation must be considered. The first is the variation in the radiation emitted by the sun. There are conflicting reports in the literature on periodic variations of intrinsic solar radiation.

It has been suggested that there are small variations (less than ± 1.5%) with different periodicities and variation related to sunspot activities. Willson et al. (1981) report variances of up to 0.2% correlated with the development of sunspots.

Others consider the measurements to be inconclusive or not indicative of regular variability. measurements from Nimbus and Mariner satellites over periods of several months showed variations within limits f ± 0.2% over a time when [4]

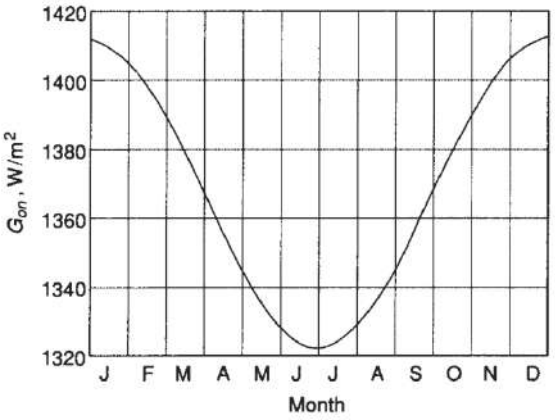



**Fig0** Variation of extraterrestrial solar radiation with time of year [3]

sunspot activity was very low (Frohlich, 1977). Data of Hickey et al. (1982) over a span of 2.5 years from the Nimbus 7 satellite suggest that the solar constant is decreasing slowly, at a rate of approximately 0.02% per year. See Coulson (1975) or Thekaekara (1976) for further discussion of this topic. For engineering purposes, in view of the uncertainties and

variability of atmospheric transmission, the energy emitted by the sun can be considered to be fixed. Variation of the earth-sun distance, however, does lead to variation of extraterrestrial radiation flux in the range of ± 3.3%. The dependence of extraterrestrial radiation on time of year is shown in Fig 1.4. A simple Eqs with accuracy adequate for most engineering calculations is given by Eqs. Spencer (1971), as cited by Iqbal (1983), provides a more accurate Eqs ( ± 0.01%) in the form of Eqs below

$$G_{on} = \begin{cases} G_{sc}\left(1 + 0.033 \cos \dfrac{360n}{365}\right) \\ G_{sc}(1.000110 + 0.034221 \cos B + 0.001280 \sin B \\ \quad +0.000719 \cos 2B + 0.000077 \sin 2B) \end{cases}$$

EQUATION (1.1)

where Gon : is the extraterrestrial radiation incident on the plane normal to the radiation on the $n^{th}$ day of the year and B is given by

$$B = (n - 1)\frac{360}{365}$$

EQUATION (1.2)

Air Mass m The ratio of the mass of atmosphere through which beam radiation passes to the mass it would pass through if the sun were at the zenith Thus at sea level m = 1 when the sun is at the zenith and m = 2 for a zenith angle θz of 60 ° . For zenith angles from 0° to 70° at sea level, to a close approximation,

$$m = \frac{1}{\cos \theta_z}$$

EQUATION (1.3)

For higher zenith angles, the effect of the earth's curvature becomes significant and must be taken into account.3 For a more complete discussion of air mass, see Robinson (1966), Kondratyev (1969), or Garg (1982).

**Beam Radiation** The solar radiation received from the sun without having been scattered by the atmosphere. (Beam radiation is often referred to as direct solar radiation; to avoid confusion between subscripts for direct and diffuse, we use the term beam radiation.)

**Diffuse Radiation** The solar radiation received from the sun after its direction has been changed by scattering by the atmosphere. (Diffuse radiation is referred to in some meteorological literature as sky radiation or solar sky radiation; the definition used here will distinguish the diffuse solar radiation from infrared radiation emitted by the atmosphere.)

**Total Solar Radiation** The sum of the beam and the diffuse solar radiation on a surface.4 (The most common measurements of solar radiation are total radiation on a horizontal surface, often referred to as global radiation on the surface.)

**Irradiance**, W / m² The rate at which radiant energy is incident on a surface per unit area of surface. The symbol G is used for solar irradiance, with appropriate subscripts for beam, diffuse, or spectral radiation.

**Irradiation or Radiant Exposure**, J / m² The incident energy per unit area on a surface, found by integration of irradiance over a specified time, usually an hour or a day.

**Insolation** is a term applying specifically to solar energy irradiation. The symbol H is used for insolation for a day. The symbol I is used for insolation for an hour (or other period if specified). The symbols H and I can represent beam, diffuse, or total and can be on surfaces of any orientation. Subscripts on G, H, and I are as follows: o refers to radiation above the earth's atmosphere, referred to as extraterrestrial radiation; b and d refer to beam and diffuse radiation; T and n refer to radiation on a tilted plane and on a plane normal to the direction of propagation. If neither T nor n appears, the radiation is on a horizontal plane.

**Radiosity or Radiant Exitance**, W / m² The rate at which radiant energy leaves a surface per unit area by combined emission, reflection, and transmission.

**Emissive Power or Radiant Self-Exitance**, W / m² The rate at which radiant energy leaves a surface per unit area by emission only.

**Solar Time Time** based on the apparent angular motion of the sun across the sky with solar noon the time the sun crosses the meridian of the observer. Solar time is the time used in all of the sun-angle relationships; it does not coincide with local clock time. It is necessary to convert standard time to solar time by applying two corrections. First, there is a constant correction for the difference in longitude between the observer's meridian (longitude) and the meridian on which the local standard time is based.5 The sun takes 4 min to transverse 1° of longitude. The second correction is from the Eqs of time, which takes into account the perturbations in the earth's rate of rotation which affect the time the sun crosses the observer's meridian. The difference in minutes between solar time and standard time is [5]

$$\text{Solar time} - \text{standard time} = 4(L_{st} - L_{loc}) + E$$

EQUATION (1.4)

where L st is the standard meridian for the local time zone, L loc is the longitude of the location in question, and longitudes are in degrees west, that is, 0 °< L < 360°

The parameter E is the Eqs of time (in minutes) from Fig 1.5. or Eqs 1.536 [fromSpencer (1971), as cited by Iqbal (1983)]:

$$E = 229.2(0.000075 + 0.001868 \cos B - 0.032077 \sin B - 0.014615 \cos 2B - 0.04089 \sin 2B)$$

EQUATION (1.5)

where B is found from Eqs  and n is the day of the year. Thus $1 \leq n \leq 365$. Note that the Eqs of time and displacement from the standard meridian are both in minutes and that there is a 60-min difference between daylight saving time and standard time. Time is usually specified in hours and minutes. Care must be exercised in applying the corrections, which can total more than 60 min.

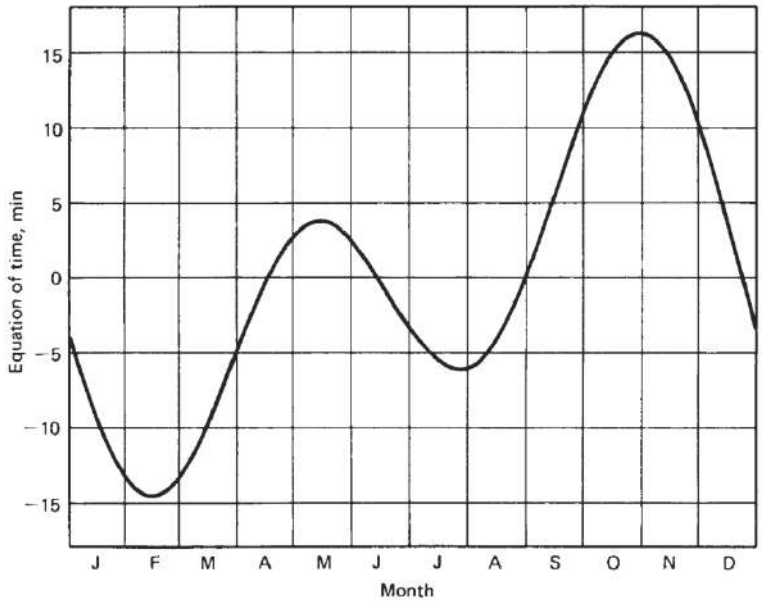



**Fig1.5** The Eqs of time E in minutes as a function of time of year.

On February 3, n = 34, and from Eqs 1.5.3 or Fig 1.5., E = − 13.5 min, so the correction to standard time is − 11 min. Thus 10:30 AM Central Standard Time is 10:19 AM solar time.  In this book time is assumed to be solar time unless indication is given otherwise.

## I.1.5 Direction of Beam Radiation:

The geometric relationships between a plane of any particular orientation relative to the earth at any time (whether that plane is fixed or moving relative to the earth) and the incoming beam solar radiation, that is,

the position of the sun relative to that plane, can be described in terms of several angles (Benford and Bock, 1939). Some of the angles are indicated below. The angles and a set of consistent sign conventions are as follows:

**φ Latitude**, the angular location north or south of the equator, north positive; $-90° \leq \varphi \leq 90°$

**δ Declination**, the angular position of the sun at solar noon (i.e., when the sun is on the local meridian) with respect to the plane of the equator, north positive; $-23.45° \leq \delta \leq 23.45°$

**β Slope**, the angle between the plane of the surface in question and the horizontal; $0° \leq \beta \leq 180°$ and $\beta > 90°$ means that the surface has a downward-facing component.

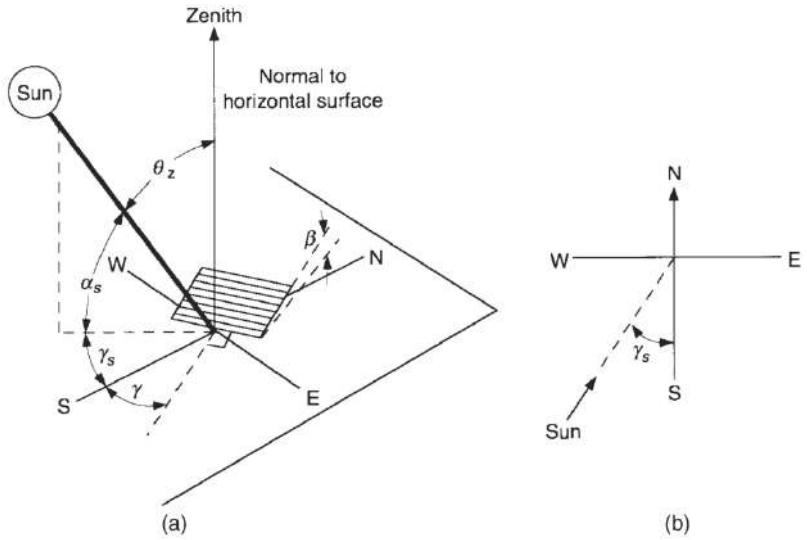



**Fig0** (a) Zenith angle, slope, surface azimuth angle, and solar azimuth angle for a tilted

(b) Plan view showing solar azimuth angle.

**γ Surface azimuth angle**, the deviation of the projection on a horizontal plane of the normal to the surface from the local meridian, with zero due south, east negative, and west positive; $-180° \leq \gamma \leq 180°$

**ω Hour angle**, the angular displacement of the sun east or west of the local meridian due to rotation of the earth on its axis at 15° per hour; morning negative, afternoon positive.

**θ Angle of incidence**, the angle between the beam radiation on a surface and the normal to that surface.

Additional angles are defined that describe the position of the sun in the sky:

**θz Zenith angle**, the angle between the vertical and the line to the sun, that is, the angle of incidence of beam radiation on a horizontal surface.

**αs Solar altitude angle**, the angle between the horizontal and the line to the sun, that is, the complement of the zenith angle.

**γs Solar azimuth angle**, the angular displacement from south of the projection of beam radiation on the horizontal plane, shown in Fig 1.6. Displacements east of south are negative and west of south are positive.

$$\delta = 23.45 \sin\left(360\frac{284+n}{365}\right)$$ EQUATION (1.6)

| Month | $n$ for $i$th Day of Month | For Average Day of Month | | |
|---|---|---|---|---|
| | | Date | $n$ | $\delta$ |
| January | $i$ | 17 | 17 | −20.9 |
| February | $31 + i$ | 16 | 47 | −13.0 |
| March | $59 + i$ | 16 | 75 | −2.4 |
| April | $90 + i$ | 15 | 105 | 9.4 |
| May | $120 + i$ | 15 | 135 | 18.8 |
| June | $151 + i$ | 11 | 162 | 23.1 |
| July | $181 + i$ | 17 | 198 | 21.2 |
| August | $212 + i$ | 16 | 228 | 13.5 |
| September | $243 + i$ | 15 | 258 | 2.2 |
| October | $273 + i$ | 15 | 288 | −9.6 |
| November | $304 + i$ | 14 | 318 | −18.9 |
| December | $334 + i$ | 10 | 344 | −23.0 |

"From Klein (1977). Do not use for $|\phi| > 66.5^\circ$.

**Tab 1.2**Recommended Average Days for Months and Values of n by Months

$$\delta = (180/\pi)(0.006918 - 0.399912\cos B + 0.070257\sin B - 0.006758\cos 2B + 0.000907\sin 2B - 0.002697\cos 3B + 0.00148\sin 3B)$$

EQUATION (1.7)

where B is from Equation 1.4.2 and the day of the year n can be conveniently obtained with the help of Table 1.2 Variation in sun-earth distance (as noted in Section 1.4), the equation of time E (asnoted in Section 1.5), and declination are all continuously varying functions of time ofyear. For many computational purposes it is customary to express the time of year in termsof n, the day of the year, and thus as an integer between 1 and 365. Eqs could be used with no integer values of n. Note that the maximum rate of changeof declination is about 0.4 °per day. The use of integer values of n is adequate for mostengineering calculations outlined in.There is a set of useful relationships among these angles. Equations relating the angleof incidence of beam radiation on a surface, θ , to the other angles are

$$\cos\theta = \sin\delta\sin\phi\cos\beta - \sin\delta\cos\phi\sin\beta\cos\gamma + \cos\delta\cos\phi\cos\beta\cos\omega + \cos\delta\sin\phi\sin\beta\cos\gamma\cos\omega + \cos\delta\sin\beta\sin\gamma\sin\omega$$

and

$$\cos\theta = \cos\theta_z\cos\beta + \sin\theta_z\sin\beta\cos(\gamma_s - \gamma)$$

EQUATION (1.8)

The angle θ may exceed 90◦, which means that the sun is behind the surface. Also, whenusing Eqs it is necessary to ensure that the earth is not blocking the sun (i.e.,that the hour angle is between sunrise and sunset).

Useful relationships for the angle of incidence of surfaces sloped due north or duesouth can be derived from the fact that surfaces with slope β to the north or south have

thesame angular relationship to beam radiation as a horizontal surface at an artificial latitudeof φ − β . The relationship is shown in Figure 1.6.2 for the northern hemisphere

$$\cos\theta = \cos(\phi - \beta)\cos\delta\cos\omega + \sin(\phi - \beta)\sin\delta$$

EQUATION (1.9)

For the southern hemisphere modify the equation by replacing φ − β by φ + β , consistentwith the sign conventions on φ and δ :

$$\cos\theta = \cos(\phi + \beta)\cos\delta\cos\omega + \sin(\phi + \beta)\sin\delta$$

For the special case of solar noon, for the south-facing sloped surface in the northernhemisphere,

$$\theta_{\text{noon}} = |\phi - \delta - \beta|$$ EQUATION (1.10)

and in the southern hemisphere

$$\theta_{\text{noon}} = |-\phi + \delta - \beta|$$

where β = 0, the angle of incidence is the zenith angle, which for the northern hemisphere is

$$\theta_{z,\text{noon}} = |\phi - \delta|$$ EQUATION (1.11)

and for the southern hemisphere

$$\theta_{z,\text{noon}} = |-\phi + \delta|$$ EQUATION (1.12)

the sunset hour angle ωs, when θz = 90◦:

$$\cos\omega_s = -\frac{\sin\phi\sin\delta}{\cos\phi\cos\delta} = -\tan\phi\tan\delta$$ EQUATION (1.13)

The sunrise hour angle is the negative of the sunset hour angle. It also follows that thenumber of daylight hours is given by

$$N = \frac{2}{15}\cos^{-1}(-\tan\phi\tan\delta)$$ EQUATION (1.14)

A convenient nomogram for determining day length has been devised by Whillier(1965) and is shown in Figure 1.6.3. Information on latitude and declination for eitherhemisphere leads directly to times of sunrise and sunset and day length.

An additional angle of interest is the profile angle of beam radiation on a receiverplane R that has a surface azimuth angle of γ . It is the projection of the solar

altitude angleon a vertical plane perpendicular to the plane in question. Expressed another way,

it is theangle through which a plane that is initially horizontal must be rotated about an axis inthe plane of the surface in question in order to include the sun. The solar altitude angleαs (i.e., angle EAD) and the profile angle αp (i.e., angle fab) for the plane R are shown inFigure 1.6.4. The plane adef includes the sun. Note that the solar altitude and profile angleare the same when the sun is in a plane perpendicular to the surface R (e.g., at solar noonfor a surface with a surface azimuth angle of 0◦or 180◦). The profile angle is useful incalculating shading by overhangs and can be determined from

$$\tan \alpha_p = \frac{\tan \alpha_s}{\cos(\gamma_s - \gamma)}$$

EQUATION (1.15)

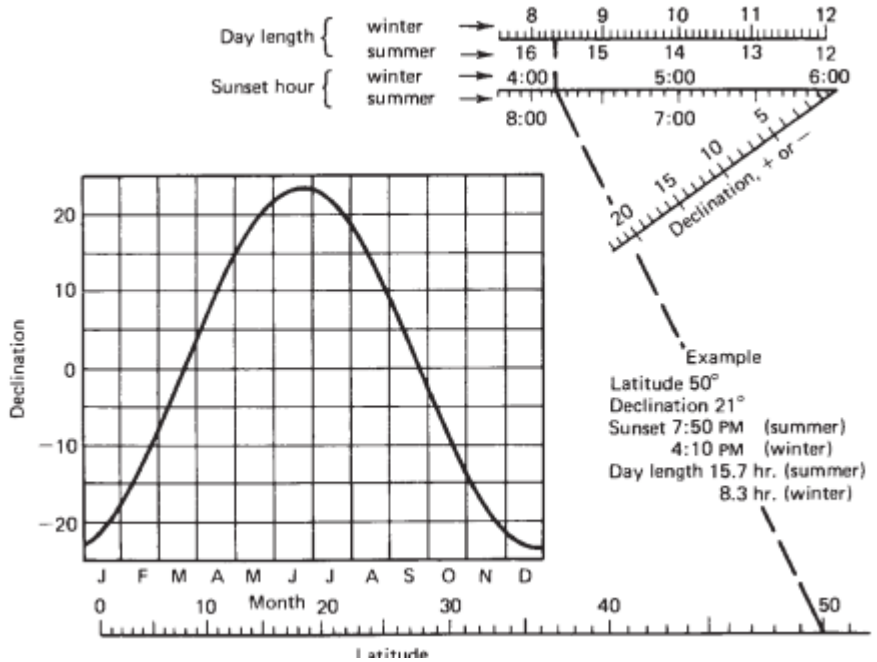



**Fig 1.7**Nomogram to determine time of sunset and day length. Adapted from Whillier

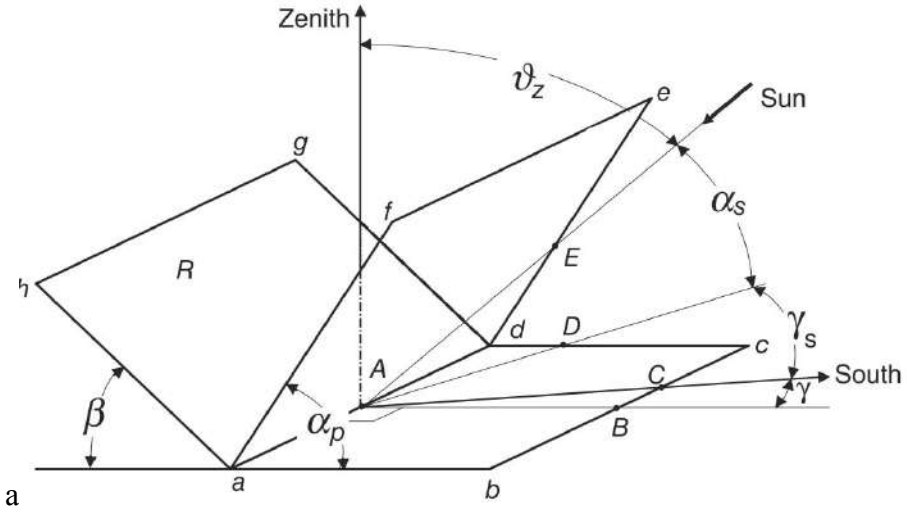



**Fig0** The solar altitude angle αs

## 1.1.6 ANGLES FOR TRACKING SURFACES:

Some solar collectors ‘‘track’’ the sun by moving in prescribed ways to minimize the angle of incidence of beam radiation on their surfaces and thus maximize the incident beam radiation. The angles of incidence and the surface azimuth angles are needed for these collectors. The relationships in this section will be useful in radiation calculations for these moving surfaces. For further information, see Eibling et al. (1953) and Braun and Mitchell (1983). [1]

Tracking systems are classified by their motions. Rotation can be about a single axis (which could have any orientation but which in practice is usually horizontal east-west, horizontal north-south, vertical, or parallel to the earth’s axis) or it can be about two axes. The following sets of Eqs are for surfaces that rotate on axes that are parallel to the surfaces. Fig 1.8. shows extraterrestrial radiation on a fixed surface with slope equal to the latitude and also on surfaces that track the sun about a horizontal north-south or east-west axis at a latitude of 45 °at the summer and winter solstices

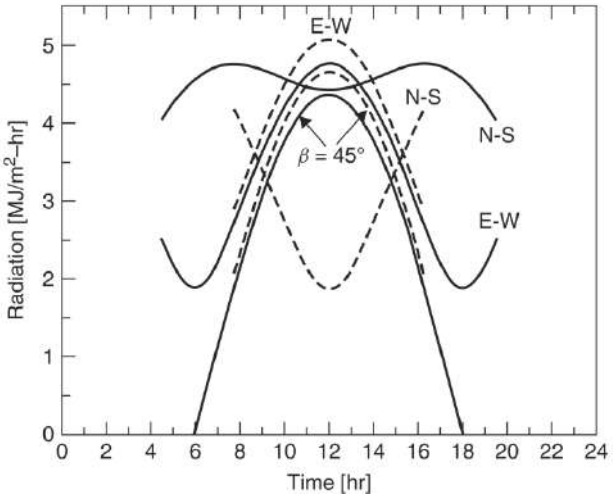


**Fig 1.9** Extraterrestrial solar radiation for φ = 45° on a stationary collector at β = 45° on north-south (N-S) and east-west (E-W) single-axis tracking collectors. The three dotted curves are for the winter solstice and the three solid curves are for the summer solstice.

It is clear that tracking can significantly change the time distribution of incident beam radiation. Tracking does not always result in increased beam radiation; compare the winter solstice radiation on the north-south tracking surface with the radiation on the fixed surface.

In practice the differences will be less than indicated by the figure due to clouds and atmospheric transmission. For a plane rotated about a horizontal east-west axis with a single daily adjustment so that the beam radiation is normal to the surface at noon each day,

$$\cos\theta = \sin^2\delta + \cos^2\delta\cos\omega \quad \text{EQUATION (1.16)}$$

The slope of this surface will be fixed for each day and will be

$$\beta = |\varphi - \delta| \quad \text{EQUATION (1.17)}$$

The surface azimuth angle for a day will be 0° or 180° depending on the latitude and declination:

$$\gamma = 0° \text{ if } \varphi - \delta > 0$$

$$180° \text{if } \varphi - \delta \leq 0$$

EQUATION (1.17)

For a plane rotated about a horizontal east-west axis with continuous adjustment to minimize the angle of incidence,

$$\cos\theta = (1 - \cos^2\delta\sin^2\omega)^{1/2} \quad \text{EQUATION (1.18)}$$

The slope of this surface is given by

$$\tan\beta = \tan\theta z|\cos\gamma_s| \quad \text{EQUATION (1.19)}$$

The surface azimuth angle for this mode of orientation will change between 0° and 180 °

If the solar azimuth angle passes through ± 90° . For either hemisphere,

$$\gamma = 0° \text{ if } |\gamma s| < 90$$

$$180° \text{ if } |\gamma s| \geq 90$$

For a plane rotated about a horizontal north-south axis with continuous adjustment to minimize the angle of incidence,

$$\cos\theta = (\cos^2\theta z + \cos^2\delta\sin^2\omega)^{1/2} \quad \text{EQUATION (1.20)}$$

The slope is given by

$$\tan \beta = \tan \theta z |\cos (\gamma - \gamma s)| \quad \text{EQUATION (1.21)}$$

The surface azimuth angle $\gamma$ will be 90° or − 90°depending on the sign of the solar azimuth angle:

$$\gamma = 90° \text{ if } \gamma s > 0$$

$$-90° \text{ if } \gamma s \leq 0$$

For a plane with a fixed slope rotated about a vertical axis, the angle of incidence is minimized when the surface azimuth and solar azimuth angles are equal.

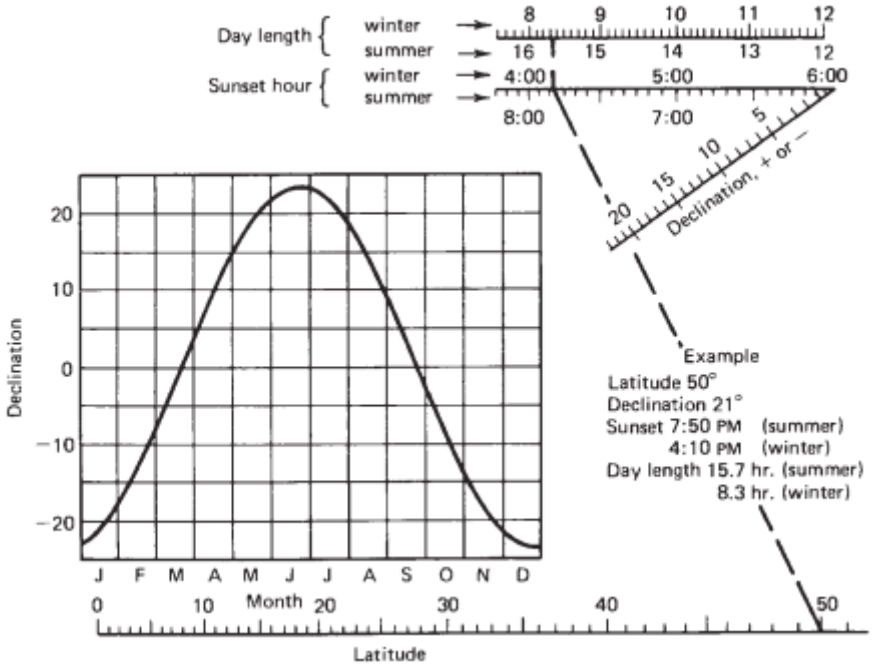



**Fig0** Nomogram to determine time of sunset and day length. Adapted from Whillier

$$\cos \theta = \cos \theta z \cos \beta + \sin \theta z \sin \beta \quad \text{EQUATION (1.22)}$$

The slope is fixed, so $\beta$ = const, The surface azimuth angle is $\gamma = \gamma s$

For a plane rotated about a north-south axis parallel to the earth's axis with continuous adjustment to minimize $\theta$ , $\cos \theta = \cos \delta$

The slope varies continuously and is $\tan \beta = \tan \varphi / \cos \gamma$

## 1.1.7 Ratio Of Beam Radiation On Tilted Surface To That On Horizontal Surface:

For purposes of solar process design and performance calculations, it is often necessary to calculate the hourly radiation on a tilted surface of a collector from measurements or estimates of solar radiation on a horizontal surface.

The most commonly available data are total radiation for hours or days on the horizontal surface, whereas the need is for beamand diffuse radiation on the plane of a collector.

The geometric factor Rb, the ratio of beam radiation on the tilted surface to that on a horizontal surface at any time, can be calculated exactly by appropriate use of

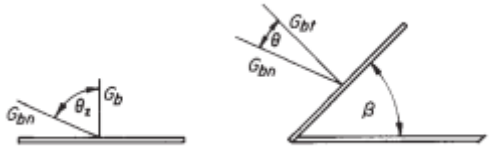



**Fig0** Beam radiation on horizontal

$$R_b = \frac{G_{b,T}}{G_b} = \frac{G_{b,n}\cos\theta}{G_{b,n}\cos\theta_z} = \frac{\cos\theta}{\cos\theta_z}$$

EQUATION (1.22)

## 1.1.8 Shading

Three types of shading problems occur so frequently that methods are needed to cope with them. The first is shading of a collector, window, or other receiver by nearby trees, buildings, or other obstructions. The geometries may be irregular,

and systematic calculations of shading of the receiver in question may be difficult. Recourse is made to diagrams of the position of the sun in the sky, for example, plots of solar altitude αs versus solar azimuth γs, on which shapes of obstructions (shading profiles) can be superimposed to determine when the path from the sun to the point in question is blocked. The second type includes shading of collectors in other than the first row of multi row arrays by the collectors on the adjoining row.

The third includes shading of windows by overhangs and wing walls. Where the geometries are regular, shading is amenable to calculation, and the results can be presented in general form. At any point in time and at a particular latitude, φ , δ , and ω are fixed. From the Eqs in; the zenith angle θz or solar altitude angle αs and the solar azimuth angle γs can be calculated. A solar position plot of θz and αs versus γs for latitudes of ± 45° is shown in

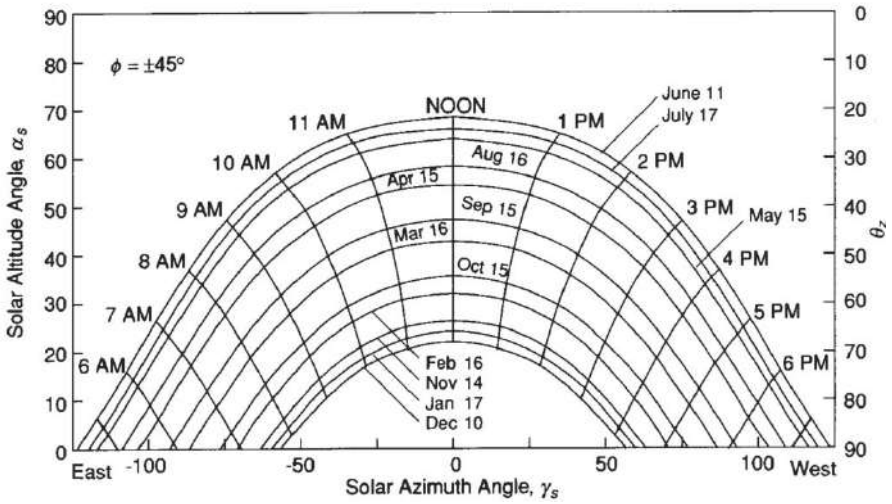



**Fig1.12**Solar position plot for ± 45◦ latitude. Solar altitude angle and solar azimuth angle are functions of declination and hour angle, indicated on the plots by dates and times. The dates shown are for northern hemisphere

Lines of constant declination are labeled by dates of mean days of the months from Tab 1.2. Lines of constant hour angles labeled by hours are also shown.

The angular position of buildings, wing walls, overhangs, or other obstructions can be entered on the same plot. For example, as observed by Mazria (1979) and Anderson (1982), if a building or other obstruction of known dimensions and orientation is located a known distance from the point of interest (i.e., the receiver, collector, or window), the angular coordinates corresponding to altitude and azimuth angles of points on the obstruction (the object azimuth angle **γo** and object altitude angle αo) can be calculated from trigonometric considerations.

This is illustrated in Examples 1.9.1. Alternatively, measurements of object altitude and azimuth angles may be made at the site of a proposed receiver and the angles plotted on the solar position plot. Instruments are available to measure the angles.

## 1.1.9 Extraterrestrial Radiation On a Horizontal Surface:

radiation levels, that is, the ratio of radiation level to the theoretically possible radiation that would be available if there were no atmosphere. For these calculations, which are discussed before, we need a method of calculating the extraterrestrial radiation. At any point in time, [7]

the solar radiation incident on a horizontal plane outside of the atmosphere is the normal incident solar radiation as given by Eqs divided by Rb

$$G_o = G_{sc}\left(1 + 0.033 \cos\frac{360n}{365}\right)\cos\theta_z \qquad \text{EQUATION (1.22)}$$

where G sc is the solar constant and n is the day of the year. cos θz with gives Go for a horizontal surface at any time between sunrise and sunset:

$$G_o = G_{sc}\left(1 + 0.033\cos\frac{360n}{365}\right)(\cos\phi\cos\delta\cos\omega + \sin\phi\sin\delta)$$

EQUATION (1.23)

It is often necessary for calculation of daily solar radiation to have the integrated daily extraterrestrial aviation on a horizontal surface, Ho.

This is obtained by integrating over the period from sunrise to sunset. If G sc is in watts per square meter, Ho in daily joules per square meter per day is

$$H_o = \frac{24 \times 3600 G_{sc}}{\pi}\left(1 + 0.033\cos\frac{360n}{365}\right) \times \left(\cos\phi\cos\delta\sin\omega_s + \frac{\pi\omega_s}{180}\sin\phi\sin\delta\right)$$

EQUATION (1.24)

**Conculsion :**

In this chapter we saw the main steps of starting of PV's Project by sizing, we saw main equations and figures to figure it out.

# Chapter II

# Operating Principle

## Introduction :

Photovoltaic solar electricity is one of the most important global disciplines in sustainable development. Currently despite the mastery of manufacturing technology solar cells and their encapsulation photovoltaic installations are still expensive; for this, the mastery of technology alone, is no longer to reduce the costs of PV installations and the dimensioning techniques used must be optimal.

## Ii.1 Reminds On The Photovoltaic Effect:

## II.1.1 Photovoltaic Effect:

The photovoltaic effect is the conversion of light photons into electricity when the light hits on solar cells (semiconductors). All the cells form a module and all the modules that give the photovoltaic field. The shock of photons on the semiconductor material transmits their energy to the carriers of the generating material as well electron-hole pairs either a voltage or an electric current.

## II.1.2 Photovoltaic history:

Discovered in 1839 by Antoine Becquerel, the photovoltaic effect allows the transformation of light energy into electricity. This principle is based on technology semiconductors. It's about using the photons to release the electrons and create a potential difference between the terminals of the cell that generates an CC

Photovoltaic electricity appeared in 1930 with copper oxide cells and then selenium. But it was not until 1954, with the realization of the first cells Silicon Photovoltaics in the Bell Telephone Laboratories, which can be sees the possibility of providing energy. Very quickly used for the supply of space vehicles towards the years 60 with space satellite equipment. Then from 1970, the first uses have concerned the electrification of isolated sites.

During the 1980s, terrestrial photovoltaic technology progressed regularly by setting up several plants of a few megawatts, and is even become familiar to consumers across many low products power using: watches, calculators, radio and weather beacons, pumps and solar refrigerators.

The progress of photovoltaic cell production techniques as well as the increase in production volumes have led, since the 1990s, to a price drop. The production of modules is done in China (nearly 60% of the production Japan, the US, Germany and Europe, with particularly large companies like Yingli Green Energy, First Solar and Suntech Power.

The production worldwide photovoltaic modules rose from 5 MWp in 1982 to over 18GWc in 2013. Concerning Algeria, the Algerian Group Condor Electronics, launched in

July 2013 in the production of photovoltaic panels whose power varies between 70 W and 285 W and at competitive prices.

As part of the implementation of Algeria's national energy program renewable energy, a 400 MW photovoltaic project has been launched as part of this project is planned for the summer of 2014. This project Photovoltaic solar power plants, in the region of high plateaus and in the southwest region; in the southern region.

In the ten years that will come, it is planned the realization of a park of energies 5539 MW renewables. The target at 2030 is 12,000 MW renewable energy for internal electricity consumption. The cumulative installed photovoltaic power worldwide reached 138.9 GW at the end of 2013.

### II.1.3.1 Basic Semiconductor Physics:

With this chapter we start with the discussion of some important concepts from semiconductor physics, which are required to understand the operation of solar cells. After giving a brief introduction into semiconductor physics in this chapter, we will discuss the most important generation and recombination mechanisms in last Chapter.

Finally, we will focus on the physics of semi- conductor junctions in Chapter. The first successful solar cell was made from crystalline silicon (c-Si), which still is by far the most widely used PV material. Therefore, we shall use c-Si as an example to explain the concepts of semiconductor physics that are relevant to solar cell operation.

This discussion will give us a basic understanding of how solar cells based on other semiconductor materials work. The central semiconductor parameters that determine thedesign and performance of a solar cell are: 1. Concentrations of doping atoms, which can be oftwo different types: donor atoms, which donate free electrons or acceptor atoms, which accept electrons. The concentrations of donor and acceptor atoms are denoted by ND and NA, r

respectively, and determine the width of the space-charge region of a junction, as we will see in Chapter coming. The mobility μ and the diffusion coefficient D of charge carriers is used to characterize the transport of carriers transport due to drift and diffusion, respectively, which we will discuss I he lifetime τ and the diffusion length L of the excess carriers characterize the recombination- generation processes, discussed in Chapter last . The band gap energy Eg, and the complex refract-ive index n − ik, where k is linked to the absorption coefficient α, characterize the ability of a semiconductor to absorb

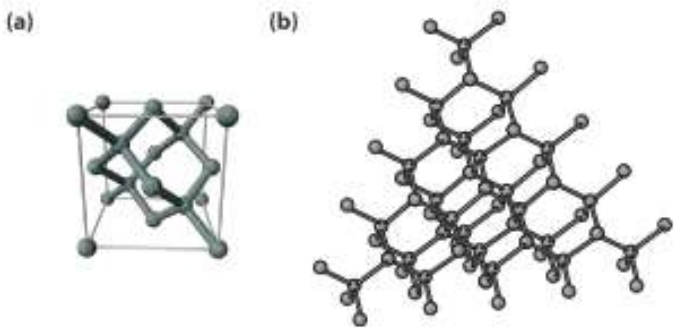



**Fig2.1** (a) A diamond lattice unit cell representing a unit cell of single crystal Si [25], (b) the atomic structure of a part of single crystal Si. [12]

The atomic number of silicon is 14, which means that are 14 electrons orbiting the nucleus. In round state con- figuration, two electrons are in the first shell, both living in the 1s orbital. Further, eight electrons are in the second shell, two in the 2s and six in the 2p orbitals. Hence, four electrons live in the third shell, which is the outermost shell for a Si atom. [8] 1eV = 1.602× 10 $-^{19}$ J

Only these four electrons interact with other atoms, for example via forming chemical bonds. They are called the valence electrons. Two Si atoms are bonded together when they share each other's valence electron. This is the so called covalent bond that is formed by two electrons. Since Si atoms have four valence electrons, they can be covalently bonded to four other Si atoms. In the crystalline form each Si atom is covalently bonded to four neighboring Si atoms,

as illustrated in Fig. 2.1. In the ground state, two valence electrons live in the 3s orbital and the other two are present in the three 3p orbitals (px, py and pz). In that state only the two electrons in the 3p orbitals can form bond as the 3s orbital is full. In a silicon crystal, where every atom is symmetrically connected to four others, the Si atoms are present as so-called sp3 hybrids.

The 3p and 3s orbitals are mixed forming 4 sp3 orbitals. Every of these four orbitals is occupied by one electron that can form a covalent bond with a valence electron from a neighboring atom. All bonds have the same length and the angles between the bonds are equal with 109.5°. The number of bonds that an atom has with its immediate neighbors in the atomic structure is called the coordination number or co- ordination. Thus, in single crystal silicon, the coordination number for all Si atoms is four, we can also say that Si atoms are fourfold coordinated

. A unit cell can be defined, from which the crystal lattice can be reproduced by duplicating the unit cell and stacking the duplicates next to each other. Such a regular atomic arrangement is described as a structure with long range order.

A diamond lattice unit cell represents the real lattice structure of monocrystalline silicon. Fig2.1 (a)

shows the arrangement of the unit cell and Fig. 2.1 (b) the atomic structure of single crystal silicon. One can determine from Fig. 2.1 (a) that there are eight Si atoms in the volume of the unit cell.

When a lattice constant of c-Si is 5.4 Å one can easily calculate that the density of atoms is approximately $5 \times 10^{22}\,cm^{-3}$. Fig2.1 (a) shows the crystalline Si atomic structure with no foreign atoms. In practice, a semiconductor sample always contains some impurity atoms. When the concentration of impurity atoms in a semiconductor is insignificant we refer to such semiconductor as an intrinsic semiconductor.

At practical operational conditions, e.g. at room temperature, 1 there are always some of the covalent bonds broken. The breaking of the bonds results in liberating the valence electrons from the bonds and making them mobile through the crystal lattice. We refer to these electrons as free electrons (henceforth simply referred to as electrons).

The position of a missing electron in a bond, which can be regarded as positively charged, is referred to as a hole. This situation can be easily visualized by using the bonding model illustrated in Fig. 2.2. In the bonding model the atomic cores (atoms without valence electrons) are represented by circles and the valence or bonding electrons are represented by lines interconnecting the circles.

In case of c-Si one Si atom has four valence electrons and four nearest neighbors. Each of the valence electron is equally shared with the nearest neighbor. There are therefore eight lines terminating on each circle. In an ideal Si crystal at 0 K all valence electrons take part in forming covalent bonds between Si atoms and therefore no free electrons are present in the lattice.

This situation is schematically shown in Fig. 2.2 (a). At temperatures higher than 0 K the bonds start to break due to absorbing thermal energy. This process results in creation of mobile electrons and holes. Fig2.2 (b) shows a situation when a covalent bond is broken and one electron departs from the bond leaving a so-called hole behind.

A single line between the atoms in Fig. 2.2 (b) represents the remaining electron of the broken bond. When a bond is broken and a hole created, a valence electron from a neighbouring bond can “jump” into this empty position and restore the bond. The consequence of this transfer is that at the same time the jumping electron creates an empty position in its original bond. The subsequent “jumps” of a valence electron can be viewed as a motion of the hole, a positive charge representing the empty position, in the direction opposite to the motion of the valence electron through the bonds. Since breaking of a covalent bond leads to the formation of an electron-hole pair,

in intrinsic semiconductors the concentration of electrons is equal to the concentration of holes. In intrinsic silicon at 300 K approximately $1.5 \times 10^{10}\,cm^{-3}$ broken bonds are present. This number then gives also the concentration of holes, p, and electrons, n. Hence, at 300 K, $n = p = 1.5 \times 10^{10}\,cm^{-3}$. This concentration is called the intrinsic carrier concentration and is denoted as $n_i$.

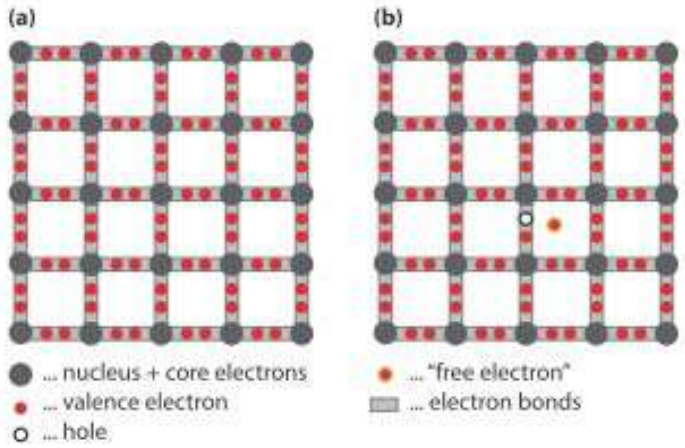



**Fig2.2** The bonding model for c-Si. (a) No bonds are broken. (b) A bond between two Si atoms is broken resulting in a free electron and hole.

### II.1.3.2 Doping:

The concentrations of electrons and holes in c-Si can be manipulated by doping. Doping of silicon means that atoms of other elements substitute Si atoms in the crystal lattice. The substitution has to be carried out by atoms with three or five valence electrons, respectively.

The most used elements to dope c-Si are boron (B) and phosphorus (P), with atomic numbers of 5 and 15, respectively. The process of doping action can best be understood with the aid of the bonding model and is illustrated in

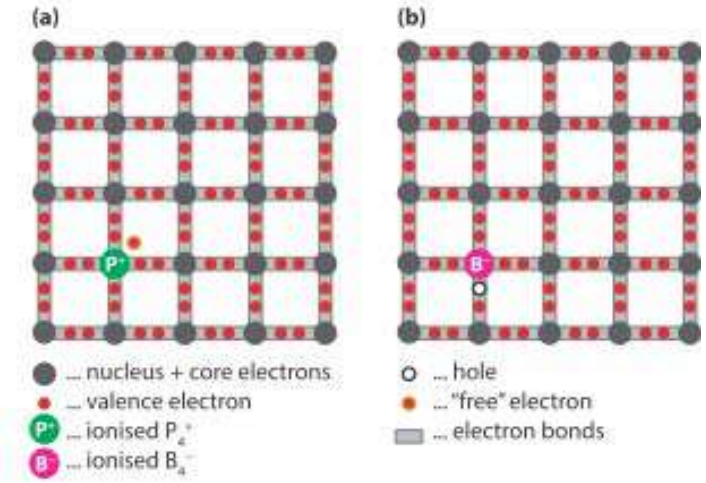



**Fig 2.3** The doping process illustrated using the bonding model. (a) A phosphorus (P) atom substitutes a Si atom in the lattice resulting in the positively-ionized P atom and a free Electron, (b) A boron (B) atom substitutes a Si atom resulting in the negatively ionized B atom and a hole.

Fig. 2.3. When introducing phosphorus atom into the c-Si lattice, four of the five phosphorus atom valence electrons will readily form bonds with the four neighboring Si atoms. The fifth valence electron cannot take part in forming a bond and becomes rather weakly bound to the phosphorus atom.

It is easily liberated from the phosphorus atom by absorbing the thermal energy, which is available in the c-Si lattice at room temperature. Once free, the electron can move throughout the lattice

. In this way the phosphorus atom that substitutes a Si atom in the lattice "donates" a free (mobile) electron into the c-Si lattice. The impurity atoms that enhance the concentration of electrons are called donors.

We denote the concentration of donors by ND. An atom with three valence electrons such as boron cannot form all bonds with four neighboring Si atoms when it substitutes a Si atom in the lattice. However, it can readily "accept" an electron from a nearby Si-Si bond.

A thermal energy that the c-Si lattice contains at room temperature is sufficient to enable an electron from a nearby Si-Si bond to attach itself to the boron atom and complete the bonding to the four Si neighbors. In this process a hole is created that can move around the lattice. The impurity atoms that enhance the concentration of holes are called acceptors. We denote the concentration of acceptors by NA.

Note that by substituting Si atoms with only one type of impurity atoms, the concentration of only one type of mobile charge carriers is increased. Charge neutrality of the material is nevertheless maintained because the sites of the bonded and thus fixed impurity atoms become charged. The donor atoms become positively ionized and the acceptor atoms become negatively ionized.

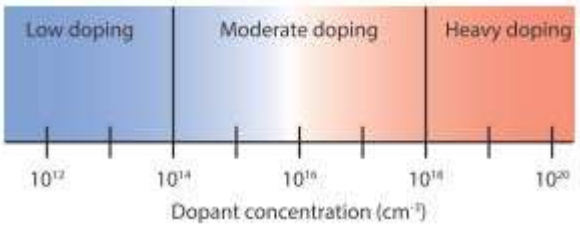



**Fig 2.4** The range of doping levels used in c-Si.

## II.1.3.3 Intrinsic semiconductors:

Any operation of a semiconductor device depends on the concentration of carriers that transport charge inside the semiconductor and hence cause electrical currents. In order to determine and to understand device operation it is important to know the precise concentration of these charge carriers.

In this section the concentrations of charge carriers inside a semiconductor are derived assuming the semiconductor is under equilibrium. The term equilibrium is used to describe the unperturbed state of a system, to which no external voltage, magnetic field, illumination, mechanical stress, or other perturbing forces are applied. In the equilibrium state the observable parameters of a semiconductor do not change with time.

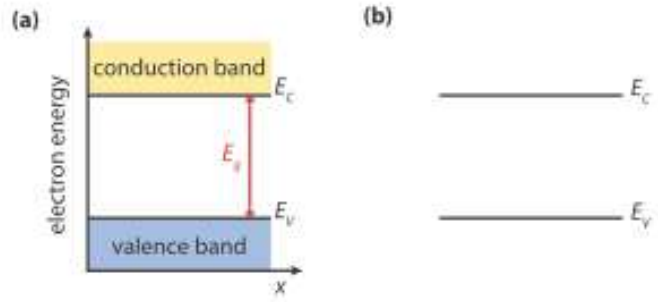



**Fig 2.5** (a) The basic energy band diagram and (b) widely used simplified version of the energy diagram.

In order to determine the carrier concentration one has to know the function of density of allowed energy states of electrons and the occupation function of the allowed energy states. The density of energy states function, g(E), describes the number of allowed states per unit volume and energy.

The occupation function is the well-known Fermi-Dirac distribution function, f (E), which describes the ratio of states filled with an electron to total allowed states at given energy E. In an isolated Si atom, electrons are allowed to have only discrete energy values. The periodic atomic structure of single crystal silicon results in the ranges of allowed energy states for electrons that are called energy bands and the excluded energy ranges, forbidden gaps or bandgaps.

Electrons that are liberated from the bonds determine the charge transport in a semiconductor. There- fore, we further discuss only those bands of energy levels, which concern the valence electrons. Valence electrons, which are involved in the covalent bonds, have their allowed energies in the valence band (VB) and the allowed energies of electrons liberated from the covalent bonds form the conduction band (CB).

The valence band is separated from the conduction band by a band of forbidden energy levels. The maximum attainable valence-band energy is denoted EV, and the minimum attainable conduction-band energy is denoted EC. The energy difference between the edges of these two bands is called the band gap energy or band gap, Eg, and it is an important material parameter.

$$EG = EC - EV.$$

At room temperature (300 K), the band gap of crystal-line silicon is 1.12 eV. 2 A plot of the allowed electron energy states as a function of position is called the energy band diagram and for intrinsic c-Si to EV are given by

$$g_c(E) = \left(\frac{4\sqrt{2}\pi m_n^*}{h^3}\right)^{\frac{3}{2}} \sqrt{E - E_C},$$

$$g_v(E) = \left(\frac{4\sqrt{2}\pi m_p^* t}{h^3}\right)^{\frac{3}{2}} \sqrt{E - E_V},$$

EQUATION (2.1)

where $M_n^*$ and $M_p^*$ is the effective mass of electrons and holes, respectively. As the electrons and holes move in the periodic potential of the c-Si crystal, the mass has to be replaced by the effective mass, which takes the effect of a periodic force into account. The effective mass is also averaged over different directions to take anisotropy into account.

The Fermi-Dirac distribution function is given by

$$f(E) = \frac{1}{1 + \exp\left(\frac{E - E_F}{kT}\right)},$$

EQUATION (2.2)

where k is Boltzmann's constant (k = 1.38 × $10^{-23}$ J/K) and EF is the so-called Fermi energy. kT is the thermal energy, at 300 K it is 0.0258 eV. The Fermi energy is the electrochemical potential of the electrons in a material and in this way it represents the averaged energy of electrons in the material.

The Fermi-Dirac distribution function for different temperatures. The carriers that contribute to charge transport are electrons in the conduction band and holes in the valence band. The total concentration of electrons in the conduction band and the total concentration of holes inthe valence band is obtained by multiplying density of states function with the distribution function and integrating across the whole energy band,

$$n = \int_{E_C}^{E_{top}} g_c(E) f(E) \mathrm{d}E,$$
$$p = \int_{E_{bottom}}^{E_V} g_v(E)\,[1 - f(E)]\,\mathrm{d}E,$$

EQUATION (2.3)

Substituting the density of states and the Fermi-Dirac distribution function into Eq. (6.4) the resulting expressions for n and p are obtained after solving the equations. The full derivation can be found for example in

$$n = N_C \exp\left(\frac{E_F - E_C}{kT}\right) \quad \text{for} \quad E_C - E_F \geq 3kT,$$
$$p = N_V \exp\left(\frac{E_V - E_F}{kT}\right) \quad \text{for} \quad E_F - E_V \geq 3kT,$$

EQUATION (2.4)

where $N_C$ and $N_V$ are the effective densities of the conduction band states and the valence band states, respectively. For crystalline silicon, we have at 300 K

$$N_C = 3.22 \times 10^{19}\,\mathrm{cm}^{-3},$$
$$N_V = 1.83 \times 10^{19}\,\mathrm{cm}^{-3}.$$

When the requirement that the Fermi level lies in the band gap more than 3kT from either band edge is

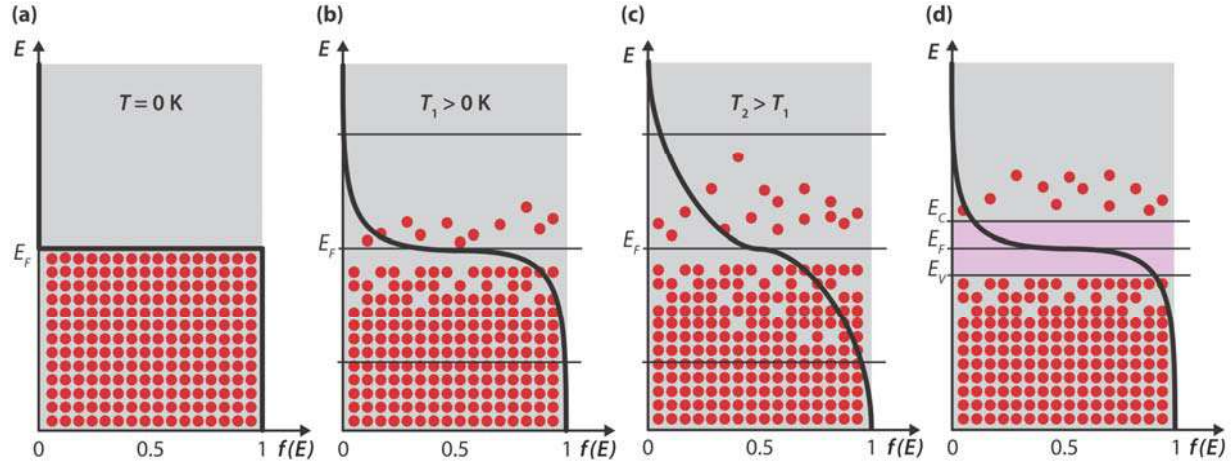



**Fig 2.6** The Fermi-Dirac distribution function. (a) For T = 0 K, all allowed states bellow the Fermi level are occupied by two electrons. (b, c) At T > 0 K not all states below the Fermi level are occupied and there are some states above the Fermi level that are occupied. (d) In an energy gap between bands no electrons are present.

satisfied the semiconductor is referred to as anon degenerate semiconductor. If an intrinsic semiconductor is in equilibrium, we have n = p = $n_i$. By multiplying the corresponding sides of Eqs

$$n = N_C \exp\left(\frac{E_F - E_C}{kT}\right) \quad \text{for} \quad E_C - E_F \geq 3kT,$$
$$p = N_V \exp\left(\frac{E_V - E_F}{kT}\right) \quad \text{for} \quad E_F - E_V \geq 3kT,$$

We obtain

$$np = n_i^2 = N_C N_V \exp\left(\frac{E_V - E_C}{kT}\right)$$
$$= N_C N_V \exp\left(-\frac{E_g}{kT}\right), \quad \text{EQUATION (2.4)}$$

which is independent of the position of the Fermi level and thus valid for doped semiconductors as well. When we denote the position of the Fermi level in the intrinsic material $E_{Fi}$ we may write

$$n_i = N_C \exp\left(\frac{E_{Fi} - E_C}{kT}\right)$$
$$= N_V \exp\left(\frac{E_V - E_{Fi}}{kT}\right).$$

From Eq. above we can easily find the position of EFi to be

$$E_{Fi} = \frac{E_C + E_V}{2} + \frac{kT}{2} \ln\left(\frac{N_V}{N_C}\right)$$
$$= E_C - \frac{E_g}{2} + \frac{kT}{2} \ln\left(\frac{N_V}{N_C}\right).$$

The Fermi level EFi lies close to the midgap [(EC+EV)/2]; a slight shift is caused by the difference in the effective densities of the valence and conduction band.

## II.1.3.4 Doped semiconductors:

It has been already mentioned in that the concentrations of electrons and holes in c-Si can be manipulated by doping. The concentration of electrons and holes is influenced by the amount of the impurity atoms that substitute silicon atoms in the lattice. Under assumption that the semiconductor is uniformly doped and in equilibrium a simple relationship between the carrier and dopant concentrations can be established. We assume that at room temperature the dopant atoms are ionized. Inside a semiconductor the local charge density is given by

$$\rho = e\left(p + N_D^+ - n - N_A^-\right), \quad \text{EQUATION (2.5)}$$

where e is the elementary charge (e = 1.602 × $10^{-19}$C). $N_D^+$ and $N_A^-$ denote the density of the ionized donor and acceptor atoms, respectively. As every ionized atom corresponds to a free atom (hole), $N_D^+$ and $N_A^-$ tell us the concentration of electrons and holes due to doping, respectively.

Under equilibrium conditions, the local charge of the uniformly doped semiconductor is zero, which means that the semiconductor is charge-neutral everywhere. We thus can write:

$$p + N_D^+ - n - N_A^- = 0.$$

As previously discussed, the thermal energy available at room temperature is sufficient to ionize almost all the dopant atoms. We therefore may assume

$$N_D^+ \approx N_D \qquad \text{and} \qquad N_A^- \approx N_A,$$

Then

$$p + N_D - n - N_A = 0,$$

which is the common form of the charge neutrality equation. Let us now consider an n-type material. At room temperature almost all donor atoms ND are ionized and donate an electron into the conduction band. Under the assumption that $N_A = 0$ ,

$$p + N_D - n = 0,$$

Under the assumption that

$$N_D \approx N_D^+ \approx n$$

we can expect that the concentration of holes is lower than that of electrons, and becomes very low when $N_D$ becomes very large. We can calculate more accurate the concentration of holes in the n-type material from Eq.

$$p = \frac{n_i^2}{n} \approx \frac{n_i^2}{N_D} \ll n.$$

In case of a p-type material almost all acceptor atoms $N_A$ are ionized at room temperature and accept an electron and leaving a hole in the valence band. Under the assumption that $N_A = 0$,

$$p - n - N_A = 0.$$

Under the assumption that

$$N_A \approx N_A^- \approx p$$

we can expect that the concentration of electrons is lower than that of holes. We can calculate more accurate the concentration of electrons in the p-type material

$$n = \frac{n_i^2}{p} \approx \frac{n_i^2}{N_A} \ll p.$$

Inserting donor and acceptor atoms into the lattice of crystalline silicon introduces allowed energy levels into the forbidden bandgap. For example, the fifth valence electron of the P atom does not take part in forming a bond, is rather weakly bound to the atom and easily liberates from the P atom. The energy of the liberated electron lies in the CB.

The energy levels, which we denote ED, of the weakly-bound valence electrons of the donor atoms have to be positioned close the CB. Notice that a dashed line represents the ED. This means that an electron that occupies the ED level, is localized to the vicinity of the donor atom.[9]

Similarly, the acceptor atoms introduce allowed energy levels EA close to the VB. Doping also influences the

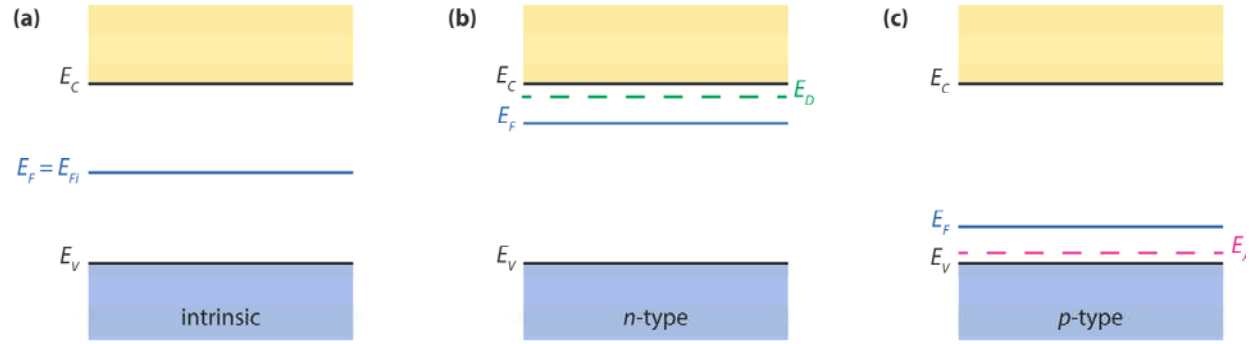



**Fig2.7** A shift of the position of the Fermi energy in the band diagram and the introduction of the allowed energy level into the bandgap due to the doping.

position of the Fermi energy. When increasing the concentration of electrons by increasing the concentration of donors the Fermi energy will increase, which is represented

by bringing the Fermi energy close to the CB in the band diagram. In the p-type material the Fermi energy is moving closer the VB.

A change in the Fermi energy position and the introduction of the allowed energy level into the bandgap due to the doping is illustrated

$$E_C - E_F = kT \ln\left(\frac{N_C}{N_D}\right) \qquad \text{for } n\text{-type},$$
$$E_F - E_V = kT \ln\left(\frac{N_V}{N_A}\right) \qquad \text{for } p\text{-type}.$$

## II.1.3.5 Transport Properties:

In contrast to the equilibrium conditions, under operational conditions a net electrical current flows through a semiconductor device.

The electrical currents are generated in a semiconductor due to the transport of charge by electrons and holes. The two basic transport mechanisms in a semiconductor are drift and diffusion.

## II.1.3.6 Drift:

Drift is charged-particle motion in response to an electric field. In an electric field the force acts on the charged particles in a semiconductor, which accelerates the positively charged holes in the direction of the electric field and the negatively charged electrons in the direction opposite to the electric field. Because of collisions with the thermally vibrating lattice atoms and ionised impurity atoms,

the carrier acceleration is frequently disturbed. The resulting motion of electrons and holes can be described by average drift velocities vdn and vdp for electrons and holes, respectively. In case of low electric fields, the average drift velocities are directly proportional to the electric field as expressed by

$$\mathbf{v}_{dn} = -\mu_n \xi,$$
$$\mathbf{v}_{dp} = \mu_p \xi.$$

The proportionality factor is called mobility μ. It is a central parameter that characterizes electron and hole transport due to drift. Although the electrons move in the opposite direction to the electric field, because the charge of an electron is negative the resulting electron drift current is in the same direction as the electric field.

This is illustrated in Fig. 2.8. The electron and hole drift-current densities are then given as

$$\mathbf{J}_{n,\,\text{drift}} = -en\mathbf{v}_{dn} = en\mu_n \xi,$$
$$\mathbf{J}_{p,\,\text{drift}} = ep\mathbf{v}_{dp} = ep\mu_p \xi.$$

Combining eqs leads to the total drift current,

$$\mathbf{J}_{\text{drift}} = e(p\mu_p + n\mu_n)\xi.$$

Mobility is a measure of how easily the charge particles can move through a semiconductor material. For example, for c-Si with a doping concentration $N_D$ or $N_A$, respectively, at 300 K, the motilities are

$$\mu_n \approx 1\,360\,\text{cm}^2\text{V}^{-1}\text{s}^{-1},$$
$$\mu_p \approx 450\,\text{cm}^2\text{V}^{-1}\text{s}^{-1}.$$

As mentioned earlier, the motion of charged carriers is frequently disturbed by collisions. When the number of collisions increases, the mobility decreases. Increasing the temperature increases the collision rate of charged carriers with the vibrating lattice atoms, which results in a lower mobility.

Increasing the doping concentration of donors or acceptors leads to more frequent collisions with the ionized dopant atoms, which results in a lower mobility as well. The dependence of mobility on doping and temperature is in more detailed discussed in standard textbooks for semiconductor physics and devices, such as Reference

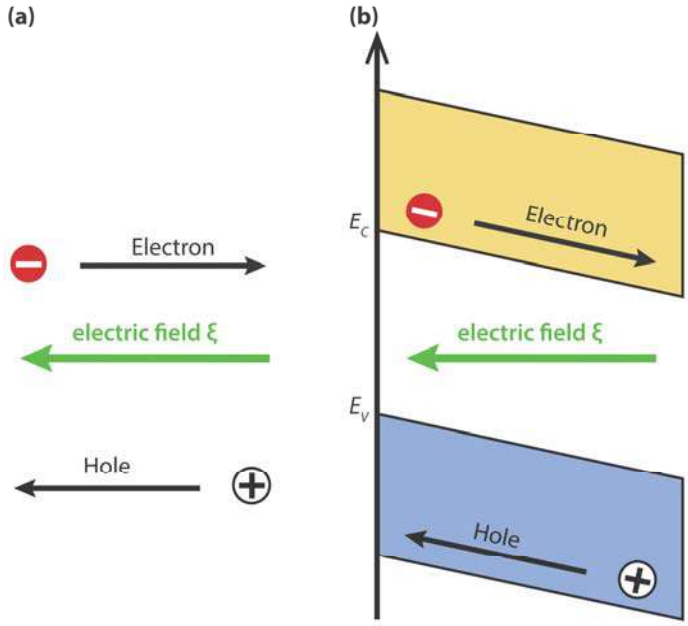



**Fig 2.8** Visualization of (a) the direction of carrier fluxes due to an electric field and (b) the corresponding band diagram.

## II.1.3.7 Diffusion :

Diffusion is a process whereby particles tend to spread out from regions of high particle concentration into regions of low particle concentration as a result of random thermal motion. The driving force of diffusion is a gradient in the particle concentration. In contrast to the drift transport mechanism,

the particles need not be charged to be involved in the diffusion process. Currents resulting from diffusion are proportional to the gradient in particle concentration. For electrons and holes, they are given by

$$\mathbf{J}_{n,\,\mathrm{diff}} = eD_n\nabla n,$$
$$\mathbf{J}_{p,\,\mathrm{diff}} = -eD_p\nabla p,$$

Combining Eqs leads to the total diffusion current,

$$\mathbf{J}_{\mathrm{diff}} = e(D_n\nabla n - D_p\nabla p).$$

The proportionality constants, Dn and Dp are called the electron and hole diffusion coefficients, respectively. The diffusion coefficients of electrons and holes are linked with

the mobilities of the corresponding charge carriers by the Einstein relationship that is given by

$$\frac{D_n}{\mu_n} = \frac{D_p}{\mu_p} = \frac{kT}{e}.$$

After we combine all equations we can have

$$\begin{aligned} \mathbf{J} &= \mathbf{J}_{\text{drift}} + \mathbf{J}_{\text{diff}} \\ &= e(p\mu_p + n\mu_n)\xi + e(D_n \nabla n - D_p \nabla p). \end{aligned}$$

## II.1.3.8 Continuity Equations :

As we have discussed in Section before, charge is a conserved quantity. Now we will have a look at how the continuity equations for the electrons and holes can be formulated. We have to take drift,

diffusion, and recombination as well as generation processes into account the latter are discussed For electrons, the rate with that the concentration changes is given by

$$\frac{\partial n}{\partial t} = \left.\frac{\partial n}{\partial t}\right|_{\text{drift}} + \left.\frac{\partial n}{\partial t}\right|_{\text{diff}} + \left.\frac{\partial n}{\partial t}\right|_{R} + \left.\frac{\partial n}{\partial t}\right|_{G},$$

where R and G denotes recombination and generation, respectively. For holes, we obtain

$$\frac{\partial p}{\partial t} = \left.\frac{\partial p}{\partial t}\right|_{\text{drift}} + \left.\frac{\partial p}{\partial t}\right|_{\text{diff}} + \left.\frac{\partial p}{\partial t}\right|_{R} + \left.\frac{\partial p}{\partial t}\right|_{G}.$$

In these equations ∂n/∂t (∂p/∂t) is the time rate change in the electron (hole) concentration Without any generation or recombination, the number of electrons and holes is conserved, . We thus obtain

$$\begin{aligned} \left.\frac{\partial n}{\partial t}\right|_{\text{drift}} + \left.\frac{\partial n}{\partial t}\right|_{\text{diff}} &= \frac{1}{e}\nabla \times \mathbf{J}_n, \\ \left.\frac{\partial p}{\partial t}\right|_{\text{drift}} + \left.\frac{\partial p}{\partial t}\right|_{\text{diff}} &= -\frac{1}{e}\nabla \times \mathbf{J}_p, \end{aligned}$$

where Jn (Jp) is the electron (hole) current density. [3]

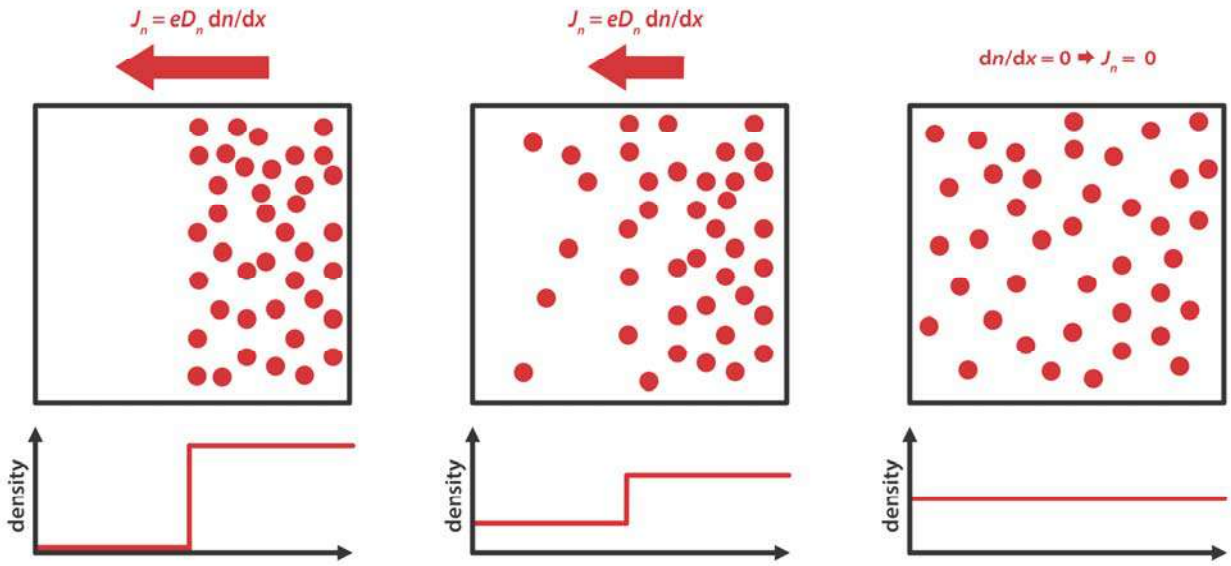



**Fig 2.9** Visualization of electron diffusion.

The equations can be written in a more compact form when introducing substitutions,

$$\left.\frac{\partial n}{\partial t}\right|_R = -R_n,$$
$$\left.\frac{\partial p}{\partial t}\right|_R = -R_p,$$

$$\left.\frac{\partial n}{\partial t}\right|_G = G_n,$$
$$\left.\frac{\partial p}{\partial t}\right|_G = G_p.$$

Rn (Rp) denotes the net thermal recombination-generation rate of electrons (holes), Gn (Gp) is the generation rate of electrons (holes) due to other processes,such as photogeneration.

We will discuss these processes in detail in. Substituting Eqs. finally leads to

$$\frac{\partial n}{\partial t} = \frac{1}{e}\nabla \times \mathbf{J}_n - R_n + G_n,$$
$$\frac{\partial p}{\partial t} = -\frac{1}{e}\nabla \times \mathbf{J}_p - R_p + G_p.$$

EQUATION (2.6)

## II.1.4 Semiconductor Junctions:

Almost all solar cells contain junctions between (different) materials of different doping. Since these junctions are crucial to the operation of the solar cell, we will discuss their physics in this semi chapter.

A p-n junction fabricated in the same semiconductor material such as c-Si is an example of an p-n homojunction. There are also other types of junctions: A p-n junction that is formed by two chemically different semi-conductors is called a p-n heterojunction. In a p-i-n junction,

the region of the internal electric field is extended by inserting an intrinsic,i, layer between the p-type and the n-type layers. The i-layer behaves like a capacitor and it stretches the electric field formed by the p-n junction across itself. Another type of the junction is a junction between a metal and a semiconductor, a so-called

## II.1.4.1 p-n homojunctions :

### II.1.4.1.1 formation of a space-charge region in P-N junction :

Fig2.1 shows schematically isolated pieces of a p-type and an n-type semiconductor and their corresponding band diagrams. In both isolated pieces the charge neutrality is maintained. In the n-type semiconductor the large concentration of negatively-charged free electrons is compensated by positively-charged ionized donor atoms.

In the p-type semiconductor holes are the majority carriers and the positive charge of holes is compensated by negatively-charged ionized acceptor atoms. For the isolated n-type semiconductor we can write

$$n = n_{n0} \approx N_D,$$
$$p = p_{n0} \approx n_i^2 / N_D .$$

For the isolated p-type semiconductor we have

$$p = p_{p0} \approx N_A,$$
$$n = n_{p0} \approx n_i^2 / N_A$$

When a p-type and an n-type semiconductor are brought together, a very large difference in electron concentration between n- and p-type regions causes a diffusion current of electrons from the n-type material across the metallurgical junction into the p-type material.

The term “metallurgical junction” denotes the interface between the n- and p-type regions. Similarly, the difference in hole concentration causes a diffusion current of holes from the p- to the n-type material.

Due to this diffusion process the region close to the metallurgical junction becomes almost completely depleted of mobile charge carriers. The gradual depletion of the charge carriers gives rise to a space charge created by the charge

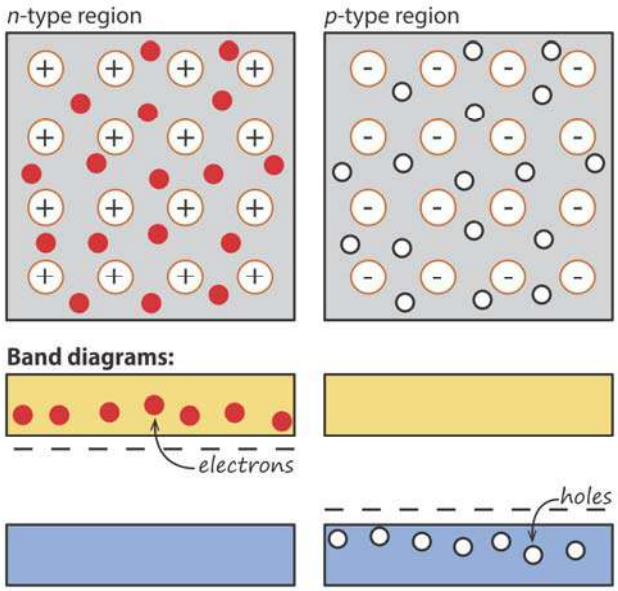



**Fig2.10** Schematic representation of an isolated n-type and p-type semiconductor and corresponding band diagrams.

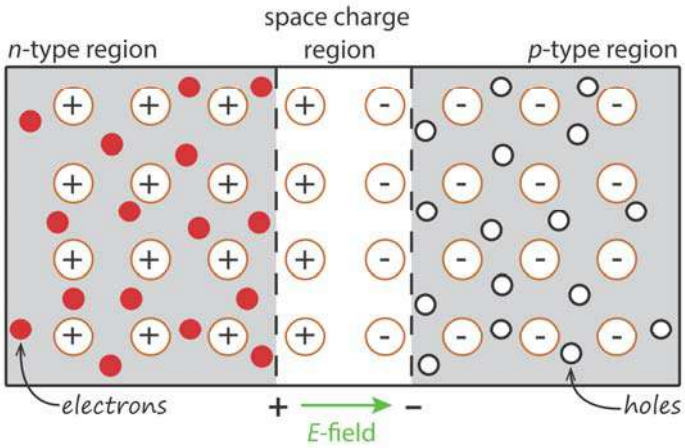



**Fig 2.11** Formation of a space-charge region, when n-type and p-type semiconductors are brought together to form a junction. The colored part represents the space-charge region.

of the ionized donor and acceptor atoms that is not compensated by the mobile charges any more.

This region of the space charge is called the space-charge region or depleted region and is schematically illustrated in Fig above. Regions outside the depletion region, in which the charge neutrality is conserved, are denoted as the quasi-neutral regions. The space charge around the metallurgical junction results in the formation of an internal electric field which forces the charge carriers to move in the opposite direction than the concentration gradient.

The diffusion currents continue to flow until the forces acting on the charge carriers, namely the concentration gradient and the internal electrical field, compensate each other. The driving force for the charge transport does not exist anymore and no net current flows through the p-n junction.

### II.1.4.1.2 The P-N junction under equilibrium:

The p-n junction represents a system of charged particles in diffusive equilibrium in which the electro-chemical potential is constant and independent of position. The electro-chemical potential describes an average energy of electrons and is represented by the Fermi energy.

It means that under equilibrium conditions the Fermi level has constant position in the band diagram of the p-n junction. Fig2.10 shows the energy-band diagram of a p-n junction under equilibrium. The distance between the Fermi level and the valence and/or conduction bands does not change in the quasi-neutral regions and is the same as in the isolated n- and p-n type semiconductors.

Inside the space-charge region, the conduction and valence bands are not represented by straight horizontal lines any more but they are curved. This indicates the presence of an electric field in this region. Due to the electric field a difference in the electrostatic potential is created between the boundaries of the space-charge region. Across the depletion region the changes in the carrier's concentration are compensated by changes in the electrostatic potential.

The electrostatic-potential profile is also drawn in Fig. coming The concentration profile of charge carriers in a p-n junction is schematically presented in Fig. 8.4. In the quasi-neutral regions, the concentration of electrons and holes is the same as in the isolated doped semiconductors. In the space-charge region the concentrations of majority charge carriers decrease very rapidly.

This fact allows us to use the assumption that the space-charge region is depleted of mobile charge carriers. This assumption means that the charge of the mobile carriers represents a negligible contribution to the total space charge in the depletion region. The space charge in this region is fully determined by the ionized dopant atoms fixed in the lattice.

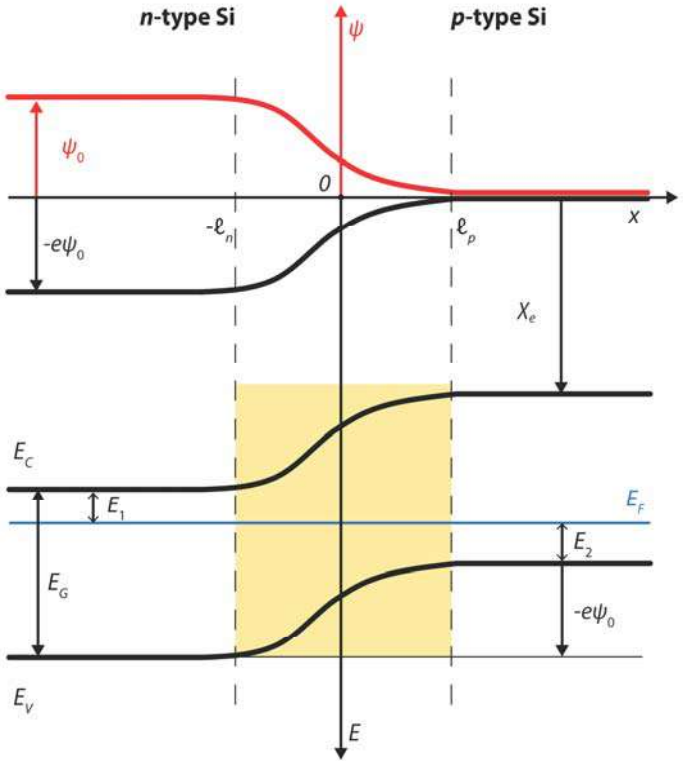



**Fig 2.12** Energy-band diagram of the p-n junction. The electrostatic potential profile (red curve) is also presented in the figure

The presence of the internal electric field inside the p-n junction means that there is an electrostatic potential difference, ψ0, across the space-charge region. We shall determine a profile of the internal electric field and electrostatic potential in the p-n junction. First we introduce an approximation,

which simplifies the calculation of the electric field and electrostatic-potential. This approximation (the depletion approximation) assumes that the space-charge density, ρ, is zero in the quasi-neutral regions and it is fully determined by the concentration of ionized dopants in the depletion region. In the depletion region of the n-types semiconductor it

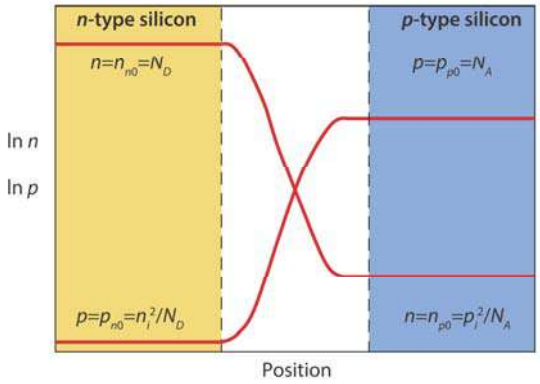



**Fig 2.13** Concentrations profile of mobile charge carriers in a p-n junction under equilibrium.

is the concentration of positively charged donor atoms, ND, which determines the space charge in this region. In the p-type semiconductor,

the concentration of negatively charged acceptor atoms, NA, determines the space charge in the depletion region. This is illustrated in Fig. 2.5. Further, we assume that the p-n junction is a step junction; it means that there is an abrupt change in doping at the metallurgical junction and the doping concentration is uniform both in the p-type and the n-type semiconductors.

According to Fig. 2.5 the position of the metallurgical junction is placed at zero, the width of the space-charge region in the n-type material is denoted as `n and the width of the space-charge region in the p-type material is denoted as `p. The space-charge density is described by

$$\begin{aligned} \rho(x) &= \quad eN_D \qquad \text{for} \qquad -\ell_n \le x \le 0, \\ \rho(x) &= -eN_A \qquad \text{for} \qquad 0 \le x \le \ell_p, \end{aligned}$$

where ND and NA is the concentration of donor and acceptor atoms, respectively. Outside the space-charge region the space-charge density is zero. The electric field is can be calculated from the Poisson's equation, in one dimension can be written as

$$\frac{\mathrm{d}^2\psi}{\mathrm{d}x^2} = -\frac{\mathrm{d}\,\xi}{\mathrm{d}x} = -\frac{\rho}{\varepsilon_r \varepsilon_0},$$

where ψ is the electrostatic potential, ξ is the electric field, ρ is the space-charge density, εr is the semiconductor dielectric onstant and ε0 is the vacuum permittivity. The vacuum permittivity is e0 = 8.854 · $10^{-14}$ F/cm and for crystalline silicon εr = 11.7..

The electric field profile can be found by integrating the spacecharge density across the space-charge region,

$$\xi = \frac{1}{\varepsilon_r \varepsilon_0} \int \rho \, \mathrm{d}x.$$

Substituting the space-charge density with Eqs and using the boundary conditions

$$\xi\,(-\ell_n) = \xi\,(\ell_p) = 0,$$

we obtain as solution for the electric field

$$\begin{aligned} \xi\ (x) &= \frac{e}{\varepsilon_r \varepsilon_0} N_D\ (\ell_n + x) \quad \text{for} \quad -\ell_n \le x \le 0, \\ \xi\ (x) &= \frac{e}{\varepsilon_r \varepsilon_0} N_A\ (\ell_p - x) \quad \text{for} \quad 0 \le x \le \ell_p. \end{aligned}$$

EQUATION (2.7)

At the metallurgical junction, x = 0, the electric field is continuous, which requires that the following condition has to be fulfilled

$$N_A \ell_p = N_D \ell_n$$

Outside the space-charge region the material is electrically neutral and therefore the electric field is zero there. The profile of the electrostatic potential is calculated by integrating the electric field throughout the space charge region and applying the boundary conditions,

$$\psi = -\int \xi \mathrm{d}x.$$

We define the zero electrostatic potential level at the outside edge of the p-type semiconductor. Since we assume no potential rop cross the quasi-neutral region the electrostatic potential at the boundary of the space charge region in the p-type material is also zero,

$$\psi(\ell_p) = 0.$$

Using two Eqs. for describing the electric field in the n-type and p-type parts of the space-charge region, respectively, and taking into account that at the metallurgical junction the electrostatic potential is continuous, the solution for the electrostatic potential can be written as

$$\left.\begin{aligned}\psi(x) = &-\frac{e}{2\varepsilon_r\varepsilon_0} N_D\ (x+\ell_n)^2 \\ &+\frac{e}{2\varepsilon_r\varepsilon_0}\left(N_D\ell_n^2 + N_A\ell_p^2\right)\end{aligned}\right\} \quad \text{for } -\ell_n \le x \le 0,$$

$$\psi(x) = \frac{e}{2\varepsilon_r\varepsilon_0} N_A\ (x-\ell_p)^2 \qquad \text{for } 0 \le x \le \ell_p.$$

Under equilibrium a difference in electrostatic potential, ψ0, develops across the space-charge region. The electrostatic potential difference across the p-n junction is an important characteristic of the junction and is denoted as the built-in voltage or diffusion potential of the p-n junction.

We can calculate ψ0 as the difference between the electrostatic potential at the edges of the space-charge region,

$$\psi_0 = \psi(-\ell_n) - \psi(\ell_p) = \psi(-\ell_n). \quad \text{EQUATION (2.8)}$$

we obtain for the built-in voltage

$$\psi_0 = \frac{e}{2\varepsilon_r\varepsilon_0}\left(N_D\ell_n^2 + N_A\ell_p^2\right) \quad \text{EQUATION (2.9)}$$

Another way to determine the built-in potential ψ0 is to use the energy-band diagram presented in Fig. 2.3.

$$e\psi_0 = E_G - E_1 - E_2.$$

Using Eqs., which determine the band gap, and the positions of the Fermi energy in the n- and p-type semiconductor, respectively,

$$\begin{aligned}E_G &= E_C - E_V, \\ E_1 &= E_C - E_F = kT\ln(N_C/N_D), \\ E_2 &= E_F - E_V = kT\ln(N_V/N_A).\end{aligned}$$

We can write

$$e\psi_0 = E_G - kT \ln\left(\frac{N_V}{N_A}\right) - kT \ln\left(\frac{N_C}{N_D}\right)$$
$$= E_G - kT \ln\left(\frac{N_V N_C}{N_A N_D}\right).$$

EQUATION (2.10)

Using the relationship between the intrinsic concentration, ni and the band gap, EG [see Eq. (6.7)],

$$n_i^2 = N_C N_V \exp\left[-\frac{E_G}{kT}\right]$$

we can rewrite Eq. (8.15) and obtain

$$\psi_0 = \frac{kT}{e} \ln\left(\frac{N_A N_D}{n_i^2}\right)$$

This equation allows us to determine the built-in potential of a p-n junction from the standard semiconductor parameters, such as doping concentrations and the intrinsic carrier concentration. With the built-in potential we can calculate the width of the space charge region of the p-n junction in the thermal equilibrium.

Substituting ψ0 using Eq. (8.16) into Eq. (8.12) and taking the boundary condition [Eq. (8.6) into account, the resulting expressions for `n and `p are obtained. The full derivation can be found for example Ref. [20].

$$\ell_n = \sqrt{\frac{2\varepsilon_r \varepsilon_0}{q} \psi_0 \frac{N_A}{N_D} \left(\frac{1}{N_A + N_D}\right)},$$
$$\ell_p = \sqrt{\frac{2\varepsilon_r \varepsilon_0}{q} \psi_0 \frac{N_D}{N_A} \left(\frac{1}{N_A + N_D}\right)}.$$

EQUATION (2.11)

The total space-charge width, W, is the sum of the partial space-charge widths in the n- and p-type semiconductors and can be calculated with

$$W = \ell_n + \ell_p = \sqrt{\frac{2\varepsilon_r \varepsilon_0}{e} \psi_0 \left(\frac{1}{N_A} + \frac{1}{N_D}\right)}.$$

EQUATION (2.12)

The space-charge region is not uniformly distributed in the n- and p- regions. The widths of the space-charge region in the n- and p-type semiconductor are determined by the doping concentrations as illustrated by Eqs.

Knowing the expressions for `n and `p we can determine the maximum value of the internal electric field, which is at the metallurgical junction. By substituting `p from expressed by Eq.

we obtain the expression for the maximum value of the internal electric field,

$$\xi_{max} = \sqrt{\frac{2e}{\varepsilon_r \varepsilon_0} \psi_0 \left(\frac{N_A N_D}{N_A + N_D}\right)}.$$

## Conclusion:

In this chapter we saw how is the operating principle of PV starting of effects and a brief of history then basic semiconductors doping and manufacturing of cells, it is a real high technology to produce and improve the effect of cell

# Chapter III

# Solar cell parameters & equivalent Circuit

## Introduction :

In this chapter we introduce the basics of electrodynamics that are required for solar cell physics. First, we introduce the electromagnetic wave eqt. The existence of these eqt explains the existence of electromagnetic waves, such as light.

From there we develop the eqt describing the interaction of an electromagnetic wave with interfaces between two materials; in this way we naturally derive the basics of optics.

Later in the chapter we introduce the Poisson equation and the continuity eqt that are very important for semiconductor physics, which we discuss, While electricity and magnetism have been known since ancient times, it took until the nineteenth century to realize that these two phenomena are two sides on one medal,

## III.1 Electrodynamic basics:

namely electromagnetism. We can easily see this by recalling that electric fields are generated by charges while magnetic fields are generated by currents, i.e. moving charges. Let us now assume that we are within an array of charges. Since charges create an electric field, we will experience such an field. Now we start moving with a constant velocity.

This is equivalent to saying that the array of charges moves with respect to us. Since moving charges are a current, we now experience an magnetic field. Thus, when changing from one, frame of reference into another one that moves with respect to the first one with a constant velocity, electric fields are transformed into magnetic fields and vice versa.

Between 1861 and 1862, the Scottish physicist James Clerk Maxwell published works in that he managed

to formulate the complete electromagnetic theory by a set of eqt, the Maxwell eqt. A modern formulation of these eqt is given in Appendix A.1. The transformation of the electric and magnetic fields between different frames of reference is correctly described by Albert Einstein's theory of special relativity published in 1905.

One of the most important prediction of the Maxwell eqt is the presence of electromagnetic waves. A derivation is given in Appendix A.2. Maxwell soon realised that the speed of these waves is (within experimental accuracy) the same as the speed of light that then already was known. He brilliantly concluded that light is an electromagnetic wave.

In the 1880s the German physicist Heinrich Hertz could experimentally confirm that electromagnetic waves can be generated and have the same speed as light. His work laid the foundation for modern radio communication that has shaped the modern world.

The electromagnetic theory can perfectly describe how light propagates. However, it fails in explaining how

light is emitted and absorbed by matter. For this purpose, quantum mechanics is required.

## III.2 Electromagnetic waves:

As shown in Appendix A.2, electromagnetic waves are described by

$$\left(\frac{\partial^2}{\partial x^2}+\frac{\partial^2}{\partial y^2}+\frac{\partial^2}{\partial z^2}\right)\mathbf{E}-\frac{n^2}{c_0^2}\left(\frac{\partial^2\mathbf{E}}{\partial t^2}\right)=0$$

EQUATION (3.1)

for the electric field E(r, t), where c0 denotes the speed of light in vacuo and n is the refractive index of the material. In a similar manner we can derive the wave equation for the magnetic field,

$$\left(\frac{\partial^2}{\partial x^2}+\frac{\partial^2}{\partial y^2}+\frac{\partial^2}{\partial z^2}\right)\mathbf{H}-\frac{n^2}{c_0^2}\left(\frac{\partial^2\mathbf{H}}{\partial t^2}\right)=0.$$

EQUATION (3.2)

The simplest solution to the wave eqt above is the plane harmonic wave, where light of constant wavelength λ propagates in one direction. Without loss of generality, we assume that the wave travels along the z direction. The electric and magnetic fields in this case are

$$\mathbf{E}(\mathbf{r},t)=\mathbf{E}_0e^{ik_zz-i\omega t},$$
$$\mathbf{H}(\mathbf{r},t)=\mathbf{H}_0e^{ik_zz-i\omega t},$$

EQUATION (3.3)

where E0 and H0 are constant vectors (the amplitudes), kz is the wave number and ω is the angular frequency. By substituting Eq. (4.2a) into Eq. (4.1a) we find that kz and ω are connected to each other via

$$k_z^2-\frac{n^2}{c_0^2}\omega^2=0.$$

EQUATION (3.4)

Thus

$$k_z=\frac{n\omega}{c}.$$

EQUATION (3.5)

The angular frequency, measured in radians per second is related to the frequency of the wave ν, measured in Hertz, via

$$\omega=2\pi\nu=\frac{2\pi}{T},$$

EQUATION (3.6)

where T = 1/ν is the period, measured in seconds. The wave number kz has the unit of an inverse length. It is related to the wavelength λ via

$$\lambda=\frac{2\pi}{k_z}=\frac{2\pi c}{n\omega}=\frac{c}{n\nu}.$$

EQUATION (3.7)

We note that ν and ω are independent of n, while k and λ change when the wave travels to media with different

Electromagnetic waves have some extraordinary properties that are derived in detail in Appendix A.3:

The electric and magnetic field vectors are perpendicular to each other and also perpendicular to thepropagation vector,

$$\mathbf{k} \cdot \mathbf{E}_0 = \mathbf{k} \cdot \mathbf{H}_0 = \mathbf{H}_0 \cdot \mathbf{E}_0 = 0. \quad \text{EQUATION (3.8)}$$

The electric and magnetic fields are proportional to the propagation direction, hence electromagnetic waves are transverse waves.

The electric and magnetic vectors have a constant, material dependent ratio. If the electric field isalong the x-direction and the magnetic field is along the y-direction, this ratio is given by

$$H_{y,0} = \frac{n}{c\mu_0} E_{x,0} = \frac{n}{Z_0} E_{x,0},$$

where

$$Z_0 = c\mu_0 = \sqrt{\frac{\mu_0}{\epsilon_0}} = 376.7\,\Omega$$

EQUATION (3.9)

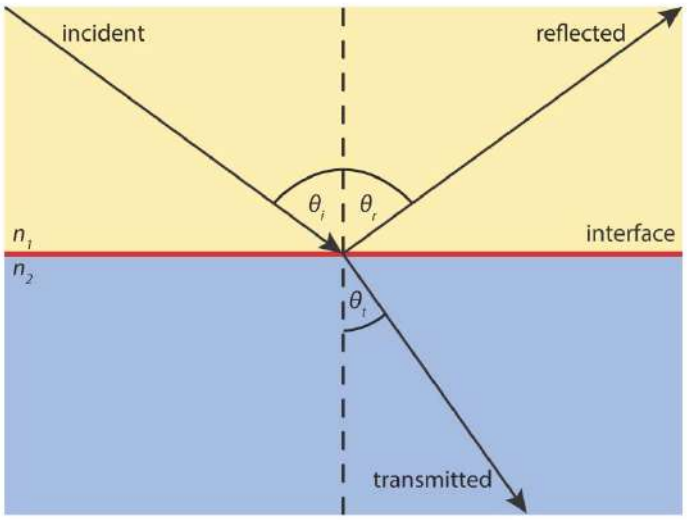



**Fig 3.1**Scheme of light, reflected and refracted by boundary.

A part of the incident light is reflected, where the angle of the scattered light θr is equal to the incident angle θi,

$$\theta_r = \theta_i.$$

The other part enters medium 2, where the angle of the refracted light θt is related to θi via Snell's law,

$$n_1 \sin\theta_i = n_2 \sin\theta_t,$$

Relations between the magnitudes of the incident, reflected and refracted fields are given by Fresnel eqt. We have to distinguish between parallel and perpendicular polarized light.

Parallel or perpendicular polarised means that the electric field is parallel or perpendicular to the plane, respectively. For perpendicular polarised light the Fresnel eqt are given by

$$t_s = \left(\frac{E_{0t}}{E_{0i}}\right)_s = \frac{2\,n_1 \cos\theta_i}{n_1 \cos\theta_i + n_2 \cos\theta_t},$$
$$r_s = \left(\frac{E_{0r}}{E_{0i}}\right)_s = \frac{n_1 \cos\theta_i - n_2 \cos\theta_t}{n_1 \cos\theta_i + n_2 \cos\theta_t},$$

EQUATION (3.10)

where the s stands for senkrecht, which is German for perpendicular. The relations for parallel polarized light are

$$t_p = \left(\frac{E_{0t}}{E_{0i}}\right)_p = \frac{2\,n_1 \cos\theta_i}{n_1 \cos\theta_t + n_2 \cos\theta_i},$$
$$r_p = \left(\frac{E_{0r}}{E_{0i}}\right)_p = \frac{n_1 \cos\theta_t - n_2 \cos\theta_i}{n_1 \cos\theta_t + n_2 \cos\theta_i}.$$

EQUATION (3.11)

The intensities are proportional to the square of the electric field, I ∝ E2 . For unpolarised light, we have to take the mean values of the two polarizations. For the reflectivity R we thus obtain

$$R = \frac{1}{2}\left(r_s^2 + r_p^2\right).$$

EQUATION (3.12)

For normal incidence this leads to

$$R(\theta_i = 0) = \left(\frac{n_1 - n_2}{n_1 + n_2}\right)^2.$$

EQUATION (3.13)

Because of conservation of energy the sum of R and the transmittance T must be 1,

$$R + T = 1.$$

EQUATION (3.14)

By combining Eqs. and doing some calculations we find

$$T = 1 - R = \frac{n_2 \cos\theta_t}{n_1 \cos\theta_i}\frac{1}{2}\left(t_s^2 + t_s^2\right),$$

EQUATION (3.15)

which leads to

$$T(\theta_i = 0) = \frac{4n_1 n_2}{(n_1 + n_2)^2}$$

EQUATION (3.16)

for normal incidence. A very important consequence of the Snell's law is total reflection. If n2 > n1, there is a critical angle at which no light can leave the layer with n2 anymore,

$$\sin\theta_{\text{crit}} = \frac{n_1}{n_2}.$$

EQUATION (3.17)

Hence if θ2 ≥ θcrit, no light will be transmitted, but everything will be reflected back into the layer. For a silicon-air interface (nSi ≈ 4.3), we find θcrit = 13.4◦ .

For the supporting layers used in solar cells, the critical angle is much larger. For a silicon-glass interface (nglass ≈ 1.5), we θcrit = 20.4 ◦ .

And for an interface between silicon and zinc oxide, which is a transparent conducting oxide often used in solar cell technology, (nZnO ≈ 2) the critical angle would be θcrit = 30.3◦

## III.3External solar cell parameters:

The main parameters that are used to characterizethe performance of solar cells are the peak power Pmax, the short-circuit current density Jsc, the open-circuit voltage Voc,

and the fill factor FF. These parameters are determined from the illuminated J-V characteristic as illustrated innext. The conversion efficiency η can be determined from these parameters.

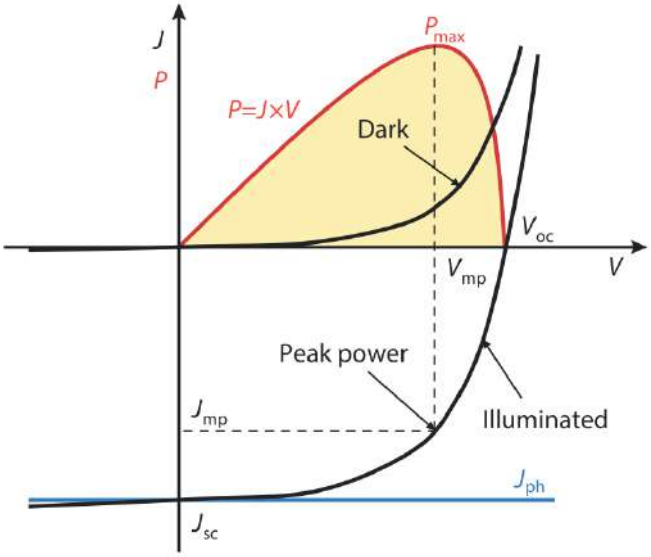



**Fig 3.2**J-V characteristics of a p-n junction in the dark and under illumination.

## III.4Short-circuit current density:

The short-circuit current Isc is the current that flows through the external circuit when the electrodes of the solar cell are short circuited. The short-circuit current of a solar cell depends on the photon flux density incident on the solar cell,

which is determined by the spectrum of the incident light. For a standard solar cell measurements, the spectrum is standardized to the AM1.5 spectrum. The Isc depends on the area of the solar cell. In order to remove the dependence of the solar cell area on Isc,

often the short-circuit current density is used to de- scribe the maximum current delivered by a solar cell. The maximum current that the solar cell can deliver strongly depends on the optical properties of the solar cell, such as absorption in the absorber layer and reflection.

In the ideal case, Jsc is equal to Jph as can be easily derived from Eq. (8.27). Jph can be approximated by Eq.(8.28), which shows that in case of an ideal diode (for example no surface recombination) and uniform generation,

the critical material parameters that determine Jph are the diffusion lengths of minority carriers. Crystalline silicon solar cells can deliver under an AM1.5 spectrum a maximum possible current density of 46 mA/cm² . In laboratory c-Si solar cells the measured Jsc is above 42 mA/cm² , while commercial solar cell have an Jsc exceeding 35 mA/cm² [22]

## III.5 Open-circuit voltage:

The open-circuit voltage is the voltage at which no current flows through the external circuit. It is the maximum voltage that a solar cell can deliver. Voc corresponds to the forward bias voltage, at which the dark current compensates the photocurrent. Voc depends on the photo-generated current density and can be calculated from Eq. assuming that the net current is zero,

$$V_{\mathrm{oc}} = \frac{kT}{e} \ln\left(\frac{J_{ph}}{J_0} + 1\right).$$

EQUATION (3.18)

This equation shows that Voc depends on the saturation current of the solar cell and the photo-generated current. While Jph typically has a small variation, the key effect is the saturation current, since this may vary by orders of magnitude. The saturation current density, J0, depends on the recombination in the solar cell.

Therefore, Voc is a measure of the amount of recombination in the device. Laboratory crystalline silicon solar cells have a Voc of up to 720 mV under the standard AM1.5 conditions, while commercial solar cells typically have Voc exceeding 600 mV.

## III.6 Fill Factor :

The fill factor is the ratio between the maximum power (Pmax = JmpVmp) generated by a solar cell and theproduct of Voc with Jsc

$$FF = \frac{J_{\mathrm{mp}} V_{\mathrm{mp}}}{J_{\mathrm{sc}} V_{oc}}.$$

EQUATION (3.19)

Assuming that the solar cell behaves as an ideal diode the fill factor can be expressed as a function of open-circuit voltage Voc

$$FF = \frac{v_{\mathrm{oc}} - \ln\left(v_{\mathrm{oc}} + 0.72\right)}{v_{\mathrm{oc}} + 1},$$

EQUATION (3.20)

where voc = Voc · e/(kT) is a normalised voltage. Eq. (9.3) is a good approximation of the ideal value of FF for voc > 10. The FF as a function of Voc is illustrated in Fig. 9.1. This figure shows that FF does not change

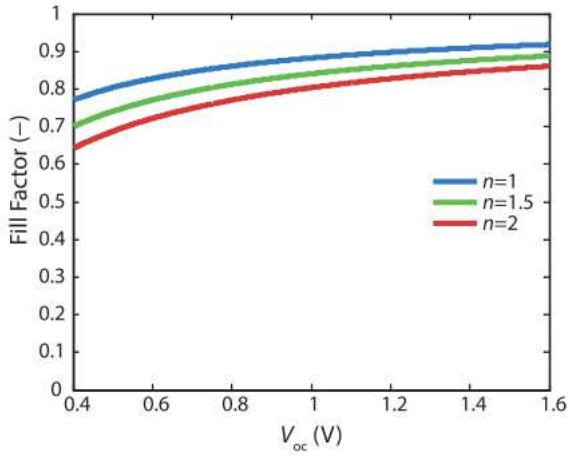



**Fig 3.3** The FF as a function of Voc for a solar cell with ideal diode behaviour.

drastically with a change in Voc. For a solar cell with a particular absorber, large variations in Voc are not common. For example, at standard illumination conditions, the difference between the maximum open-circuit voltage measured for a silicon laboratory device and a typical commercial solar cell is about 120 mV,

giving a maximal FF of 0.85 and 0.83, respectively. However, the variation in maximum FF can be significant for solar cells made from different materials. For example, a GaAs solar cell may have a FF approaching 0.89. However, in practical solar cells the dark diode current Eq. (8.23) does not obey the Boltzmann approximation. The non-ideal diode is approximated by introducing an ideality factor n, into the Boltzmann factor,

$$\exp \frac{eV_a}{nkT}.$$

also demonstrates the importance of the diode ideality factor when introduced into the normalized voltage in Eq. The ideality factor is a measure of the junction quality and the type of recombination in a solar cell. For the ideal junction where the recombination is represented by the recombination of the minority carriers in the quasi-neutral regions the n is equal to 1

. However, when other recombination mechanisms occur, the n can have a value of 2. A high n value not only lowers the FF, but since it signals a high recombination, it leads to a low Voc. Eq. 9.3) describes a maximum achievable FF. In practice the FF is often lower due to the presence of parasitic resistive losses.

## III.7 Conversion efficiency:

The conversion efficiency is calculated as the ratio between the maximal generated power and the incident power. The irradiance value Pin of 1000 W/m$^2$ for the AM1.5 spectrum has become a standard for Measuring the conversion efficiency of solar cells,

$$\eta = \frac{P_{\max}}{P_{in}} = \frac{J_{\mathrm{mp}}\, V_{\mathrm{mp}}}{P_{\mathrm{in}}} = \frac{J_{\mathrm{sc}}\, V_{\mathrm{oc}}\, FF}{P_{\mathrm{in}}}.$$

EQUATION (3.21)

Typical external parameters of a crystalline silicon solar cell as shown are; Jsc ≈ 35 mA/cm² , Voc up to 0.65 V and FF in the range 0.75 to 0.80. The conversion efficiency lies in the range of 17 to 18%.

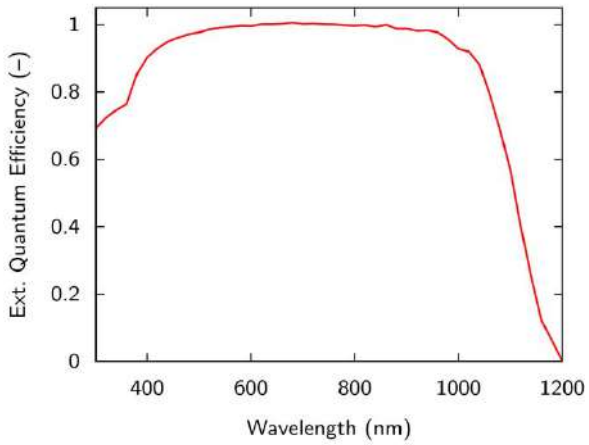



**Fig 3.4**The external quantum efficiency of a high-quality crystalline silicon based solar cell.

## III.8 The External Quantum efficiency:

The external quantum efficiency EQE(λ0) is the fraction of photons incident on the solar cell that create electron-hole pairs in the absorber, which are successfully collected. It is wavelength dependent and is usually measured by illuminating the solar cell with monochromatic light of wavelength λ0 and measuring the photocurrent Iph through the solar cell.

The external quantum efficiency is then determined as

$$\mathrm{EQE}(\lambda_0) = \frac{I_{\mathrm{ph}}(\lambda_0)}{e\,\Phi_{\mathrm{ph}}(\lambda_0)},$$

EQUATION (3.22)

where e is the elementary charge and Φ ph is the photon flux incident on the solar cell. Since Iph is dependent on the bias voltage, the bias voltage must be fixed. The photon flux is usually determined by measuring the EQE of a calibrated photodiode under the same light source.

Fig above illustrates a typical EQE for a high quality crystalline silicon based solar cell. We can identify the major optical loss mechanisms for such a solar cell: For short wavelengths only a small fraction of the light is converted into electron-hole pairs.

Most photons are already absorbed in the layers that the light traverses prior to the absorber layer. For long wavelengths, the penetration depth of the light exceeds the optical thickness of the absorber. Then the absorber itself becomes transparent so that most of the light leaves the solar cell before it can be absorbed. We can see that for this type of solar cells the EQE is close to 1 for a broad wavelength band. Hence,

in this band almost all absorbed photons are converted into electron-hole pairs that can leave the solar cell.

When a bias voltage of 0 V is applied, the measured photocurrent density equals the short circuit current density. When applying a sufficiently large reversed bias voltage, it can be assured that nearly all photo-

generated charge carriers in the intrinsic layer are collected. Thus, this measurement can be used to study the optical effectiveness of the design, i.e. light trapping and light absorption in inactive layers, such as the TCO layer, doped layers and the back reflector.

**Measuring the EQE**

EQE spectra are measured using an EQE-setup that also called spectral response setup. For this measurement, usually a wavelength selective light source, a calibrated light detector and a current meter are required. Usually, the used light sours is a xenon gas discharge lamp that as a very broad spectrum covering all the wavelengths important for the solar cell performance.

With the help of filters and monochromators a very narrow wavelength band of photon energies can be selected that then can be incident on the solar cell.

As already seen in Eq. (9.5), EQE(λ) is proportional to the the current divided by the photon flux. While the current can be easily determined using an Ampere meter, the photon flux must be determined indirectly.

This is done by performing a measurement with a calibrated photodetector (or solar cell), whose EQE is known. Via this measurement we find

$$\Phi_{\mathrm{ph}}(\lambda_0) = \frac{I_{\mathrm{ph}}^{\mathrm{ref}}(\lambda_0)}{e\,\mathrm{EQE}^{\mathrm{ref}}(\lambda_0)},$$ EQUATION (3.22)

By combining Eqs. we therefore find

$$\mathrm{EQE}(\lambda_0) = \mathrm{EQE}^{\mathrm{ref}}(\lambda_0)\frac{I_{\mathrm{ph}}(\lambda_0)}{I_{\mathrm{ph}}^{\mathrm{ref}}(\lambda_0)}.$$ EQUATION (3.23)

The EQE therefore can be determined by performing two current measurements. Of course it is very important that the light source is sufficiently stable during the whole measurement as we assume that the photon flux in the reference measurement and the actual measurement is unchanged.

If we perform the EQE measurement under short circuit conditions, the measurement can be used to determine the short circuit current density Jsc. Determining Jsc via the EQE has the advantage that it is independent of the spectral shape of the used light source, in contrast to determining the Jsc via an JV measurement. Secondly, on lab scale the real contact area of solar cells is not accurately determined during JV measurements.

When using shading masks, the EQE measurement is independent on the contact area. Hence, for accurately measuring the sort circuit current density, it is not sufficient to rely on JV measurements only, but EQE setups have to be used.

For determining Jsc we combine that the photon flux at a certain wavelength with the EQE at this wavelength, leading to the flow of electrons leaving the solar cell at this wavelength. Jsc then is obtained by integrating across all the relevant wavelength,

$$J_{sc} = -e \int_{\lambda_1}^{\lambda_2} \mathrm{EQE}(\lambda)\Phi_{\mathrm{AM1.5}}(\lambda)\,\mathrm{d}\lambda. \qquad \text{EQUATION (3.24)}$$

For crystalline silicon, the important range would be from 300 to 1200 nm.

## III.9 The Equivalent Circuit:

The J-V characteristic of an illuminated solar cell that behaves as the ideal diode is given by Eq

$$\begin{aligned} J(V_a) &= J_{\mathrm{rec}}(V_a) - J_{\mathrm{gen}}(V_a) - J_{\mathrm{ph}} \\ &= J_0\left[\exp\left(\frac{eV_a}{kT}\right) - 1\right] - J_{\mathrm{ph}}. \end{aligned} \qquad \text{EQUATION (3.25)}$$

This behavior can be described by a simple equivalent circuit, illustrated in Fig. 9.3 (a), in which a diode and a current source are connected in parallel. The diode is formed by a p-n junction. The first term in Eq.

above describes the dark diode current density while the second term describes the photo-generated current density. In practice the FF is influenced by a series resistance Rs, and a shunt resistance Rp. The influence of

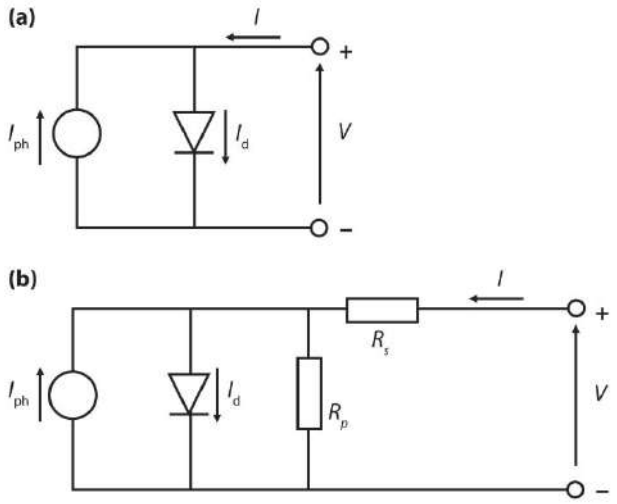



**Fig 3.5** The equivalent circuit of an (a) ideal solar cell and a (b) solar cell with a series resistance Rs and a shunt resistanceb Rp.

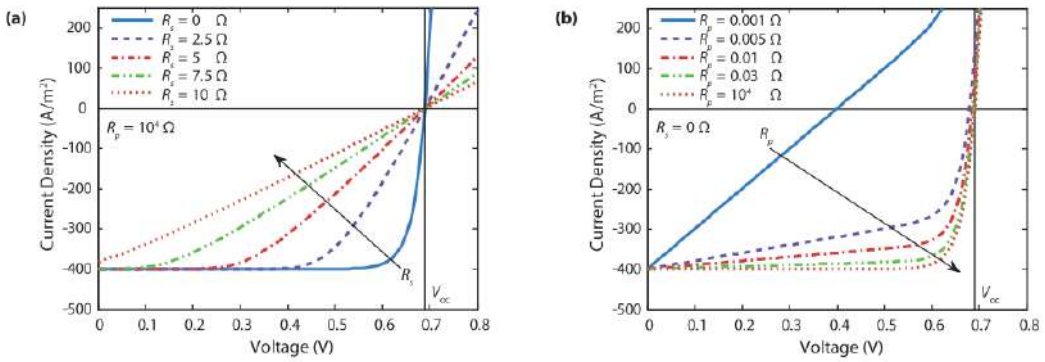



**Fig 3.6** Effect of the (a) series resistance and (b) parallel resistance on the J-V characteristic of a solar cell.

these parameters on the J-V characteristic of the solar cell can be studied using the equivalent circuit presented in Fig. 3.6 (b).

The J-V characteristic of the one diode equivalent circuit with the series resistance and the shunt resistance is given by

$$J = J_0 \left\{ \exp\left[\frac{e\,(V - AJR_s)}{kT}\right] - 1 \right\} + \frac{V - AJR_s}{R_p} - J_{\text{ph}}, \qquad \text{EQUATION (3.26)}$$

where A is the area of the solar cell. The effect of Rs and Rp on the J-V characteristic is illustrated in Fig. 9.4. In real solar cells the FF is influenced by additional re-combination occurring in the p-n junction. This non-ideal diode is often represented in the equivalent circuit by two diodes, an ideal one with an ideality factor equal to unity and a non-ideal diode with an ideality factor larger than one.[22]

The equivalent circuit of a real solar cell is presented in Fig. 3.5. The J-V characteristic of the two-diode equivalent circuit is given by

$$\begin{aligned} J = {} & J_{01}\left[\exp\left(\frac{e\,(V - AJR_s)}{n_1 kT}\right) - 1\right] \\ & + J_{02}\left[\exp\left(\frac{e\,(V - AJR_s)}{n_2 kT}\right) - 1\right] \\ & + \frac{V - AJR_s}{R_p} - J_{\text{ph}}, \end{aligned} \qquad \text{EQUATION (3.27)}$$

where J01 and J02 are the saturation currents of the two diodes, respectively. n1 and n2 are the ideality factors of the two diodes.

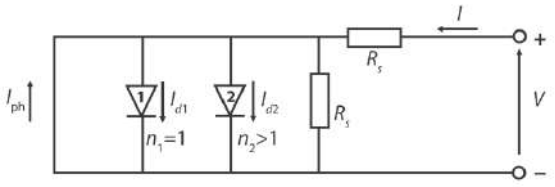



**Fig 3.7** The equivalent circuit of a solar cell based on the two-diode model.

**Conclusion**

In this chapter we saw the equivalent circuit of solar cell with diode parameter and some electrodynamic basics and electromagnetic waves

# Chapter IV

# PV System

## Introduction

After we have discussed the fundamental scientific theories required for solar cells in Part II and have taken a look at modern PV technology in Part III, we now will use the gained knowledge to discuss complete PV systems.

## IV.1External solar cell parameters:

A PV system contains many different components besides the PV modules. For successfully planning a PV system it is crucial to understand the function of the different components and to know their major specifications. Further, it is important to know the effect on the location of the (expected) performance of a PV system.

## IV.2 Types of PV systems:

PV systems can be very simple, consisting of just a PV module and load, as in the direct powering of a water pump motor, which only needs to operate when the sun shines. However, when for example a whole house should be powered, the system must be operational day and night. It also may have to feed both AC and DC loads, have reserve power and may even include a back-up generator. Depending on the system configuration,

we can distinguish three main types of PV systems: stand-alone, grid-connected, and hybrid. The basic PV system principles and elements remain the same. Systems are adapted to meet particular requirements by varying the type and quantity of the basic elements. A modular system design allows easy expansion, when power demands change. [14]

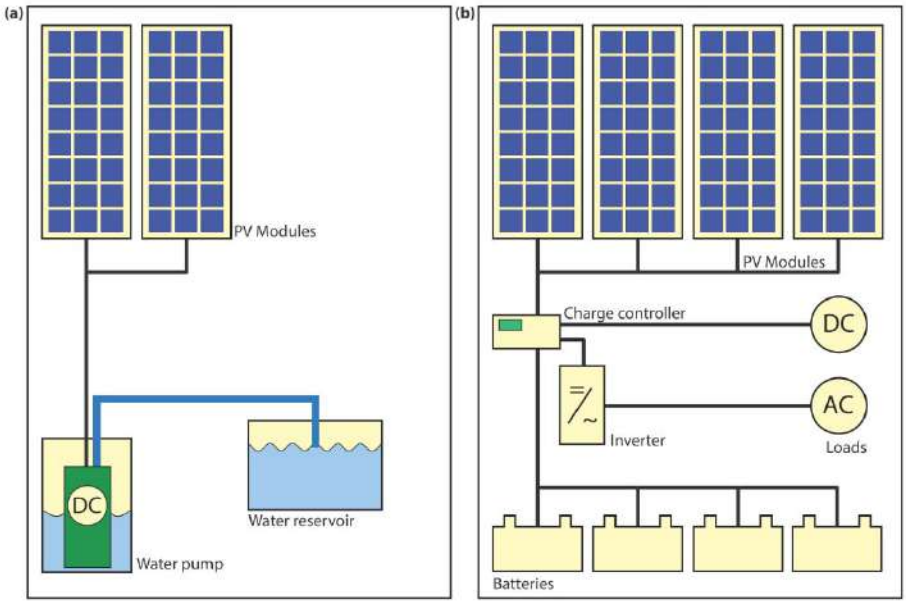



**Fig 4.1**Schematic representation of (a) a simple DC PV system to power a water pump with no energy storage and (b) a complex PV system including batteries, power conditioners, and both DC and AC loads.

## IV.2.1 Stand-alone systems:

Stand-alone systems rely on solar power only. These systems can consist of the PV modules and a load only or they can include batteries for energy storage. When using batteries charge regulators are included, which switch off the PV modules when batteries are fully charged, and may switch off the load to prevent the batteries from being discharged below a certain limit.

The batteries must have enough capacity to store the energy produced during the day to be used at night and during periods of poor weather. Fig4.1 shows schematically examples of stand-alone systems; (a) a simple DC PV system without a battery and (b) a large PV system with both DC and AC loads.

## IV.2.2 Grid-connected systems:

Grid-connected PV systems have become increasingly popular for building integrated applications. As illustrated in Fig. 4.2, they are connected to the grid via inverters, which convert the DC power into AC electricity. In small systems as they are installed in residential homes, the inverter is connected to the distribution board, from where the PV-generated power is transferred into the electricity grid or to AC appliances in the house.

These systems do not require batteries, since they are connected to the grid, which acts as a buffer into that an oversupply of PV electricity is transported while the grid also supplies the house with electricity in times of insufficient PV power generation. Large PV fields act as power stations from that all the generated PV electricity is directly transported to the electricity grid. They can reach peak powers of up to several hundreds of MWp. Fig4.3 shows a 25.7 MWp system installed in Germany.

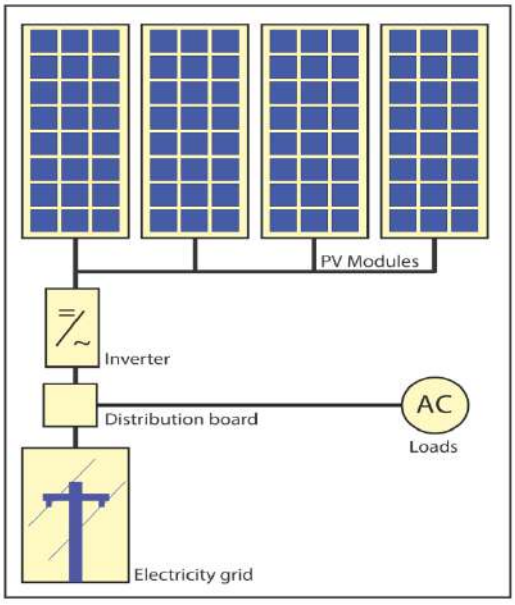



**Fig 4.2**Schematic representation of a grid-connected PV system

## IV.2.3 Hybrid systems:

Hybrid systems consist of combination of PV modules and a complementary method of electricity generation such as a diesel, gas or wind generator. A schematic of a hybrid system shown in Fig. 4.4. In order to optimize the different methods of electricity generation, hybrid systems typically require more sophisticated controls than stand-alone or grid-connected PV systems. For example,

in the case of an PV/diesel system, the diesel engine must be started when the battery reaches a given discharge level and stopped again when battery reaches an adequate state of charge. The back-up generator can be used to recharge batteries only or to supply the load as well.



**Fig 4.3**The 25.7 MWp Lauingen Energy Park in Bavarian Swabia, Germany

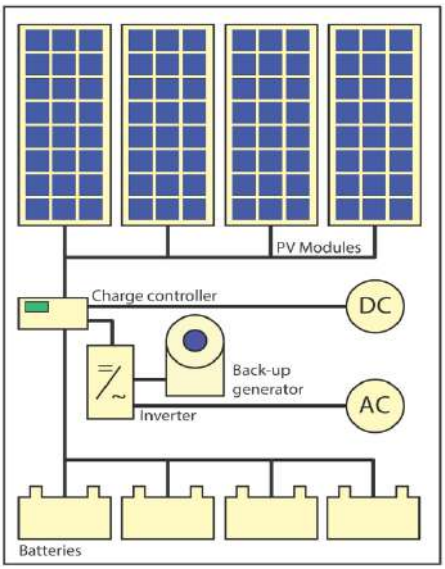



**Fig 4.4**Schematic representation of a hybrid PV system that has a diesel generator as alternative electricity source.

## IV.3 Components of a PV system:

As we have seen earlier in this book, a solar cell can convert the energy contained in the solar radiation into electrical energy. Due to the limited size of the solar cell it only delivers a limited amount of power under fixed current-voltage conditions that are not practical for most applications. In order to use solar electricity for practical devices, which require a particular voltage and/or current for their operation, a number of solar cells have to be connected together to form a solar panel, also called a PV module. For large-scale generation of solar electricity solar panels are connected together into a solar array.

Although, the solar panels are the heart of a PV system, many other components are required for a working system, that we already discussed very briefly above. Together, these components are called the Balance of System (BOS). Which components are required depends on whether the system is connected to the electricity grid or whether it is designed as a stand-alone system. The most important components belonging to the BOS are:

A mounting structure is used to fix the modules and to direct them towards the sun.Energy storage is a vital part of stand-alone systems because it assures that the system can deliver electricity during the night and in periods of bad weather. Usually, batteries are used as energy storage units.

DC-DC converters are used to convert the module output, which will have a variable voltage depending on the time of the day and the weather conditions, to a fixed voltage output that e. g. can beused to charge a battery or that is used as input foran inverter in a grid-connected system.

Inverters or DC-AC converters are used in grid-connected systems to convert the DC electricity originating from the PV modules into AC electricity that can be fed into the electricity grid.

Cables are used to connect the different components of the PV system with each other and to the electrical load. It is important to choose cables of sufficient thickness in order to minimize resistive losses.

Even though not a part of the PV system itself, the electric load, i.e. all the electric appliances that are connected to it have to be taken into account during the planning phase. Further, it has to be considered whether the loads are AC or DC loads.

The different components of a PV system are schematically presented in Fig below and will be discussed in detail in coming

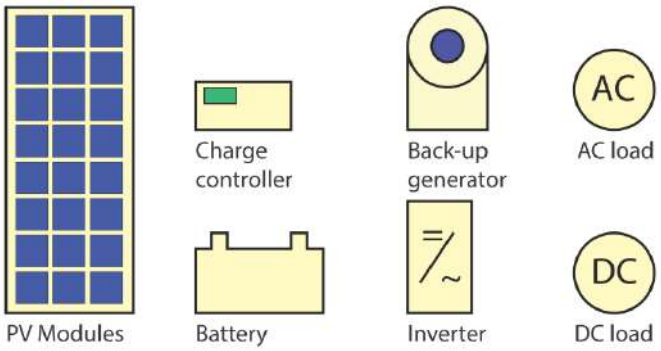



**Fig 4.5**A schematic of the different components of a PV system.

## IV.3.1 PV modules :

In this section we will discuss PV modules (or solar modules), their fabrication and how to to determine their performance.Before we start with the actual treatment of PV modules, we briefly want to introduce different terms (a) shows a crystalline solar cell, which we discussed before . For the moment we will consideronly modules that are made from this type of solarcells.

A PV module, is a larger device in which manysolar cells are connected, as illustrated in The names PV module and solar module are often usedinterchangeably. A solar panel, as illustrated in Fig. coming in c), consists of several PV modules that are electrically connected and mounted on a supporting structure.

Finally, a PV array consists of several solar panels. An example of such an array is shown in Fig. 4.6 (d). This array consists of two strings of two solar panels each, where string means that these panels are connected in series.

## IV.3.2 Monocrystalline, Polycrystalline, Amorphous PV Panels :

When approaching the photovoltaic domain, it is fundamental to have a basic knowledge about different types of solar panels and their differences. The choice among different modules should be based not only on cost but also on space and efficiency issues.

we are going to understand which are the features and the consequent advantages and disadvantages of monocrystalline, polycrystalline and amorphous solar panels.

Monocrystalline and polycrystalline panels differ in the cells used for their production. The formers use monocrystalline cells, characterized by black color and beveled angles. They are made of monocrystalline silicon. This material is composed of aligned crystals that better absorb light when sunbeams are perpendicular to the cell. They have an average efficiency of 18-22% and they ensure the highest power output compared to other panels thus requiring the least amount of space.

However, they have scarcer performances in low-light conditions. For this reason, they are not suitable for shaded areas or for diffused light situations. On the contrary they are recommended if exposed to direct light. Furthermore, due to the high costs involved in production these panels are more expensive.

On the contrary, polycrystalline cells are made of polycrystalline silicon that is composed of non-aligned crystals. These crystals can produce energy even with low or diffused light ensuring a more constant output production during the day. Polycrystalline cells are characterized by a slightly inferior efficiency (about 14-16%) compared to monocrystalline cells. Nonetheless,

they can reach the same levels of output of monocrystalline cells because they can produce more constantly. However, these cells are bigger and thus they require wider surfaces to produce the same amount of energy compared to monocrystalline cells.

Amorphous panels can be composed of a minimum of 30 to a maximum of 70 square cells positioned under a blue or gray sheet of glass for a total thickness of few millimeters. They are characterized by a uniform appearance and great flexibility and lightness. They are the cheapest panels but they are less efficient than mono- and polycrystalline panels (efficiency of 6-8%) and they require twice the amount of surface. On the other hand,

amorphous silicon absorbs light differently and assures a better power output compared to crystalline silicon because it produces energy even in low-light conditions. These features make amorphous panels suitable for architectural structures that do not require as much high power output, but rather a good aesthetic appearance.

The following table shortly summarizes the most relevant features of the different photovoltaic modules:

| MONOCRYSTALLINE PANELS | POLYCRISTALLINE PANELS | AMORPHOUS PANELS |
|---|---|---|
| ▪ High efficiency (18-22%)<br>▪ Space-effective<br>▪ Higher power output with direct light<br>▪ Uniform appearance<br>▪ Highest price | ▪ Lower efficiency (14-16%)<br>▪ Wider surface required for same power output<br>▪ Constant Energy production, even with low light<br>▪ Non-uniform appearance<br>▪ Lower price compared to monocrystalline | ▪ Lower efficiency (6-8%)<br>▪ Twice amount of surface for same power output<br>▪ Constant Energy production, even with diffused light<br>▪ Uniform appearance<br>▪ Thin structure (3mm)<br>▪ Lowest price |

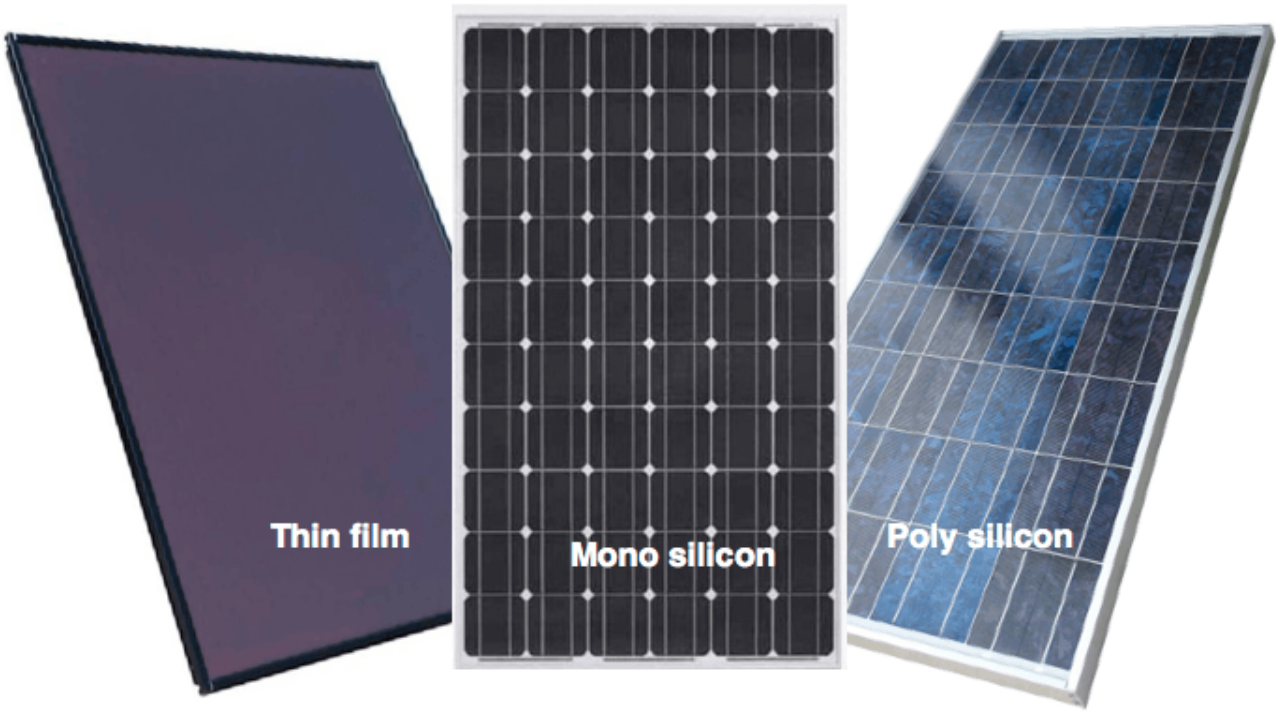



**Fig 4.6** Different types of Panels [16]

## IV.3.3 Series and parallel connections in PV modules:

If we make a solar module out of an ensemble of solar cells, we can connect the solar cells in different ways: first, we can connect them in a series connection as shown in Fig. Upcoming In a series connection the voltages add up. For example,

if the open circuit voltage of one cell is equal to 0.6 V, a string of three cells will deliver an open circuit voltage of 1.8 V. For solar cells with a classical front metal grid, a series connection can be established by connecting the bus bars at the front side with the back contact of the neighbouring cell,

as illustrated in Fig upcoming. For series connected cells, the current does not add up but is determined by the photocurrent in each solar cell. Hence, the total current in a string of solar cells is equal to the current generated by one single solar cell.

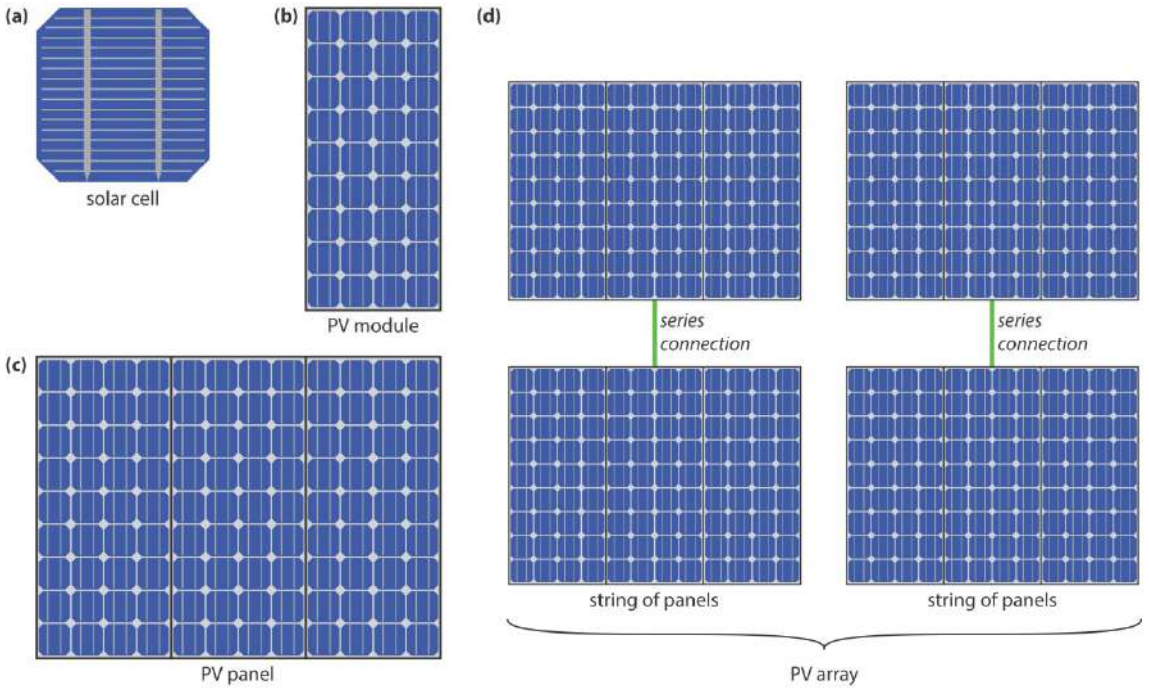



**Fig 4.7** Illustrating (a) a solar cell, (b) a PV module, (c) a solar panel, and (d) a PV array.

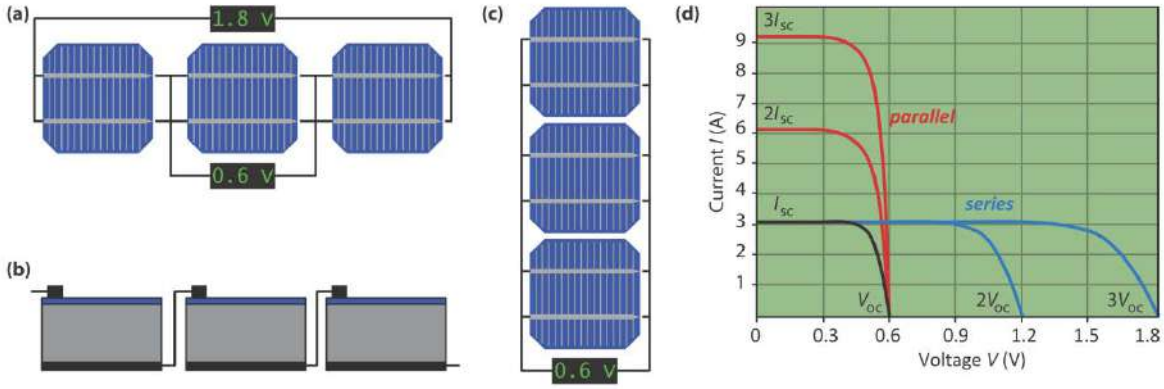



**Fig 4.8** Illustrating (a) a series connection of three solar cells and (b) realisation of such a series connection for cells with a classical front metal grid. (c) Illustrating a parallel connection of three solar cells. (d) I-V curves of solar cells connected in series and parallel

Fig.b above shows the I-V curve of solar cells connected in series. If we connect two solar cells in series, the voltages add up while the current stays the same. The resulting open circuit voltage is two times that of the single cell. If we connect three solar cells in series, the open circuit voltage becomes three times as large, whereas the current still is that of one single solar cell.[18]

Secondly, we can connect solar cells in parallel as illustrated in Fig. (c), which shows three solar cells connected in parallel. If cells are connected in parallel, the voltage is the same over all solar cells, while the currents of the solar cells add up. If we connect

e.g. three cells in parallel, the current becomes three times as large, while the voltage is the same as for a single cell, as illustrated in Fig. (d).

The reader may have noticed that we used I-V curves, i.e. the current-voltage characteristics, in the previous paragraphs. This is different to Parts II and III, where we used I-V curves instead, i.e. the current density - voltage characteristics. The reason for this switch from J to I is that on module level,

the total current that the module can generate is of higher interest than the current density. As the area of a module is a constant, the shapes of the I-V and J-V curves of a module are similar.

For a total module, therefore the voltage and current output can be partially tuned via the arrangements of the solar cell connections. Fig4.8 (a) shows a typical PV module that contains 36 solar cells connected in series. If a single junction solar cell would have a short circuit current of 5 A, and an open circuit voltage of 0.6 V,

the total module would have an output of Voc = 36 · 0.6 V = 21.6 V and Isc = 5 A. However, if two strings of 18 series-connected cells are connected in parallel, as illustrated in Fig. 4.8 (b), the output of the module will be Voc = 18 · 0.6 V = 10.8 V and Isc = 2 × 5 A = 10 A. In general, for the I-V characteristics of a module consisting of m identical cells in series and n identical cells in parallel the voltage multiplies by a factor m while the current multiplies by a factor n. Modern PV modules often contain 60 (10 × 6), 72 (9 × 8) or 96 (12 × 8) solar cells that are usually all connected in series in order to minimize resistive losses.

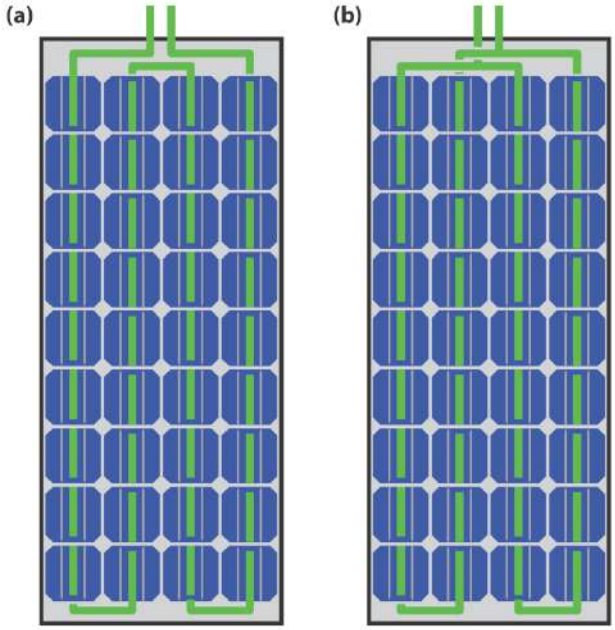



**Fig 4.9** Illustrating a PV module consisting (a) of a string of 36 solar cells connected in series and (b) of two strings of 18 solar cells each that are connected in parallel.

In a nutshell, for a PV module a set of parameters can be defined, similar than for solar cells. The most common parameters are the open circuit voltage Voc, the short circuit current Isc and the module fill factor FFM. On module level, we have to distinguish between the aperture area efficiency and the module efficiency.

The aperture area is defined as the area of the PV-active parts only. The total module area is given as the aperture area plus the dead area consisting of the interconnections and the edges of the module. Clearly, the aperture area efficiency is larger than the module efficiency.

Determining the the efficiency and the fill factor of a PV module is less straight-forward than determining voltage and current. In an ideal world with perfectly matched solar cells and no losses, one would expect that the efficiency and fill factor at both the module and cell levels to be the same. This is not the case in real life.

As mentioned above. The cells are connected with each other using interconnects that induce resistive losses. Further, there might be small mismatches in the interconnected cells. For example, if m × n cells are interconnected, the cell with the lowest current in a string of m cells in series determines the module current.

Similarly, the string with the lowest voltage in the n strings that are connected in parallel dictates the module voltage. The reason for mismatch between individual cells are in homogeneities that occur during

the production process. Hence, in practice PV module perform a little less than what one would expect from ideally matched and interconnected solar cells. This loss in performance translates to a lower fill factor and efficiency at module level. If the illumination across the module is not constant or if the module is heats up non-uniformly, the module performance reduces even further.

Often, differences between cell and module performance are mentioned in datasheets that are provide by the module manufacturers. For example, the datasheet of a Sanyo HIT-N240SE10 module gives a cell level efficiency of 21.6%, but a module level efficiency of only 19%. Despite all the technological advancements being made at solar cell level for improving the efficiency, still a lot must be done at the PV systems level to ensure a healthy PV yield. For the performance of a PV system, not only the module performance is important, but also the yield of the PV system.

## IV.3.4 Partial shading and bypass diodes:

PV modules have so-called bypass diodes integrated. To understand the reason for using such diodes, we have to consider modules in real-life conditions, where they can be partially shaded, as illustrated in Fig. 4.9 (a). The shade can be from an object nearby, like a tree, a chimney or a neighbouring building. It also can be caused by a leaf that has fallen from a tree. Partial shading can have significant consequences for the output of the solar module. To understand this,

we consider the situation in which one solar cell in the module shaded for a large part shaded. For simplicity, we assume that all six cells are connected in series. This means that the current generated in the shaded cell is significantly reduced. In a series connection the current is limited by the cell that generates the lowest current, this cell thus dictates the maximum current flowing through the module.

In Fig. 4.9 (b) the theoretical I-V curve of the five unshaded solar cells and the shaded solar cell is shown. If the cells are connected to a constant load R, the voltage across the module is dropping due to the lower current generated. However, since the five unshaded solar cells are forced to produce high voltages, they act like a reverse bias source on the shaded solar cell. The dashed line in Fig. (b) represents the reverse bias load put on the shaded cell, which is the I-V curve of the five cells,

reflected across the vertical axis equal to 0 V. Hence, the shaded solar cell does not generate energy, but starts to dissipate energy and heats up. The temperature can increase to such a critical level, that the encapsulation material cracks, or other materials wear out. Further, high temperatures generally lead to a decrease of the PV output as well.

These problems occurring from partial shading can be

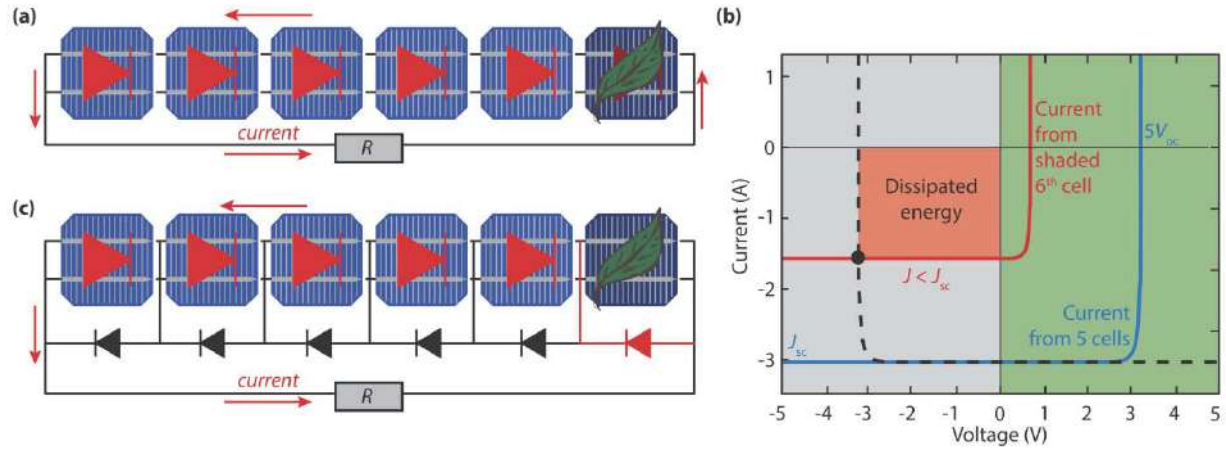



**Fig 4.10** Illustrating (a) string of six solar cells of which one is partially shaded, which (b) has dramatic effects on the I-V curve of this string. (c) Bypass diodes can solve the problem of partial shading.

prevented by including bypass diodes in the module, as illustrated in .4.10 (c). As discussed in previous a diode blocks the current when it is under negative voltage, but conducts a current when it is under positive voltage. If no cell is shaded, no current is flowing through the bypass diodes. However, if one cell is (partially) shaded, the bypass diode starts to pass current through because of the biasing from the other cells. As a result current can flow around the shaded cell and the module can still produce the current equal to that of a unshaded single solar cell.

For cells that are connected in parallel, partial shading is less of a problem, because the currents generated in the others cells do not need to travel through the shaded cell. However, a module consisting of 36 cells in parallel have very high currents (above 100 A) combined with a very low voltage (approx. 0.6 V). This combination would lead to very high resistive losses in the cables; further an inverter that has only 0.6 V as input will not be very efficient, as we will see in Section Therefore, combining the cells in series and using bypass diodes is much better an option to do.

## IV.3.5 Lifetime testing of PV Modules:

The typical lifetime of PV systems is about 25 years. In these as little maintenance as possible should be required on the system components, especially the PV modules are required to be maintenance free. Further- more, degradation in the different components of that

the module is made should be little: manufacturers typically guarantee a power between 80% and 90% of the initial power after 25 years. During the lifetime of 25 years or more, PV modules are exposed to various external stress from various sources

• temperature changes between night and day as well as between winter and summer,

• mechanical stress for example from wind, snow and hail,

• stress by agents transported via the atmosphere such as dust, sand, salty mist and other agents,

• moisture originating from rain, dew and frost,

• humidity originating from the atmosphere,

• irradiance consisting of direct and indirect irradiance from the sun; mainly the highly-energetic UV radiation is challenging for many materials.

Before PV modules are brought to the market, they are usually tested extensively in order to assure their stability against these various stresses. The required tests are extensively defined in the standards IEC 61215 for modules based on crystalline silicon solar cells and in IEC 61646 for thin-film modules.

Since the modules cannot be tested during a period of 25 years, accelerated stress testing must be performed. The required tests are [91]:

•Thermal cycles for studying whether thermal stress leads to broken interconnects, broken cells, electrical bond failure, adhesion of the junction box, . . .

•Humidity freeze testing in order to test delamination, adhesion of the junction box, . . .

• UV testing, because UV light can lead to delamination, loss of adhesion and elasticity of the encapsulate, ground fault due to back sheet degradation. Mainly, UV light can lead to a

discoloration of the encapsulant and back sheet, which means that they get yellow. This can lead to losses in the amount of light that reaches the solar cells.

• Static mechanical loads in order to test whether strong winds or heavy snow loads lead to structural failures, broken glass, broken interconnect ribbons or broken cells.

• Dynamic mechanical load, which can lead to rokenglass, broken interconnect ribbons or broken cells.

• Hot spot testing in order to see whether hot spotsdue to shunts in cells or inadequate bypass diodeprotection are present.

• Hail testing to see whether the module can handlethe mechanical stress induced by hail.

• Bypass diode thermal testing to study whether over-heating of these diodes causes degradation of the encapsulant, backsheet or the junction box.

• Salt spray testing to see whether salt that is present in salty mist or that is used in salty water for snow and ice removal leads to corrosion of PV module components.

How these tests are to be performed is defined in other standards, for example IEC 61345 for UV testing and IV 61701 for salt-mist corrosion testing Usually these tests are carried out by organisations like TÜV Rhein-land. Refining the test requirements and understanding which accelerated tests are required to guarantee a lifetime of 25 years and more is subject to ongoing research and development.

## IV.3.6 Maximum power point tracking:

In this section we discuss the concept of Maximum power point tracking (MPPT). This concept is very unique to the field of PV Systems, and hence brings a very special application of power electronics to the field of photovoltaics. The concepts discussed in this section are equally valid for cells, modules, and arrays, although MPPT usually is employed at PV module/array level.

As discussed earlier, the behaviour of an illuminated solar cell can be characterised by an I-V curve. Inter-connecting several solar cells in series or in parallel merely increases the overall voltage and/or current, but does not change the shape of the I-V curve. Therefore, for understanding the concept of MPPT,

it is sufficient to consider the I-V curve of a solar cell. The I-V curve is dependent on the module temperature on the irradiance, For example, an increasing irradiance leads to an increased current and slightly increased voltage, as illustrated in Fig. above.

The same figure shows that an increasing temperature has a detrimental effect on the voltage.

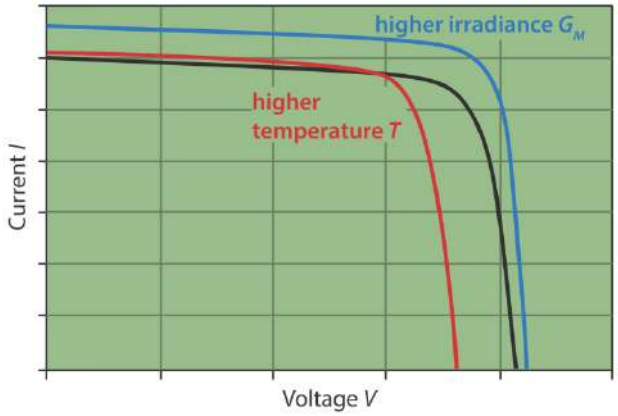



**Fig 4.11** Effect of increased temperature T or irradiance GM on the I-V curve.

does not change the shape of the I-V curve. Therefore, for understnding the concept of MPPT, it is sufficient to consider the I-V curve of a solar cell. The I-V curve is dependent on the module temperature on the irradiance, as we will discuss in detail in coming . For example, an increasing irradiance leads to an increased current and slightly increased voltage, as illustrated in Fig above. The same figure shows that an increasing temperature has a detrimental effect on the voltage.

Now we take a look at the concept of the operating point, which is the defined as the particular voltage and current, at that the PV module operates at any given point in time. For a given irradiance and temperature, the operating point corresponds to a unique (I, V) pair which lies onto the I-V curve. The power output at this operating point is given by

$$P = I \cdot V. \quad \text{EQUATION (4.1)}$$

The operating point (I, V) corresponds to a point on the power-voltage (P-V) curve, shown in Fig coming . For generating the highest power output at a given irradiance and temperature, the operating point should such correspond to the maximum of the (P-V) curve, which is called the maximum power point (MPP).

If a PV module (or array) is directly connected to an electrical load, the operating point is dictated by that load. For getting the maximal power out of the module, it thus is imperative to force the module to operate at the maximum power point. The simplest way of forcing the module to operate at the MPP,

is either to force the voltage of the PV module to be that at the MPP (called Vmpp) or to regulate the current to be that of the MPP (called Impp). However, the MPP is dependent on the ambient conditions.

If the irradiance or temperature change, the I-V and the P-V characteristics will change as well and hence the position of the MPP will shift. Therefore, changes in the I-V curve have to be tracked continuously such that the operating point can be adjusted to

be at the MPP after changes of the ambient conditions. This process is called Maximum Power Point Tracking or MPPT. The devices that perform this process are called MPP trackers. We can distinguish between two categories of MPP tracking:

• Indirect MPP tracking, for example performed with the Fractional Open Circuit Voltage method.

• Direct MPP tracking, for example performed with the Perturb and Observe method or the Incremental Conductance method. All the MPPT algorithms that we discuss in this section are based on finding the and tuning the voltage until VMPP is found. Other algorithms, which are not discussed in this section, work with the power instead and aim to find IMPP.

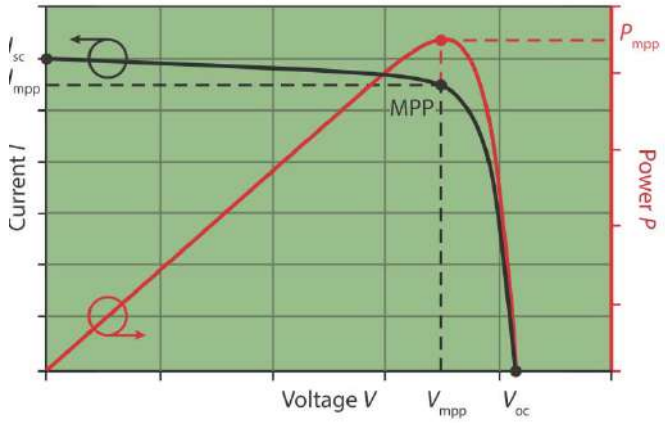



**Fig 4.12** A generic I-V curve and the associated P-V curve. The maximum power point (MPP) is indicated.

## IV.3.7 Indirect MPPT:

First, we discuss indirect MPP Tracking, where simple assumptions are made for estimating the MPP based on a few measurements.

## IV.3.7.1.Fixed voltage method:

For example, in the fixed voltage method (also called constant voltage method), the operating voltage of the solar module is adjusted only on a seasonal basis. This model is based on the assumption that for the same level of irradiance higher MPP voltages are expected during winter than during summer.

It is obvious that this method is not very accurate. It works best at locations with minimal irradiance fluctuations between different days.

**Fractional open circuit voltage method**

One of the most common indirect MPPT techniques is the fractional open circuit voltage method. This method exploits the fact that – in a very good approximation –the Vmpp is given by

$$Vmpp = k \cdot Voc, \quad \text{EQUATION (4.2)}$$

where k is a constant. For crystalline silicon, k usually takes values in between 0.7 and 0.8. In general, k of course is dependent on the type of solar cells. As changes in the open circuit voltage can be easily tracked, changes in the Vmpp can be easily estimated just by multiplying with k. This method thus can be implemented easily. However, there are also certain draw-backs. First, using a constant factor k only allows to roughly estimate the position of the MPP.

Therefore, the operating point usually will not be exactly on the MPP but in its proximity, with is called the MPP region. Secondly, every time the system needs to respond to a change in illumination conditions, the Voc must be measured. For this measurement, the PV module needs to be disconnected from the load for a short while,

which will lead to a reduced total output of the PV system. The more often the Voc is determined, the larger the loss in output will be. This drawback can be overcome my slightly modifying the method. For this modification a pilot PV cell is required,

which is highly matched with the rest of the cells in the module. The pilot cell receives the same irradiance as the rest of the PV module, and a measurement of the pilot PV cell's Voc also gives an accurate representation of that of the PV module, hence it can be used for estimating Vmpp. Therefore, the operating point of the module can be adjusted without needing to disconnect the PV module.

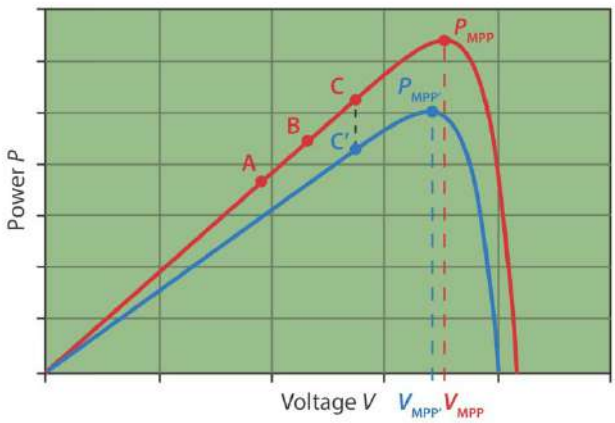



**Fig 4.13** The perturb&observe algorithm struggles from rapidly changing illumination conditions.

| Prior Perturbation | Change in Power | Next Perturbation |
|---|---|---|
| Positive | Positive | Positive |
| Positive | Negative | Negative |
| Negative | Positive | Negative |
| Negative | Negative | Positive |

**Fig 4.14** A summary of the possible options in the P&O algorithm.

## IV.3.7.2.Direct MPPT:

Now we discuss direct MPP tracking, which is more involved than indirect MPPT, because current, voltage or power measurements are required. Further, the system must response more accurately and faster than in indirect MPPT. We shall look at a couple of the most popular kind of algorithms.

**Perturb and observe (P&O) algorithm**

The first algorithm that we discuss is the Perturb and Observe (P&O) algorithm, which also is known as "hill climbing" algorithm. In this algorithm, a perturbation is provided to the voltage at that the module is currently driven.

This perturbation in voltage will lead to a change in the power output. If an increasing voltage leads to an increasing in power, the operating point is at a lower voltage than the MPP, and hence further voltage perturbation towards higher voltages is required to reach the MPP. In contrast,

if an increasing voltage leads to a decreasing power, further perturbation towards lower voltages is required in order to reach the MPP. Hence, the algorithm will converge towards the MPP over several perturbations. This principle is summarized in Table above

A problem with this algorithm is that the operating point is never steady at the MPP but meandering around the MPP. If very small perturbation steps are used around the MPP, this meandering, however, can be minimized.

Additionally, the P&O algorithm struggles from rapidly changing illuminations. For example, if the illumination (and hence the irradiance) changes in between two sampling instants in the process of convergence, then the algorithm essentially fails in its convergence efforts, as illustrated in Fig. 4.13 In the latest perturbation, the algorithm has determined that the MPP lies to the at a higher voltage than of point B, and hence the next step is a perturbation to converge towards the MPP accordingly.

If the illumination was constant, it would end up at C and the algorithm would conclude that the MPP is at still higher voltages, which is correct. However, as the illumination changes rapidly before the next perturbation, the next perturbation shifts the operating point to C’ instead to C, such that

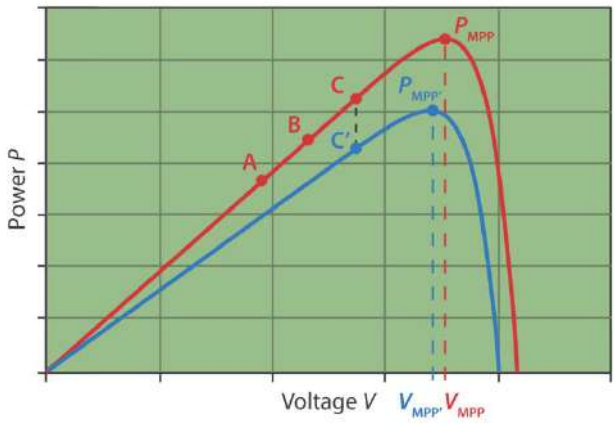



**Fig 4.15** The perturb observe algorithm

The perturb&observe algorithm struggles from rapidly changing illumination conditions. ing point is never steady at the MPP but meandering around the MPP. If very small perturbation steps are used around the MPP, this meandering, however, can be minimized. Additionally, the P&O algorithm struggles from rapidly changing illuminations.

For example, if the illumination (and hence the irradiance) changes in between two sampling instants in the process of convergence, then the algorithm essentially fails in its convergence efforts, as illustrated in Fig. above In the latest perturbation, the algorithm has determined that the MPP lies to the at a higher voltage than of point B, and hence the next step is a perturbation to converge towards the MPP accordingly.

If the illumination was constant, it would end up at C and the algorithm would conclude that the MPP is at still higher voltages, which is correct. However, as the illumination changes rapidly before the next perturbation, the next perturbation shifts the operating point to C' instead to C, such that PC'< PB

While the MPP still lies to the right of C', the P&O algorithm thinks that it is on the left of C'.

This wrong assumption is detrimental to the speed of convergence of the P&O algorithm, which is one of the critical figures of merit for MPPT techniques. Thus, drastic changes in weather conditions severely affect the efficacy of the P&O algorithm's.

**Incremental conductance method**

Next, we look at the Incremental Conductance Method. The conductance G1 of an electrical component is

defined as

$$G = I / V \quad \text{EQUATION (4.3)}$$

At the MPP, the slope of the P-V curve is zero, hence

$$dP / dV = 0$$

We can write

$$\frac{dP}{dV} = \frac{d(IV)}{dV} = I + V\frac{dI}{dV}. \quad \text{EQUATION (4.4)}$$

If the sampling steps are small enough, the approximation

$$\frac{dI}{dV} \approx \frac{\Delta I}{\Delta V}$$

can be used. We call ΔI/ΔV the incremental conductance and I/V the coinstantaneous conductance. Hence, we have

$$\begin{aligned} \frac{\Delta I}{\Delta V} &= -\frac{I}{V} && \text{if} && V = V_{\text{mpp}}, \\ \frac{\Delta I}{\Delta V} &> -\frac{I}{V} && \text{if} && V < V_{\text{mpp}}, \\ \frac{\Delta I}{\Delta V} &< -\frac{I}{V} && \text{if} && V > V_{\text{mpp}}. \end{aligned}$$

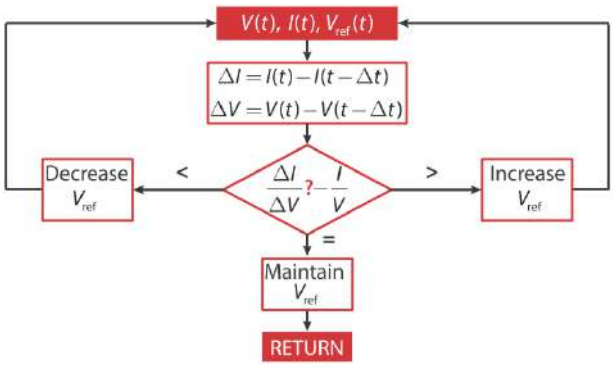



**Fig 4.16** A conceptual flowchart of the incremental conductance algorithm.

These relationships are exploited by the incremental conductance algorithm.

Fig above shows a conceptual flowchart. Note that this flowchart is not exhaustive. While both, the instantaneous voltage and current are the observable parameters, the instantaneous voltage is also the controllabl parameter. Vref is the voltage value forced on the PV module by the MPPT device.

It is the latest approximation of the Vmpp. For any change of the operating point, the algorithm compares the instantaneous with the incremental conductance values. If the incremental conductance is larger than the negative of the instantaneous conductance, the current operating point is to the left of the MPP; consequently, Vref must be incremented. In contrast, if the incremental conductance is lower than the negative of the instantaneous conductance, the current operating point is to the left of the MPP and the is consequently decremented.

This process is iterated until the incremental conductance is the same as the negative instantaneous conductance, in which case Vref= Vmpp.

The incremental conductance algorithm can be more efficient than the P&O algorithm as it does not meander around the MPP under steady state conditions. Further, small sampling intervals make it less susceptible to changing illumination conditions. However, under conditions that are strongly varying and under partial shading, the incremental conductance method might also become less efficient.

The major drawback of this algorithm is the complexity of its hardware implementation. Not only currents and voltages must be measured, but also the instantaneous and incremental conductance's must be calculated and compared.

**IV.3.7.2.1.Photovoltaic Converters:**

A core technology associated with PV systems is the power electronic converter. An ideal PV converter should draw the maximum power from the PV panel and supply it to the load side. In case of grid connected systems, this should be done with the minimum harmonic content in the current and at a power factor close to unity. For stand-alone systems the output voltage should also be regulated to the desired value.

In this section a short review of different topologies often associated with PV systems is given. The semiconductor switches in the following are assumed to be ideal.

## IV.3.7.3.System configurations:

Before digging into details about different converter topologies used for power conversion in PV systems, a general overview of different system architecture will be presented. The system architecture determines how PV modules are interconnected and how the interface with the grid is established.

Which of these system architectures will be employed in a particular PV plant depends on many factors such as environment of the plant (whether the plant is situated in an urban environment or at an open area), scalability, costs etc. Fig down an overview of different system architectures is given.

The main advantages and disadvantages of the different architectures are discussed below.

In general, solar inverters should have the following characteristics:

• Inverters should be highly efficient because the owner of the solar system requires the absolute maximum possible generated energy to be de-livered to the grid/load.

• Special demands regarding the potential between solar generator and earth (depending on the solar

module type).

• Special safety features like active islanding detection capability.

• Low limits for harmonics of the line currents. This requirement is enforced by law in most countries since the harmonic limits of both sources and loads connected to the grid are regulated.

• Special demands on electromagnetic interference (EMI), which are regulated by law in most countries. The goal of these minimize the unwanted influence of EMI on other equipment in the vicinity or connected to the same supply. Think for example of the influence of a mobile phone on an old radio.

• In many instances the solar system is to be installed outdoors and inverters should adhere to certain specification regarding temperature and humidity conditions, e.g. IP 54.

• Design for high ambient temperatures.

• Designed for 20 years operation under harsh environmental conditions.

• Silent operation (no audible noise).

We have to distinguish between single-phase and three-phase inverters. For low powers, as they are common small residential PV systems, single-phase inverter are used. They are connected to one phase of the grid For higher powers, three-phase inverters are used that are connected to all phases of the grid.

If a high power would be delivered to one phase, the currents flowing across the three phases would become very asymmetric

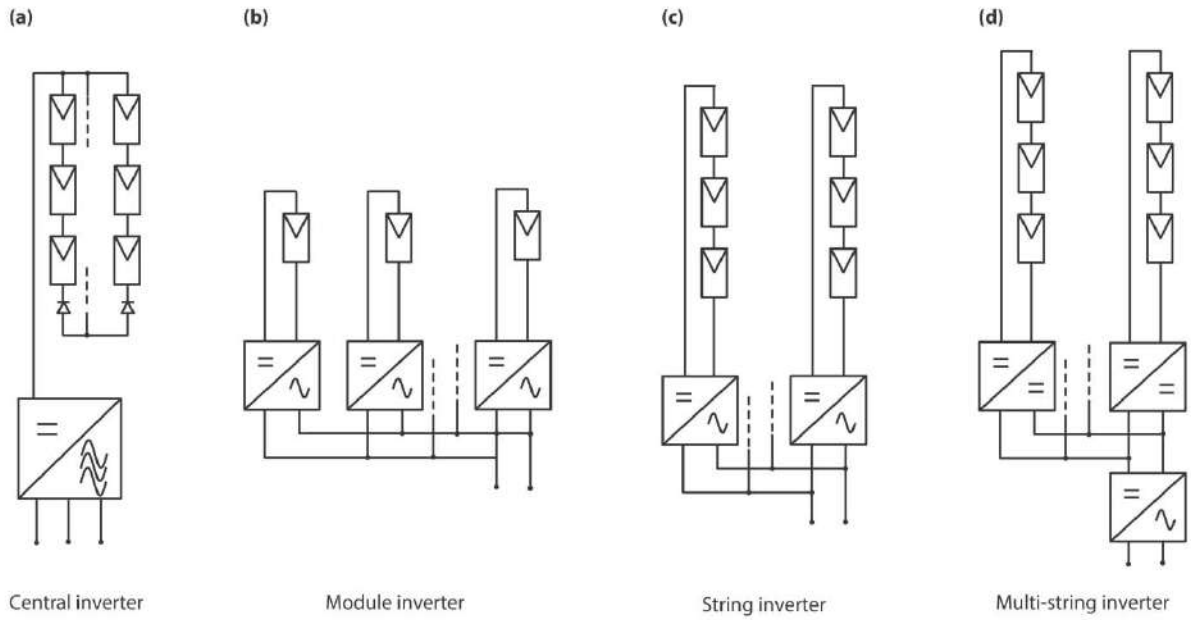



**Fig 4.17** Different system architectures employed in PV systems.

leading to several problems in the electricity grid. Note that the term inverter is often used for two different things: First, it is used for the actual inverter, which is the electronic building block that performs the DC-to-AC conversion, as described in section 17.3.3. Secondly, the term inverter also is used for the total unit produced by manufacturers, that nowadays usually contains, an MPP tracker, a DC-DC converter, an DC-AC converter and possibly also a charge controller of also a battery is connected.

**Central inverters**

This is the simplest architecture employed in PV systems. Here, PV modules are connected in strings leading to an increased system voltage. Many strings are then connected in parallel forming a PV array, which connected to one central inverter. The inverter performs maximum power point tracking and power conversion as shown in Fig. 4.13 (a), where a three-phase inverter is depicted. This configuration is mostly employed in very-large scale PV production, with central inverter usually being DC to three phase [94]. Many different inverter topologies are utilized as a three phase inverter. Sometimes they are organized as a single DC to three phase unit but sometimes as a three separate DC-to-AC single phase units working with a phase displacement of 120 degrees each. Having

all the PV modes connected in a single array in such a centralized configuration offers the lowest specific cost (cost per kWpp of installed power). Since central inverters only use a few components, they are very reliable what makes them the preferred option in large scale PV power plants. [19]

In spite of their simplicity and low specific cost, central inverters suffer from the following disadvantages:

1. Due to the layout of the system, a large amount of power is carried over considerable distances using DC wiring. This can cause safety issues because fault DC currents are difficult to interrupt. Special precaution measures must to be taken such as ticker insulation on the DC cabling and special circuit breakers, which can increase the costs.

2. All strings operate at the same maximum power point, which leads to mismatch losses in the modules. This is significant disadvantage. Mismatch losses increase even more with ageing and with partial shading of sections of the array. Mismatch between the different strings may significantly reduce the overall system output.

3. Low flexibility and expandability of the system. Due to the high ratings a system is normally designed as a unit and hence difficult to extend. In other words the system design is not very flexible.

4. Power losses in the string diodes, which are put in series with each string to prevent current circulation inside strings.

**Module Integrated or module oriented inverters**

A very different architecture is that of the module integrated inverters, as shown in 17.12 (b). These inverters operate directly at one or several PV modules and have power ratings of several hundreds of watts. Because of the low voltage rating of the PV module, these inverters require often require a two stage power conversion. In a first stage boosts the DC voltage is boosted to the required value while it is inverted to AC in the second stage. Often, a high frequency transformer is incorporated providing full galvanic isolation, which enhances the system flexibility even further.

As their name suggests, these inverters are usually integrated with PV panel (so called 'AC PV panels'). In this way the highest flexibility and the expandability of system is obtained. One of the most distinguishing features of this system is the "plug and play" characteristic, which allows to build a complete (and readily expandable) PV system at a low investment cost. Another advantage of these inverters, is minimization of the mismatch losses that can occur because of non-optimal MPPT.

All these advantages come at certain expenses. Because these inverters are be mounted on a PV module, they must operate in harsh environment such as high temperature and large daily and seasonal temperature variations. Also,

the specific are the highest of all the inverter topologies. Many topologies for module integrated inverters have been proposed, with some of them being already implemented in commercially available inverters.

**String Inverters**

String inverter, as illustrated in 17.12 (c), combine the advantages of central and module integrated nverter concepts with little tradeoffs. A number of PV mod-ules that are connected in series form a PV string with a power rating of up to 5 kWp and with the open circuit voltage of up to 1 kV.

Now, a number of smaller inverters can be used to connect the PV system to the grid.

One disadvantage of the topology is the fact that the high DC voltage requires special consideration, similarly as this already was the case for the central inverter architecture. Here, this issue is even more important because string inverters are usually being installed in households or on office buildings,

without designated support structure or increased safety requirements. In general a qualified electrician is needed to perform the interconnections between the modules and the inverter. The protection of the system also requires special consideration, with emphasis on proper DC cabling.

Although partial shading of the string will influence the overall efficiency of the system, each string can independently be operated at its MPP. Also, because no strings are connected in parallel, there is no need for series diodes as in the case of PV arrays with many parallel strings.

This reduces losses associated with these diodes. However, it still is a risk that within a string hot-spot occurs because of unequal current and power sharing inside the string.

**Multi String Inverters**

The Multi String inverter concept, illustrated in Fig above (d), as been developed to combine the advantage of the higher energy yield of a string inverter with the lower costs of a central inverter [95]. Lower power AC- DC converters are connected to individual PV strings each having its own MPP tracking, which ndependently optimises the energy output from each PV string.

To expand the system within a certain power range only a new string with a DC-DC converter has to be included. All DC-DC converters are connected via a DC bus through a central inverter to the grid.

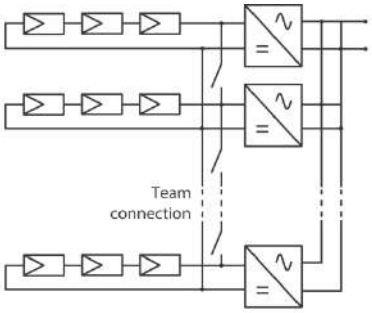



**Fig 4.18** The team concept of inverters.

## IV.3.8.batteries:

In this section we discuss a vital component not only of PV systems but of renewable energy systems in general. Energy storage is very important at both small and large scales in order to tackle the intermittency of renewable energy sources. In the case of PV systems, the intermittency of the electricity generation is of two kinds: first, diurnal fluctuations, i.e. the difference of irradiance during the 24-hour period.

Secondly, the seasonal fluctuations, i.e. the difference of irradiance between the summer and winter months. There are several technological options for realizing storage of energy. Therefore, it is important to make an optimal choice.

Fig. 4.18 shows a Ragone chart, where the specific energy is plotted against the peak power density. Because it uses a double-logarithmic chart storage technology with very different storage properties can be compared in one plot. Solar energy application requires a high energy density and – depending on the application – also a reasonably high power density. For example, [19]

we cannot use capacitors because of their very poor energy density. For short term to medium term storage, the most common storage technology of course is the battery. Batteries have both the right energy density and power density to meet the daily storage

demand in small and medium-size PV systems. However, the seasonal storage problem at large scales is yet to be solved.

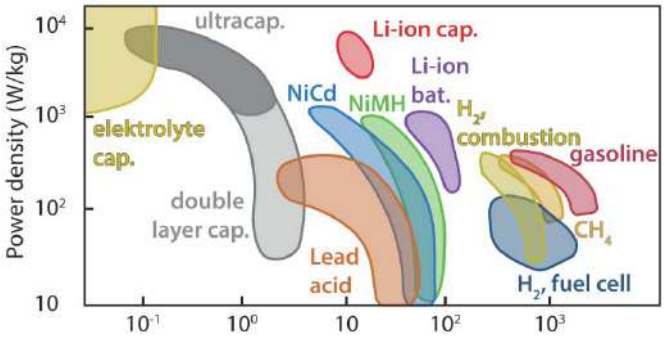



**Fig 4.19** A Ragone chart of different energy storage methods. Capacitors are indicated with "cap".

The ease of implementation and efficiency of the batteries is still superior to that of other technologies, like pumping water to higher levels, compressed air energy storage, conversion to hydrogen, flywheels, and others. Therefore we will focus on battery technology as a viable storage option for PV systems.

Batteries are electrochemical devices that convert chemical energy into electrical energy. We can distinguish between primary or secondary batteries. Primary batteries convert chemical energy to electrical energy irreversibly. For example, zinc carbon and alkaline batteries are primary batteries.

Secondary batteries or rechargeable batteries, as they are more commonly called, convert chemical energy to electrical energy reversibly.

This means that they can be recharged when an over-potential is used. In other words, excess electrical energy is stored in these secondary batteries in the form of chemical energy. Typical examples for rechargeable batteries are lead acid or lithium ion batteries. For PV systems only secondary batteries are of interest.

## IV.3.8.1.Types of batteries:

Lead-acid batteries are the oldest and most mature technology available. They will be discussed in detail later in this section.

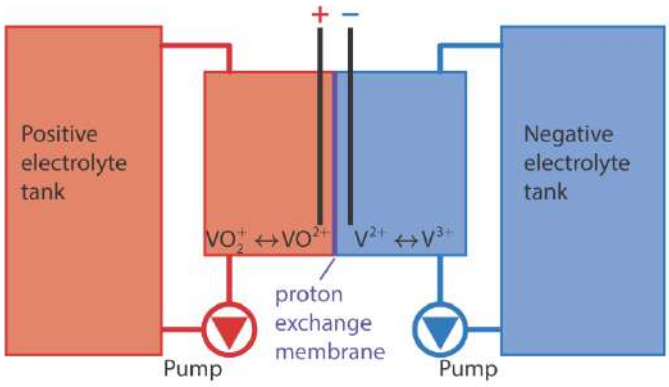



**Fig 4.20** Schematic on a vanadium redox-flow battery that employs vanadium ions.

Other examples are nickel-metal hydride (NiMH) and nickel cadmium (NiCd) batteries. NiMH batteries have a high energy density, which is comparable to that of lithium-ion batteries (discussed below). However, NiMH batteries suffer from a high rate of self discharge. On the other hand, NiCd batteries have much lower energy density than lithium ion batteries. Furthermore, because of the toxicity of cadmium,

NiCd batteries are widely banned in the European Union for consumer use. Additionally, NiCd batteries suffer from what is called the memory effect: the batteries loose their usable energy capacity if they are repeatedly charged after only being partially discharged. These disadvantages make NiMH and NiCD batteries unsuitable candidates for PV storage systems.

Lithium ion batteries (LIB) and lithium-ion polymer batteries, which are often referred to as lithium polymer (LiPo) batteries, have been heavily investigated in recent years. Their high energy density already has made them the favorite technology for light-weight storage applications for example in mobile telephones. However,

these technologies still suffer from high costs an low maturity.

The last and the most recent category of batteries that we will discuss in this treatise are redox-flow batteries.

Lead-acid batteries and LIB, the two main storage options for PV systems, are similar in the sense that their electrodes undergo chemical conversion during charging and discharging, which makes their electrodes degenerate with time, leading to inevitable “ageing” of the battery. In contrast, redox flow batteries combine properties of both batteries and fuel cells, as illustrated in Fig. 4.20.

Two liquids, a positive electrolyte and a negative electrolyte are brought together only separated by a membrane, which only is permeable for protons. The cell thus can be charged and discharged without the reactants being mixed, which in principle prevents the liquids from ageing. The chemical energy in a redox flow battery is stored in its 2 electrolytes, which are stored in two separate tanks.

Since it is easy to make the tanks larger, the maximal energy that can be stored in such a battery thus is not restricted. Further, the maximal output power can easily be increased by increasing the area of the membrane,

for example, by using more cells at the same time. The major disadvantages is that such a battery system requires additional components such as pumps, which makes them more complicated than other types of batteries.

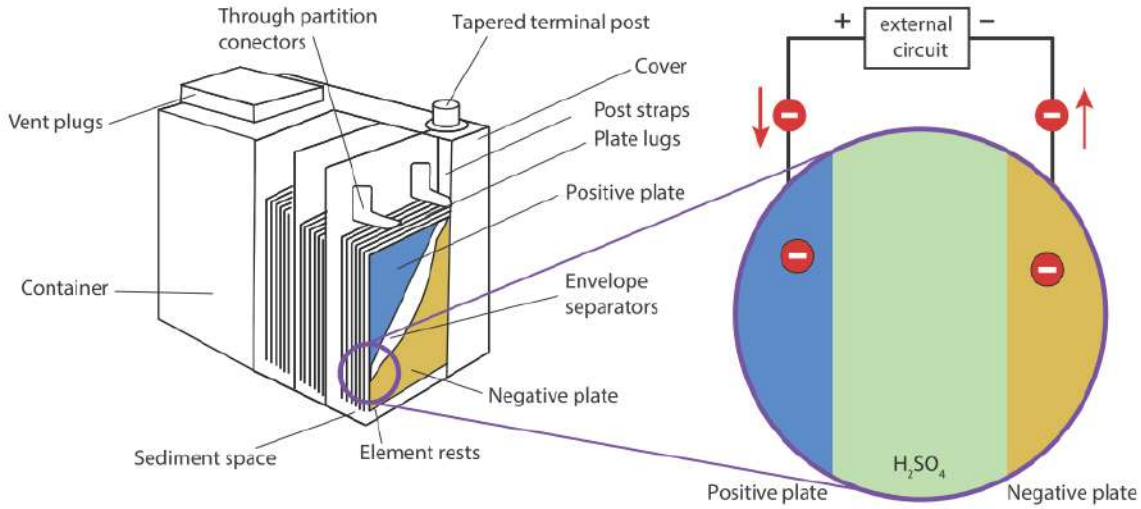



**Fig 4.21** Schematic of a lead-acid battery.

## IV.3.8.2.Battery parameters:

Let us now discuss some parameters that are used to characterise batteries.

**Voltage :**

First, we will discuss the voltage rating of the battery. The voltage at that the battery is rated is the nominal voltage at which the battery is supposed to operate. The so called solar batteries or lead acid grid plate batteries are usually rated at 12 V, 24 V or 48 V.

**Capacity**

When talking about batteries, the term capacity refers to the amount of charge that the battery can deliver at the rated voltage. The capacity is directly proportional to the amount of electrode material in the battery. This explains why a small cell has a lower capacity than a large cell that is based on the same chemistry, even though the open circuit voltage across the cell will be the same for both the cells. Thus, the voltage of the cell is more chemistry based, while the capacity is more based on the quantity of the active materials used. The capacity Cbat is measured in ampere-hours (Ah).

Note that charge usually is measured in coulomb (C). As the electric current is defined as the rate of flow of electric charge, Ah is another unit of charge. Since 1 C = 1 As, 1 Ah = 3600 C. For batteries, Ah is the more convenient unit, because in the field of electricity the amount of energy usually is measured in watt-hours (Wh).

The energy capacity of a battery is simply given by multiplying the rated battery voltage measured in Volt by the battery capacity measured in Amp-hours, Ebat = CbatV, which results in the battery energy capacity in Watt-hours.

**C-rate**

A brand new battery with 10 Ah capacity theoretically can deliver 1 A current for 10 hours at room temperature. Of course, in practice this is seldom the case due to several factors. Therefore, the C-rate is used, which is a measure of the rate of discharge of the battery relative to its capacity. It is defined as the multiple of the current over the discharge current that the battry can sustain over one hour. For example, a C-rate of 1 for a 10Ah battery corresponds to a discharge current of 10 A over 1 hour.

A C-rate of 2 for the same battery would correspond to a discharge current of 20 A over half an hour. Similarly, a C-rate of 0.5 implies a discharge current of 5 A over 2 hours. In general, it can be said that a C-rate of n corresponds to the battery getting fully discharged in 1/n hours, irrespective of the battery capacity

**Battery efficiency.**

For designing PV systems it is very importent to know the efficiency of the storage system. For storage systems, usually the round-trip efficiency is used, which is given as the ratio of total storage system input to the total storage system output,

$$\eta_{\text{bat}} = \frac{E_{\text{out}}}{E_{\text{in}}} 100\%. \qquad \text{EQUATION (4.5)}$$

For example, if 10 kWh is pumped into the storage system during charging, but only 8 kWh can be retrieved during discharging, the round trip efficiency of the storage system is 80%. The round-trip efficiency of batteries can be broken down into two efficiencies: first, the voltaic efficiency, which is the ratio of the average discharging voltage to the average charging voltage,

$$\eta_V = \frac{V_{\text{discharge}}}{V_{\text{charge}}} 100\%. \qquad \text{EQUATION (4.6)}$$

This efficiency covers the fact that the charging voltage is always a little above the rated voltage in order to drive the reverse chemical (charging) reaction in the battery. Secondly, we have the coulombic efficiency (or Faraday efficiency),

which is defined as the ratio of the total charge got out of the battery to the total charge put into the battery over a full charge cycle,

$$\eta_C = \frac{Q_{\text{discharge}}}{Q_{\text{charge}}} 100\%.$$

EQUATION (4.7)

The battery efficiency then is defined as the product of these two efficiencies,

$$\eta_{\text{bat}} = \eta_V \cdot \eta_C = \frac{V_{\text{discharge}}}{V_{\text{charge}}} \frac{Q_{\text{discharge}}}{Q_{\text{charge}}} 100\%.$$

EQUATION (4.8)

When comparing different storage devices, usually this round-trip efficiency is considered. It includes all the effects of the different chemical and electrical non-idealities occurring in the battery.

**State of charge and depth of discharge**

At another important battery parameter is the State of Charge (SoC), which is defined as the percentage of the battery capacity available for discharge,

$$\text{SoC} = \frac{E_{\text{bat}}}{C_{\text{bat}} V}$$

EQUATION (4.9)

Thus, a 10 Ah rated battery that has been drained by 2 Ah is said to have a SoC of 80%. Also the Depth of Discharge (DoD) is an important parameter. It is defined as the percentage of the battery capacity that has been discharged,

$$\text{DoD} = \frac{C_{\text{bat}} V - E_{\text{bat}}}{C_{\text{bat}} V}.$$

EQUATION (4.10)

For example, a 10 Ah battery that has been drained by 2 Ah has a DoD of 20%. The SoC and the DoD are complimentary to each other.

**Cycle lifetime**

The cycle lifetime is a very important parameter. It is defined as the number of charging and discharging cycles after that the battery capacity drops below 80% of the nominal value. Usually, the cycle lifetime is specified by the battery manufacturer as an absolute number. However, stating the battery lifetime as a single number is a oversimplification because the different battery parameters discussed so far are not only related to each other but are also dependent on the temperature. Fig4.22 (a) shows the cycle lifetime as a function of the DoD for different temperatures. Clearly, colder operating temperatures mean longer cycle lifetimes. Furthermore, the cycle lifetime depends strongly on the

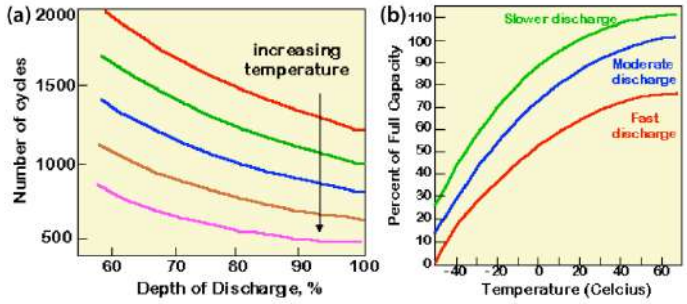



**Fig 4.22** Qualitative illustration of the cycle lifetime of a lead-acid battery in dependence of the DoD and temperature [100]. (b) Effect of the temperature on the battery capacity

DoD. The smaller the DoD, the higher the cycle life-time. Thus, that the battery will last longer if the average DoD can be reduced during the lifetime of thebattery. Also, battery overheating should be strictly controlled. Overheating can because of overcharging andsubsequent over-voltage of the lead acid battery. To prevent this, charge controllers are used that we address inthe next section.

**Temperature effects**

While the battery lifetime is increased at lower temperatures, one more effect must to be considered. The temperature affects the battery capacity during regular use too. As seen from Fig. 4.22 (b), the lower the temperature, the lower the battery capacity. This is because, the chemicals in the battery are more active at higher temperatures, and the increased chemical activity leads to increased battery capacity.

It is even possible to reach an above rated battery capacity at high temperatures. However, such high temperatures are severely detrimental to the battery health.

**Ageing**

The major cause for ageing of the battery is sulphation. If the battery is insufficiently recharged after being dis- charged, sulphate crystals start to grow, which cannot be completely transformed back into lead or lead oxide. Thus the battery slowly loses its active material mass and hence its discharge capacity.

Corrosion of the lead grid at the electrode is another common ageing mechanism. Corrosion leads to increased grid resistance due to high positive potentials. Further, the electrolyte can dry out. At high charging voltages, gassing can occur, which results in the loss of water. Thus, demineralized water should be used to refill the battery from time to time.

## IV.3.9.Charge controllers:

After having discussed different types of batteries and different battery characteristics, it is now time to discuss charge controllers. Charge controllers are used in PV systems that use batteries, which are stand-alone systems in most cases. As we have

seen before, it is very important to charge and discharge batteries at the right voltage and current levels in order to ensure a long battery lifetime. A battery is an electrochemical device that requires a small over-potential to be charged. However, batteries have strict voltage limits, which are necessary for their optimal functioning

. Further, the amount of current sent to the battery by the PV array and the current flowing through the battery while being discharged have to be within well-defined limits for proper functioning of the battery. We have seen before that lead acid batteries suffer from over-charge and over-discharge. On the other hand, the PV array responds dynamically to ambient conditions like irradiance, temperature and other factors like shading. Thus, directly coupling the battery to the PV array and the loads is detrimental to the battery lifetime.

Therefore a device is needed that controls the currents flowing between the battery, the PV array and the load and that ensures that the electrical parameters present at the battery are kept within the specifications given by the battery manufacturer. These tasks are done by a charge controller, that nowadays has several different

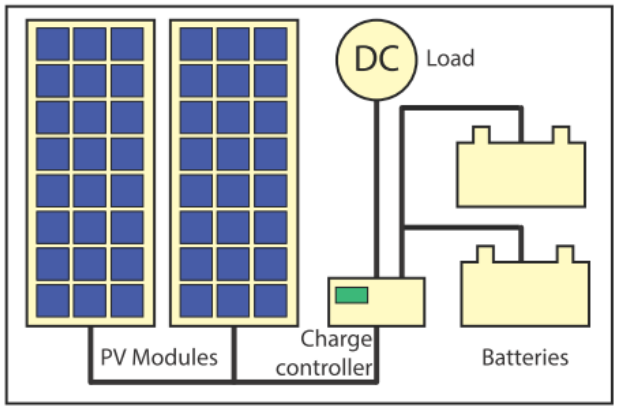



**Fig 4.23** Illustrating the position of the charge controller in a generic PV system with batteries.

functionalities, which also depend on the manufacturer. We will discuss the most important functionalities. A schematic of its location in a PV system is shown in Fig. 17.30. When the sun is shining at peak hours during summer, the generated PV power excesses the load. The excess energy is sent to the battery. When the battery is fully charged, and the PV array is still connected to the battery, the battery might overcharge, which can cause several problems like gas formation, capacity loss or overheating. Here, the charge controller plays a vital role by de-coupling the PV array from the battery. Similarly,

during severe winter days at low irradiance, the load exceeds the power generated by the PV array, such that the battery is heavily discharged. Over-discharging the battery has a detrimental effect on the cycle lifetime,

as discussed above. The charge controller prevents the battery from being over-discharged by disconnecting the battery from the load. For optimal performance, the

battery voltage has to be within specified limits. The charge controller can help in maintaining an allowed voltage range in order to ensure a healthy operation. Further, the PV array will have its Vmpp at different levels, based on the temperature and irradiance conditions. Hence, the charge controller needs to perform appropriate voltage regulation to ensure the battery operates in the specified voltage range,

while the PV array is operating at the MPP. Modern charge controllers often have an MPP tracker integrated. As we have seen above, certain C-rates are used as bat- tery specifications. The higher the charge/discharge rates, the lower the coulombic efficiency of the battery. The optimal charge rates, as specified by the manufacturer, can be reached by manipulating the current flowing into the battery.

A charge controller that contains a proper current regulation is also able to control the C-rates. Finally, the charge controller can impose the limits on the maximal currents flowing into and from the battery.

if no blocking diodes are used, it is even possible that the battery can “load” the PV array, when the PV array is operating at a very low voltage. This means that the battery will impose a forward bias on the PV modules and make them consume the battery power, which leads to heating up the solar cells. Traditionally, blocking diodes are used at the PV panel or string level to prevent this back discharge of the battery through the PV array. However, this function is also easily integrated in the charge controller. We distinguish between series and shunt controllers, [20]

In a series controller, overcharging is prevented by disconnecting the PV array until a particular voltage drop is detected, at which point the array is connected to the battery again. On the other hand, in a parallel or shunt controller, overcharging is prevented by short-circuiting the PV array. This means that the PV modules work under short circuit mode, and that no current flows into the battery. These topologies also ensure over-discharge protection using  ower switches for the load connection,

which are appropriately controlled by the algorithms implemented into the charge controller algorithm. As charge controllers are a necessary component of of stand-alone PV systems, they should have a very high efficiency. As we have seen above, temperature plays a crucial role in the functioning of the battery. Not only does temperature affect the lifespan of the battery, but it also changes its electrical parameters significantly. Thus, modern charge controllers have a temperature sensor included, which allows the charge controller to adjust the electrical parameters of the battery,

like the operating voltage, to the temperature. The charge controller thus keeps the operating range of the battery within the optimal range of voltages. The charge controller is usually kept in close proximity to the battery, such that the operating temperature of the battery is close to that of the charge controller. However, when the battery is heavily loaded, the battery might heat up,

leading to differences between the temperature expected by the charge controller and the actual temperature of the battery. Therefore, high end charge controllers also take temperature effects due to high currents into account.

## IV.3.10.Cables:

The overall performance of PV systems also is strongly dependent on the correct choice of the cables. We there-fore will discuss how to choose suitable cables. But we start our discussion with color conventions. PV systems usually contain DC and AC parts. For correcty installing a PV system, it is important to know

the color conventions. For DC cables,

• red is used for connecting the +-contacts of the different system components with each other while

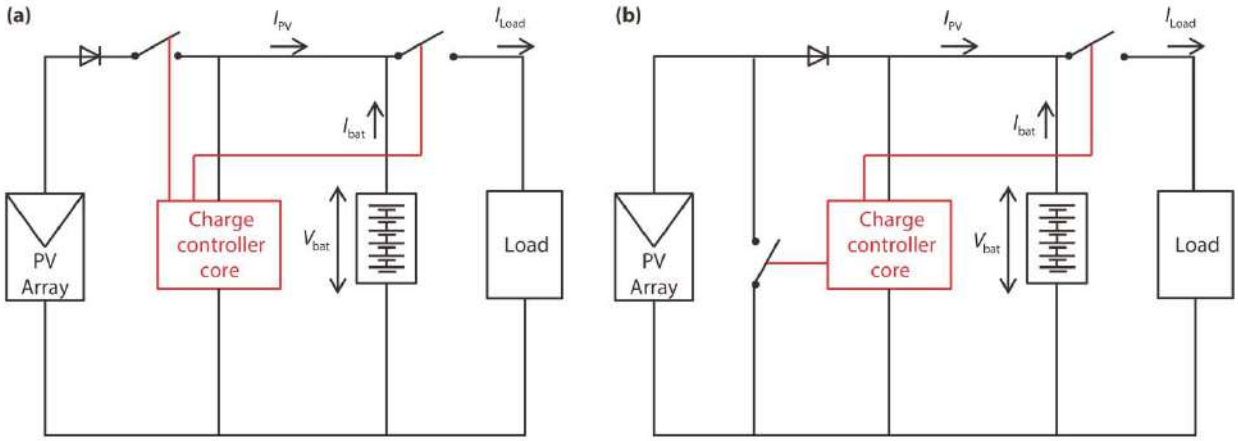



**Fig 4.24** Basic wiring scheme of (a) a series and (b) a shunt charge controller.

• black is used for interconnecting the contacts.For AC wiring, different colour conventions are used around the world.

• For example, in the European Union, blue is used for neutral, green-yellow is used for the protective earth and brown (or another color) is used for the phase.

• In the United States and Canada, silver is used for neutral, green-yellow, green or a bare conductor is used for the protective earth and black (or another color) is used for the phase.

• In India and Pakistan, black is used for neutral, green is used for the protective earth and blue, red, or yellow is used for the phase.

## IV.3. 11.A simple approach for designing off-grid systems:

In this section, we will design a simple off-grid system, as depicted in Fig. 18.1. The design presented here is based on very simple assumptions and does not take any weather-dependent performance changes into account.

Nonetheless, we will see the major steps that are necessary for designing a system. Such a simple design can be performed in a six step plan:

1. **Determine the total load current and operational time**

Before starting determining the current requirements of loads of a PV system one has to decide the nominal operational voltage of the PV system. Usual nominal voltages are 12 V or 24 V. When knowing the voltage, the next step is to express the daily energy requirements of loads in terms of current and average operational time expressed in Ampere-hours [Ah]. In case of DC loads the daily energy [Wh] requirement is calculated by multiplying the power rating [W] of an individual appliance with the average daily operational time [h]. Dividing the Wh by the nominal PV system operational voltage, the required Ah of the appliance is obtained.

In case of AC loads the energy use has to be expressedas a DC energy requirement since PV modules generate DC electricity. The DC equivalent of the energy use of an AC load is determined by dividing the AC load energy use by the efficiency of the inverter, which typically can be assumed to be 85%. By dividing the DC energy requirement by the nominal PV system voltage the Ah is determined.

2. **Add system losses**

Some components of the PV system, such as charge regulators and batteries require energy to perform their functions. We denote the use of energy by the system components as system energy losses.

Therefore, the total energy requirements of loads, which were determined in step 1, are increase with 20 to 30% in order to compensate for the system losses.

3. **Determine the solar irradiation in daily equivalent sun hours (ESH)**

How much energy a PV module delivers depends on several factors, such as local weather conditions, seasonal changes, and installation of modules. PV modules should be installed under the optimal tilt-angle in order to achieve best year-round performance. It is also important to know whether a PV system is expected to be used all-year round or only during a certain period of a year.

The power output during winter is much less than the yearly average and in the summer months the power output will be above the average. In the PV community, 1 equivalent sun means a solar irradiance of 1000 $W/m^2$ . This value corresponds to the standard, at which the performance of solar cells and modules is determined. The rated parameters of modules are determined at solar irradiance of 1 sun. When solar irradiation data are available for a particular location than the equivalent sun hours can be determined. For example, in the Netherlands the average annual solar irradiation is 1000 $kWh/m^2$ . According to the AM1.5 spectrum, 1 sun delivers 1000 $W/m^2 = 1\ kW/m^2$ . Hence, the Dutch average annual solar irradiation can be expressed as

$$\frac{1000\,\mathrm{kWh}\cdot\mathrm{m}^{-2}}{1\,\mathrm{kW}\cdot\mathrm{m}^{-2}} = 1000\,\mathrm{h},$$

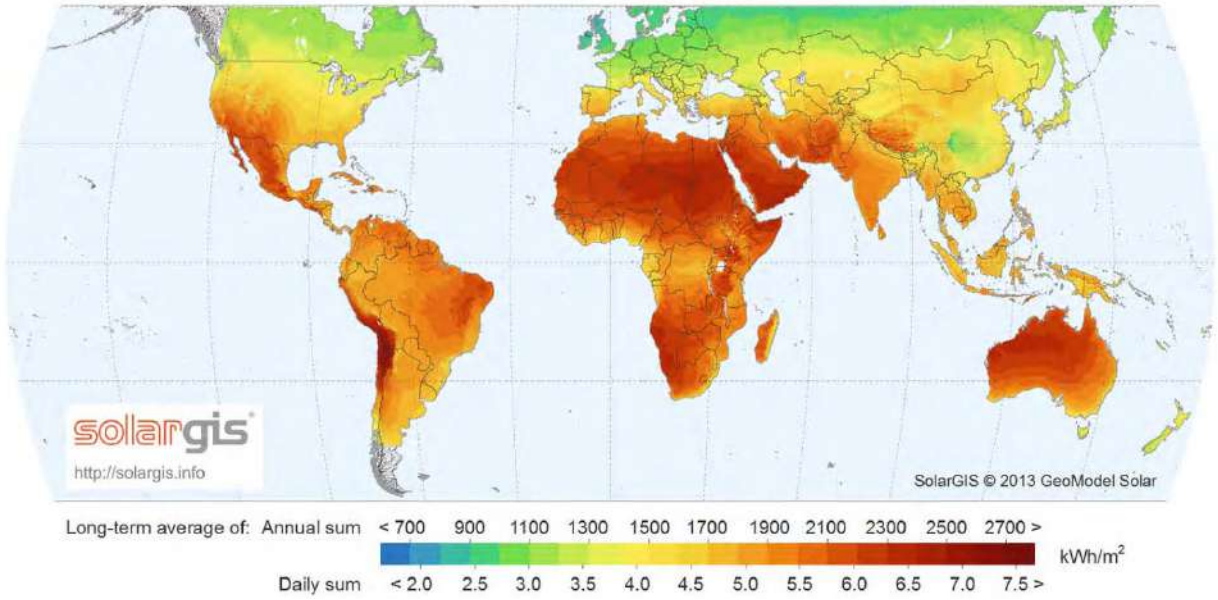



**Fig 4.25**: The average global horizontal insolation of the World given in kWh/year and PSH/day [21]. Note that this map only shows latitudes in between 60° N and 60° S.

i.e. 1000 equivalent sun hours, which corresponds to 2.8 h per day. Figs 4.24 and 4.25 show the globalhorizontal irradiation given in units of daily equivalentsun hours (ESH) and in kWh/year. Note that these Figs show horizontal values, meaning that a PV module would get this irradiance if it would be flat. For atilted module, the annual irradiance can be considerably higher, as we have seen in before

**4. Determine total solar array current requirements**

The current that has to be generated by the solar array is determined by dividing the total DC energy requirement of the PV system including loads and system losses (calculated in step 2 and expressed in Ah) by the daily equivalent sun hours (determined in step 3).




**Fig 4.26** The average global horizontal insolation of the Netherlands given in kWh/year and PSH/day [11]

**5. Determine optimum module arrangement for solar array**

Usually, PV manufacturers produce modules in a whole serie of different output powers. In the optimum arrangement of modules the required total solar array current (as determined in step 4) is obtained with the minimum number of modules. Modules can be either connected in series or in parallel to form an array. When modules are connected in series, the nominal voltage of the PV system is increased, while the parallel connection of modules results in a higher current.

The required number of modules in parallel is calculated by dividing the total current required from the solar array (determined in step 4) by the current generated by module at peak power (rated current in the specification sheet). The number of modules in series is determined by dividing the nominal PV system voltage with the nominal module voltage (in the specification sheet under configuration). The total number of modules is the product of the number of modules required in parallel and the number required in series.

**6. Determine battery size for recommended reserve time**

Batteries are a major component of stand-alone PV systems. The batteries provide load operation at night or in combination with the PV modules during periods of limited sunlight. For a safe operation of the PV system one has to anticipate periods with cloudy weather and plan a reserve energy capacity stored in the batteries.

This reserve capacity is referred to as PV system autonomy, which means the period of time that the system is not dependent on energy generated by PV modules. It is given in days. The system autonomy depends on the type of loads. For critical loads such as telecommunications components the autonomy can be 10 days and more, for residential use it is usually 5 days or less.

The capacity [Ah] of the batteries is calculated by multiplying the daily total DC energy requirement of the PV system including loads and system losses (calculated in step 2 and expressed in Ah) by the number ofdays of recommended reserve time. In order to prolong [13]

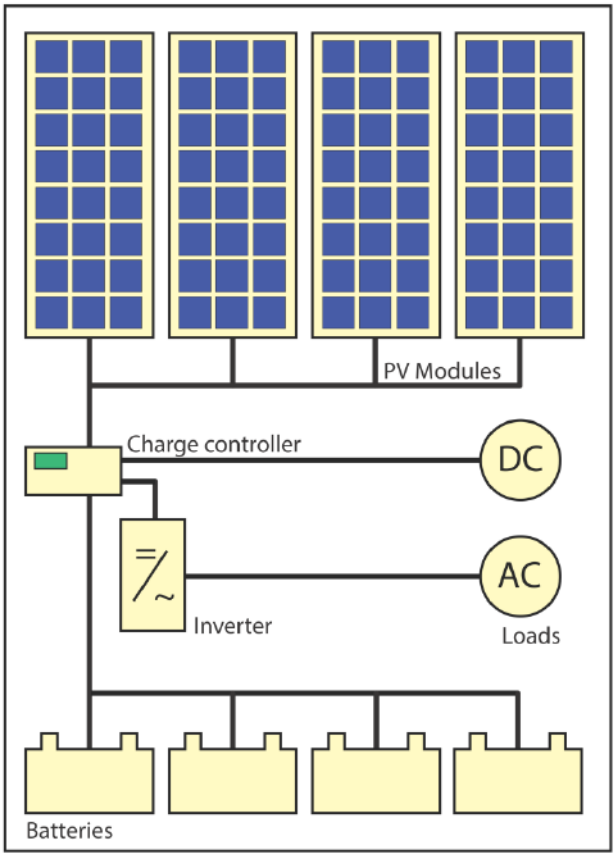
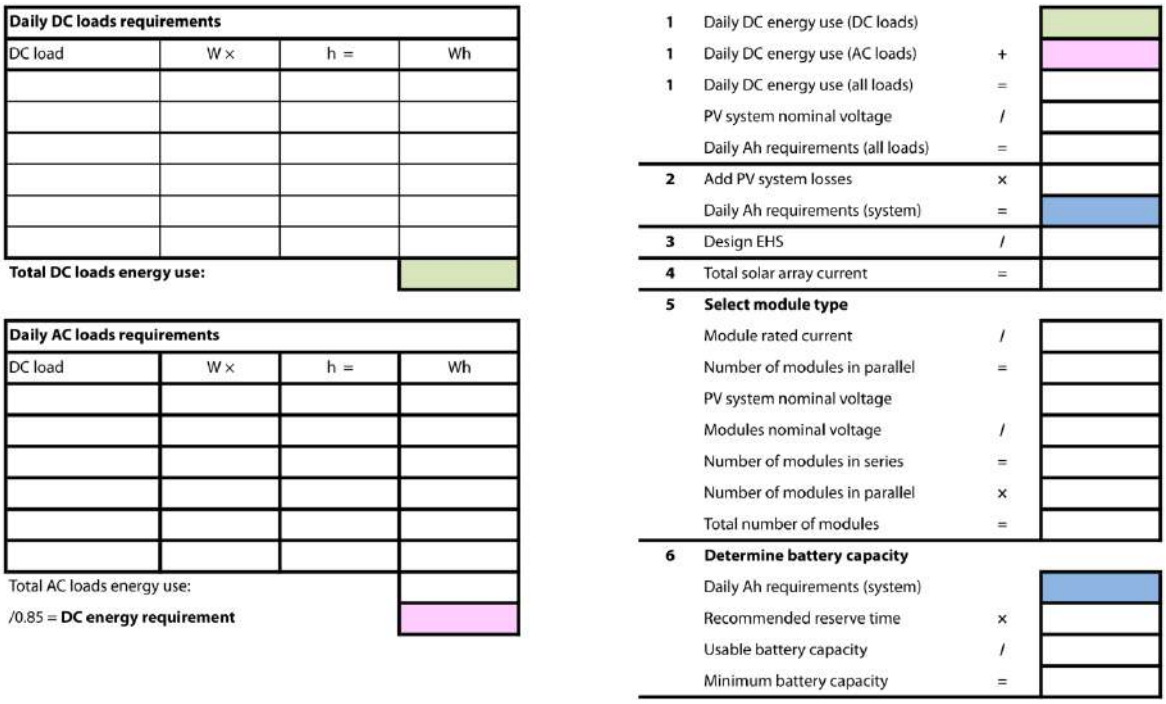



**Fig4.27**: Illustrating a simple off-grid PV system with AC and DC loads (see also Fig. 15.1 b).



| Daily DC loads requirements | | | |
|---|---|---|---|
| DC load | W × | h = | Wh |
| | | | |
| | | | |
| | | | |
| | | | |
| | | | |
| | | | |
| **Total DC loads energy use:** | | | |

| Daily AC loads requirements | | | |
|---|---|---|---|
| DC load | W × | h = | Wh |
| | | | |
| | | | |
| | | | |
| | | | |
| | | | |
| | | | |
| Total AC loads energy use: | | | |
| /0.85 = **DC energy requirement** | | | |

| | | | |
|---|---|---|---|
| 1 | Daily DC energy use (DC loads) | | |
| 1 | Daily DC energy use (AC loads) | + | |
| 1 | Daily DC energy use (all loads) | = | |
| | PV system nominal voltage | / | |
| | Daily Ah requirements (all loads) | = | |
| 2 | Add PV system losses | × | |
| | Daily Ah requirements (system) | = | |
| 3 | Design EHS | / | |
| 4 | Total solar array current | = | |
| 5 | **Select module type** | | |
| | Module rated current | / | |
| | Number of modules in parallel | = | |
| | PV system nominal voltage | | |
| | Modules nominal voltage | / | |
| | Number of modules in series | = | |
| | Number of modules in parallel | × | |
| | Total number of modules | = | |
| 6 | **Determine battery capacity** | | |
| | Daily Ah requirements (system) | | |
| | Recommended reserve time | × | |
| | Usable battery capacity | / | |
| | Minimum battery capacity | = | |

**Fig 4.28**: Worksheet for designing a simple off-grid PV system based on rough assumptions.

**Conclusion**:

In this chapter we saw the main continent of PV's system, and how we transfer power DC AC, type and well choosing of batteries and cables, and some tricks

# Chapter V

# Simulating of PV System

## Introduction

In this chapter we're going to see some result of simulating of PV system using MATLAB 2012R

## V.1 External solar cell parameters:

The building block of PV arrays is the solar cell, which is basically a p-n junction that directly converts light energy into electricity: it has an equivalent circuit as shown below in Figure

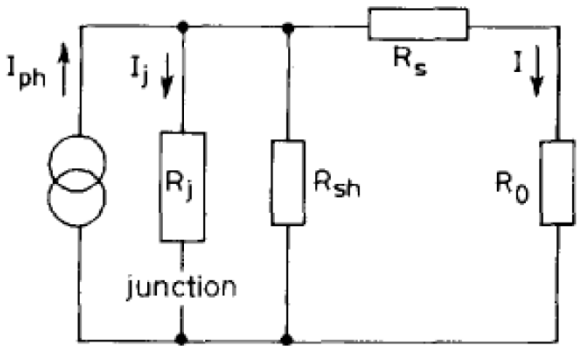



**Fig 5.1** Equivalent circuit of a PV cell

The current source Iph represents the cell photo current; Rj is used to represent the non-linear impedance of the p-n junction; R sh and R s are used to represent the intrinsic series and shunt resistance of the cell respectively. Usually the value of R sh is very large and that of R s is very small, hence they may be neglected to simplify the analysis.

PV cells are grouped in larger units called PV modules which are further interconnected in series-parallel configuration to form PV arrays or PV generators.The PV mathematical model used to simplify our PV array is represented by the equation:

$$I=n_pI_{ph}-n_pI_{rs}[\exp(\frac{q}{KTA}*\frac{V}{n_s}) -1]$$

EQUATION (5.1)

where I is the PV array output current; V is the PV array output voltage; n s is the number of cells in series and n p is the number of cells in parallel; q is the charge of an electron; k is the Boltzmann's constant; A is the p-n junction ideality factor; T is the cell temperature (K); I rs is the cell reverse saturation current. The factor A in equation (3.5) determines the cell deviation from the ideal p-n junction characteristics; it ranges between 1-5 but for our case A=2.46. The cell reverse saturation current I rs varies with temperature according to the following

equation:

$$I_{rs}=I_{rr}[\frac{T}{T_r}]^3\exp(\frac{qE_G}{KA}[\frac{1}{T_r}-\frac{1}{T}])$$

EQUATION (5.2)

I'll give some result of simulating from MATLAB

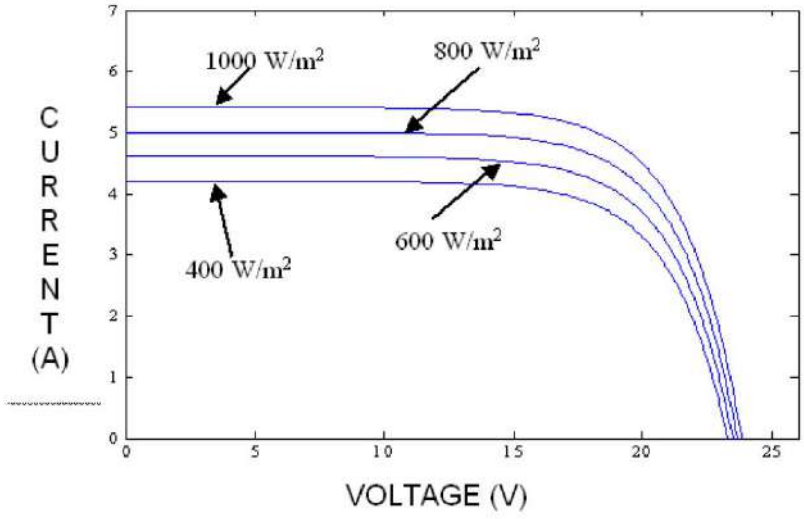



**Fig 5.2** characteristic of a solar array for a fixed temperature but varying irradiance

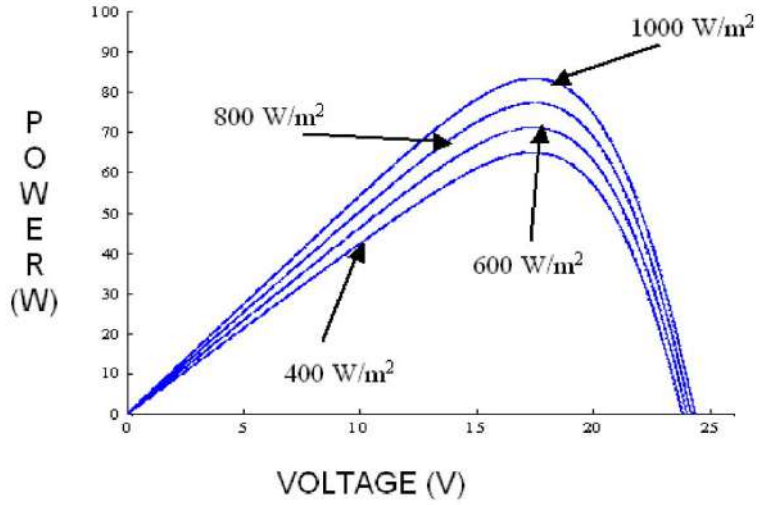



**Fig 5.3** characteristic of a solar array for a fixed temperature but varying irradiance

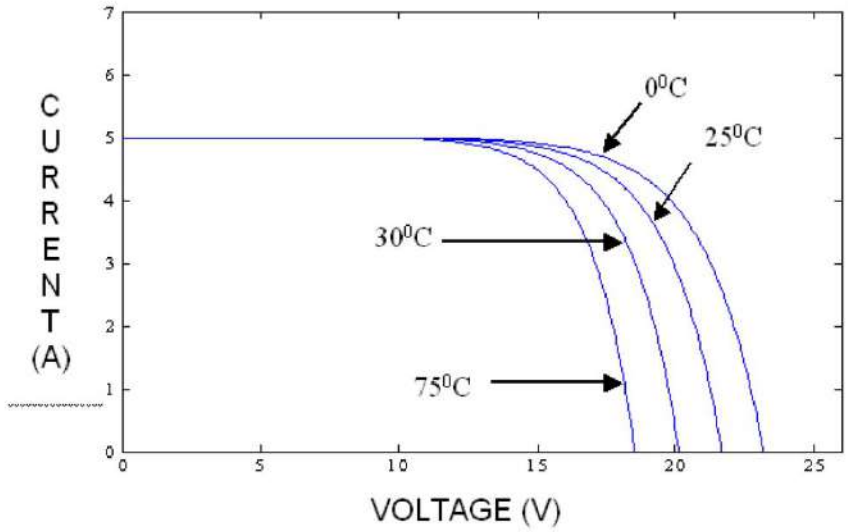



**Fig 5.4** Characteristic of a PV array under a fixed irradiance but varying temperatures Current

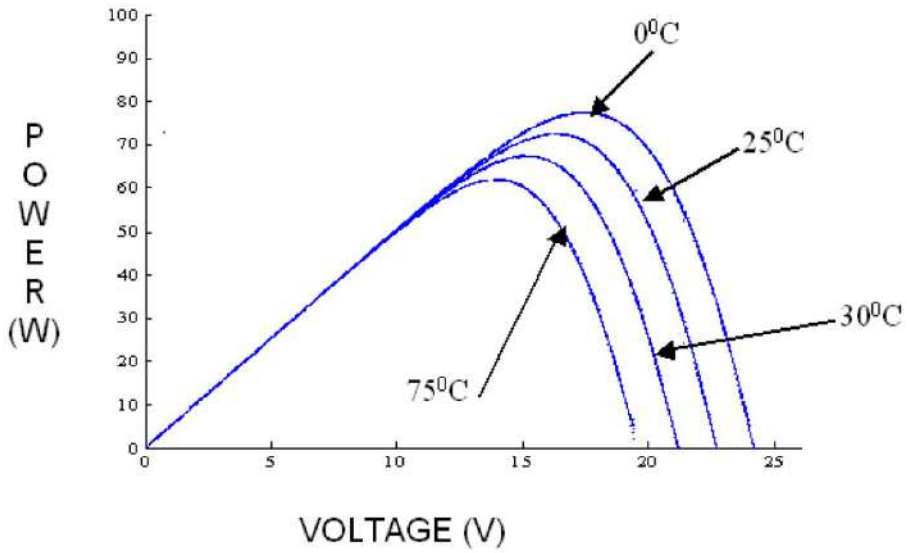



**Fig 5.5** Characteristic of a PV array under a fixed irradiance but varying temperatures.

Power

## V.2Matlab Code For Pv Array :

```
T=28+273;

Tr1=40;  %   Reference temperature in degree fahrenheit

Tr=((Tr1-32)*

 )+273;  %   Reference temperature in kelvin
```

```
S=[100 80 60 40 20];    %   Solar radiation in mW/sq.cm
%S=70;
ki=0.00023;  %   in A/K
Iscr=3.75; %    SC Current at ref. temp. in A
Irr=0.000021;   % in A
k=1.38065*10^(-23);  %   Boltzmann constant
q=1.6022*10^(-19);  %   charge of an electron
A=2.15;
Eg(0)=1.166;
alpha=0.473;
beta=636;
Eg=Eg0-(alpha*T*T)/(T+beta)*q;          %      band  gap  energy  of
semiconductor used
cell in joules
Np=4;
Ns=60;
V0=[0:1:300];
for i=1:5
Iph=(Iscr+ki*(T-Tr))*((S(i))/100);
Irs=Irr*((T/Tr)^3)*exp(q*Eg/(k*A)*((1/Tr)-(1/T)));
I0=Np*Iph-Np*Irs*(exp(q/(k*T*A)*V0./Ns)-1);
P0 = V0.*I0;
figure(1)
plot(V0,I0);
axis([0 50 0 20]);
xlabel('Voltage in volt');
ylabel('Current in amp');
hold on;
figure(2)
```

```
plot(V0,P0);

axis([0 50 0 400]);

xlabel('Voltage in volt');

ylabel('Power in watt');

hold on;

figure(3)

plot(I0,P0);

axis([0 20 0 400]);

xlabel('Current in amp');

ylabel('Power in watt');

hold on;

end
```

## V.3Interfacing Of The Pv Array With Boost Converter :

The PV array has been interfaced with the boost converter using a controlled voltage source as

shown in the circuit diagram below:

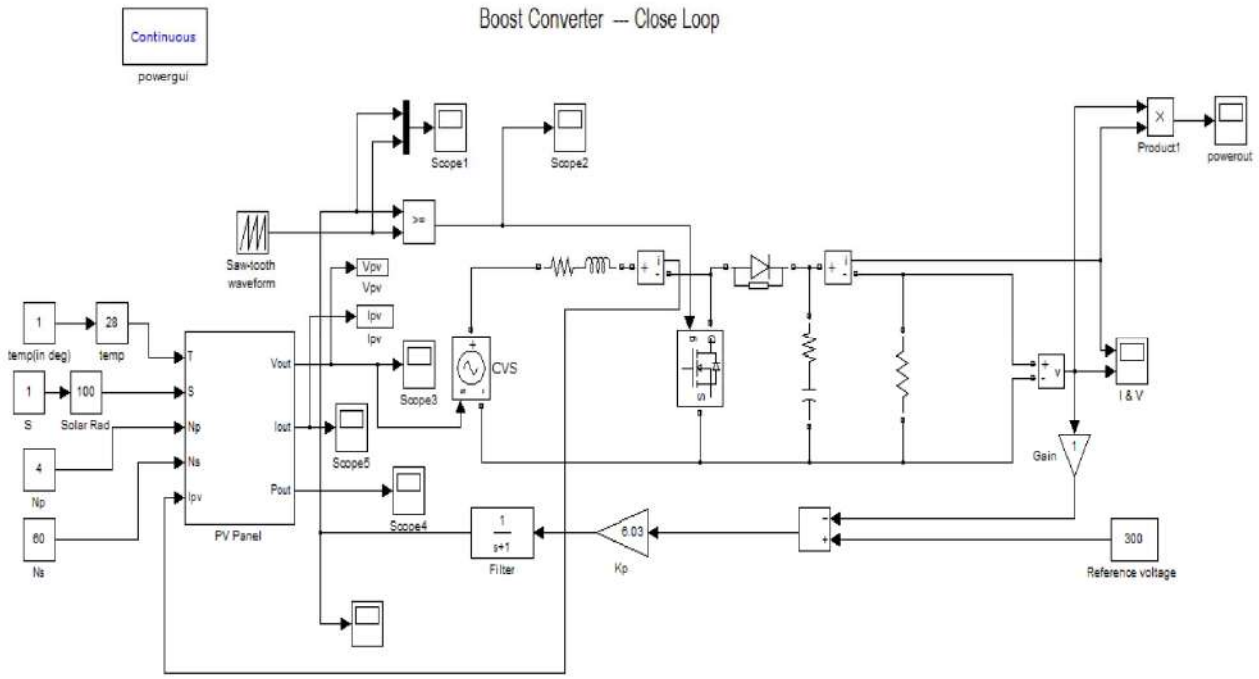



**Fig 5.6** The complete simulink circuit model showing the coupling of PV array with the boost

Converter

The PV array has been designed taken into consideration its dependence upon the irradiance, temperature, number of PV cells connected in series and parallel as explained in previous chapter

. The detailed internal circuit of the PV array showing the design is given below:

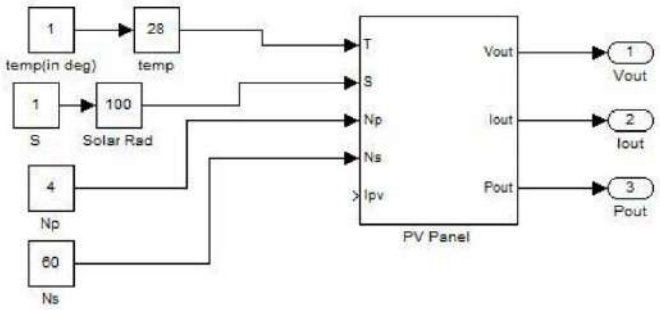



**Fig 5.7** PV panel block diagram

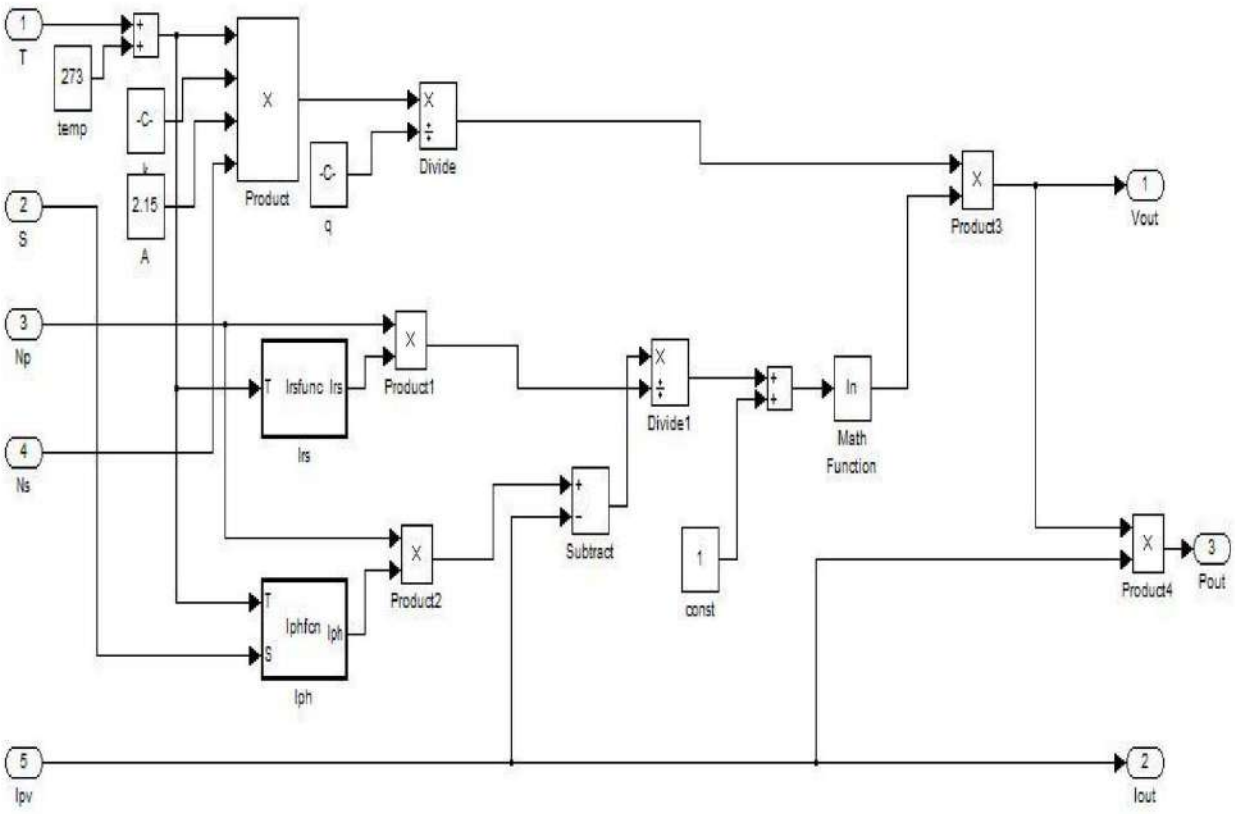



**Fig 5.8** Detailed internal circuit diagram of PV array in Simulink

The M-file for I rs function has been developed using the equation and that for the I ph

function using equation The PV array has been modeled using the equations

The interfacing of the PV array with the boost converter has been achieved using a voltage

controlled source. The inductor current which is same as the load current of the PV system is

used as feedback for designing the PV array.

$$I_{rs}=I_{rr}[\frac{T}{T_r}]^3 \exp(\frac{qE_G}{KA}[\frac{1}{T_r}-\frac{1}{T}])$$

EQUATION (5.3)

$$E_G= E_G(0)-\frac{\alpha T^2}{T+\beta}$$

EQUATION (5.4)

$$I_{ph}=[\ I_{scr} + K_i(T - T_r)]\ \frac{S}{100}$$

EQUATION (5.5)

$$P=IV= n_p I_{ph} V[(\frac{q}{KTA} * \frac{V}{n_s})-1]$$

EQUATION (5.6)

## V.4Parameters Used In The Matlab Code:

The values of the parameters used in developing the MATLAB code for the Photovoltaic array

have been tabled below

| PARAMETERS | VALUES |
|---|---|
| $N_p$ | 4 |
| $N_s$ | 60 |
| $I_{scr}$ | 3.75 A |
| $T_{r1}$ | 40 $^0$C |
| $K_i$ | 0.00023 A/K |
| $I_{rr}$ | 0.000021 A |
| K | 1.38065 * $10^{-23}$ J/$^0$K |
| q | 1.6022* $10^{-19}$ C |
| A | 2.15 |
| $E_g0$ | 1.66 eV |
| α | 4.73* 10^-4 eV/K |
| β | 636 K |

**Tab 5.1** Value of dev on matlab

## V.5OUTPUT WAVEFORMS OF THE PV ARRAY:

The waveforms obtained by varying the solar insolation and temperatures which are fed into the PV array model have been plotted as shown below:

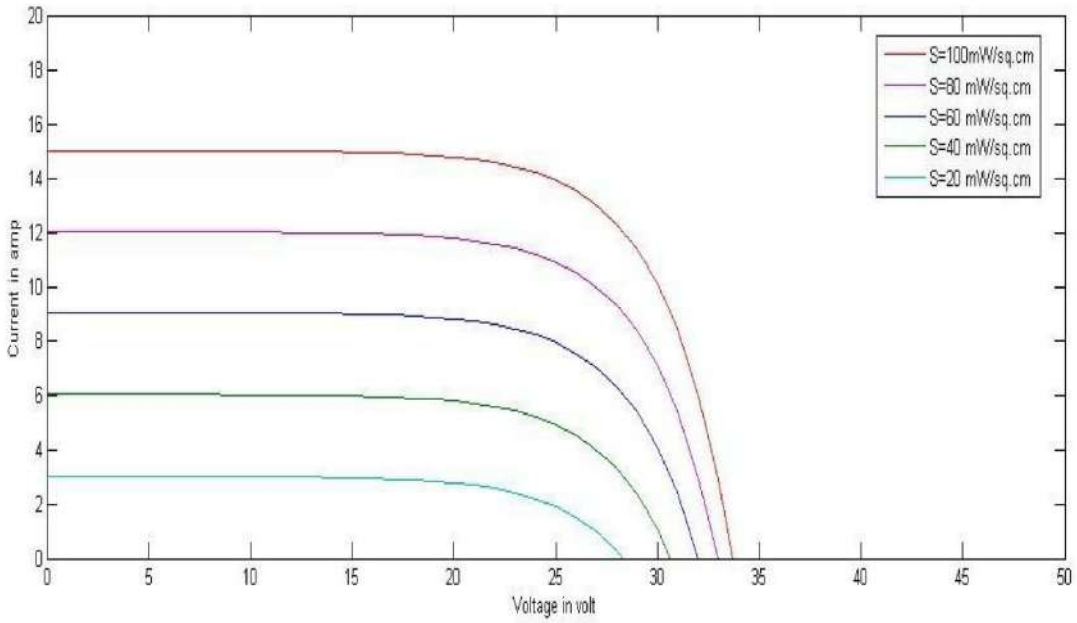



**Fig 5.9** curves obtained at 28° C for various irradiance levels

From this fig we observed that by increasing the solar radiation at constant temperature the voltage and current output from PV array also increases.Hence at higher insolation we can get our required level voltage.

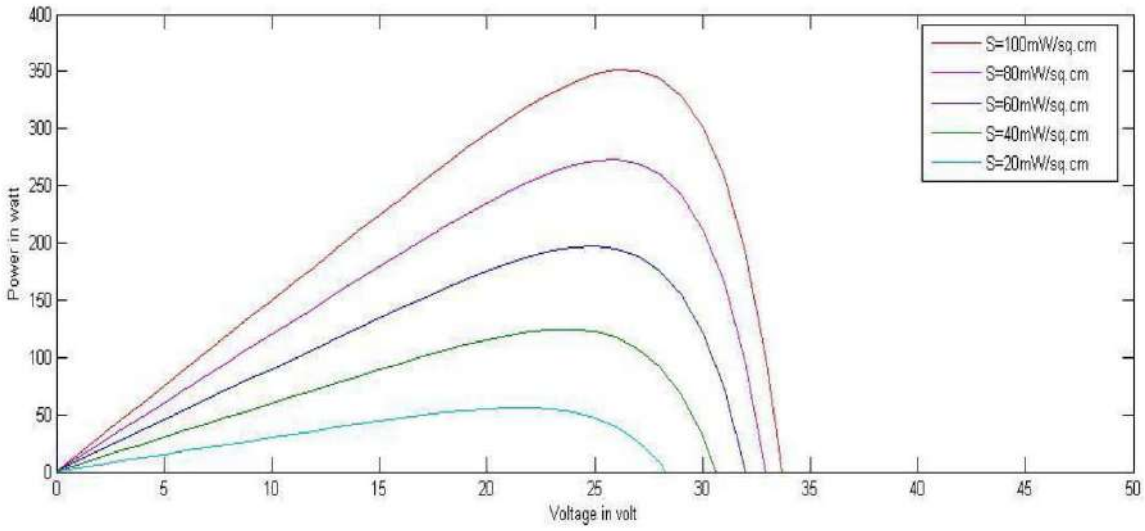



**Fig 5.10** P-V curves obtained at 28° C for various irradiance levels

we observed that by increasing the solar insolation level, the power output from PV array increases

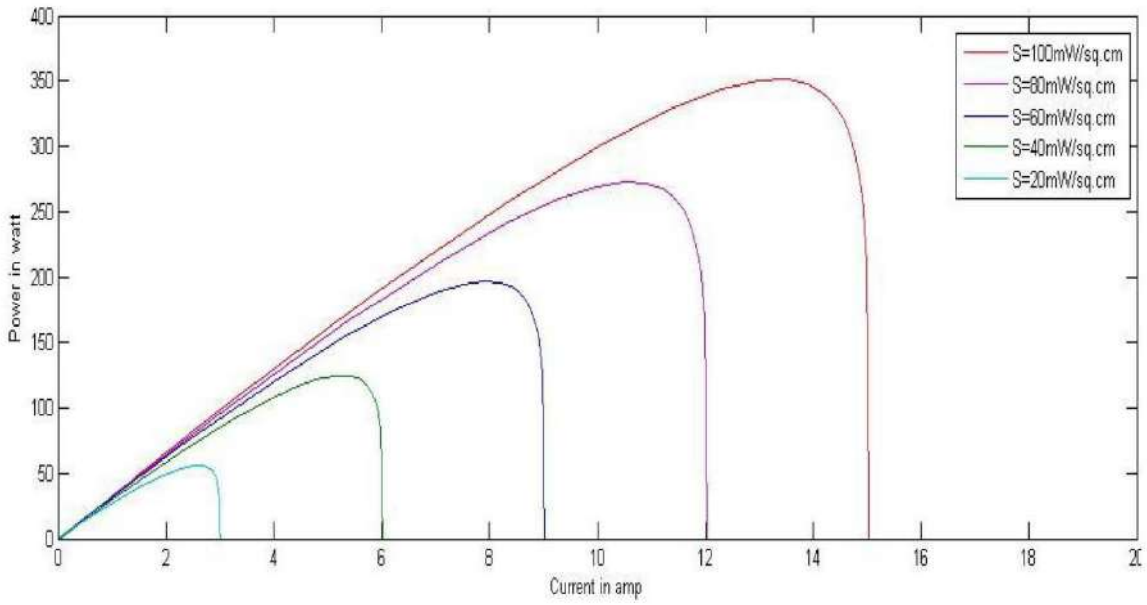



**Fig 5.11** P-I curves obtained at 28° C for various irradiance levels

we observed that by increasing the solar radiation level, the current and power output from PV array increases.

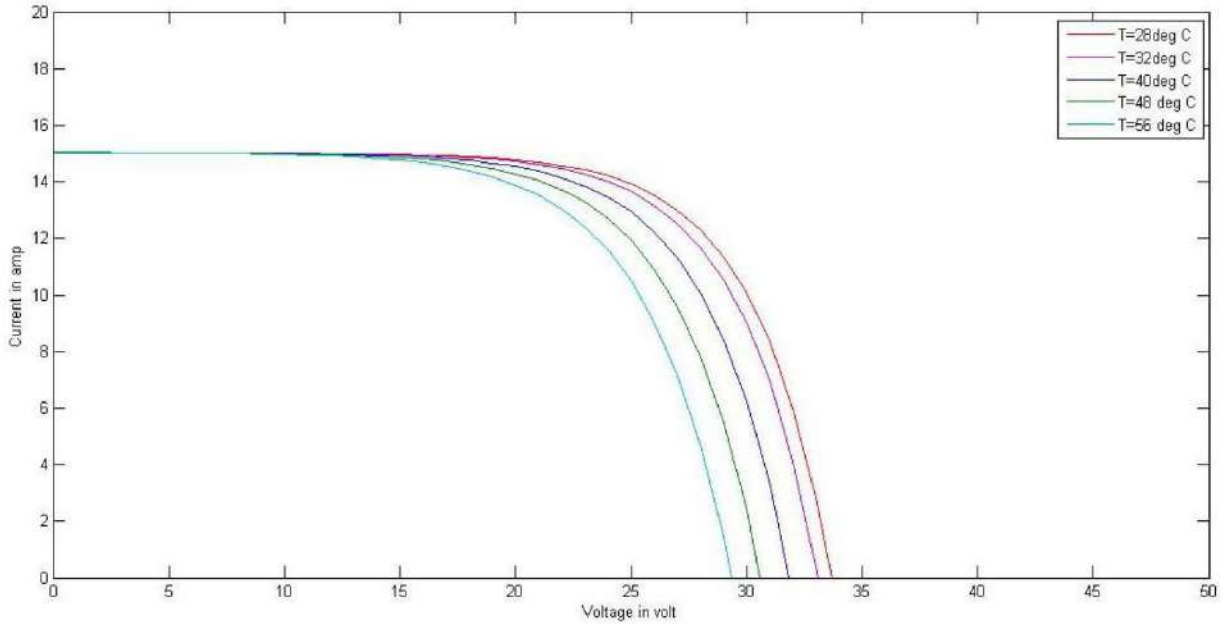



**Fig 5.12** curves obtained at an irradiance of 100 mW /cm² for various temperatures.

we observed that by increasing the temperature level at constant irradiance, the voltage output from PV array decreases but current output increases slightly with respect to voltage and, hence the power output from PV array decreases.

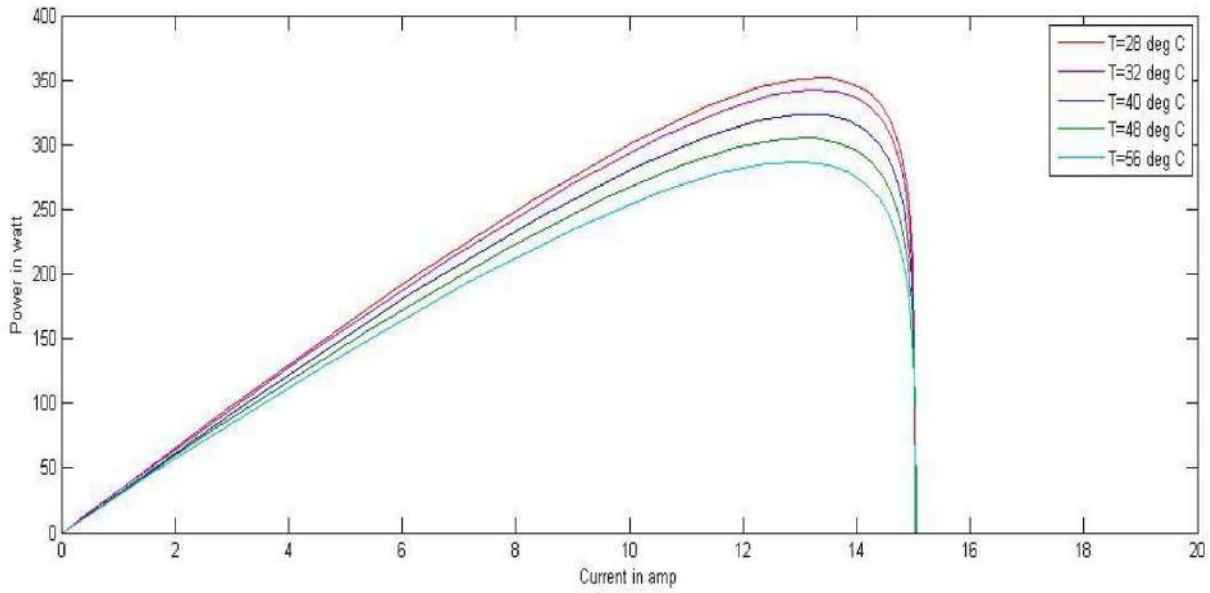



**Fig 5.13** P-I curves obtained at an irradiance of 100 mW/cm² for various temperatures.

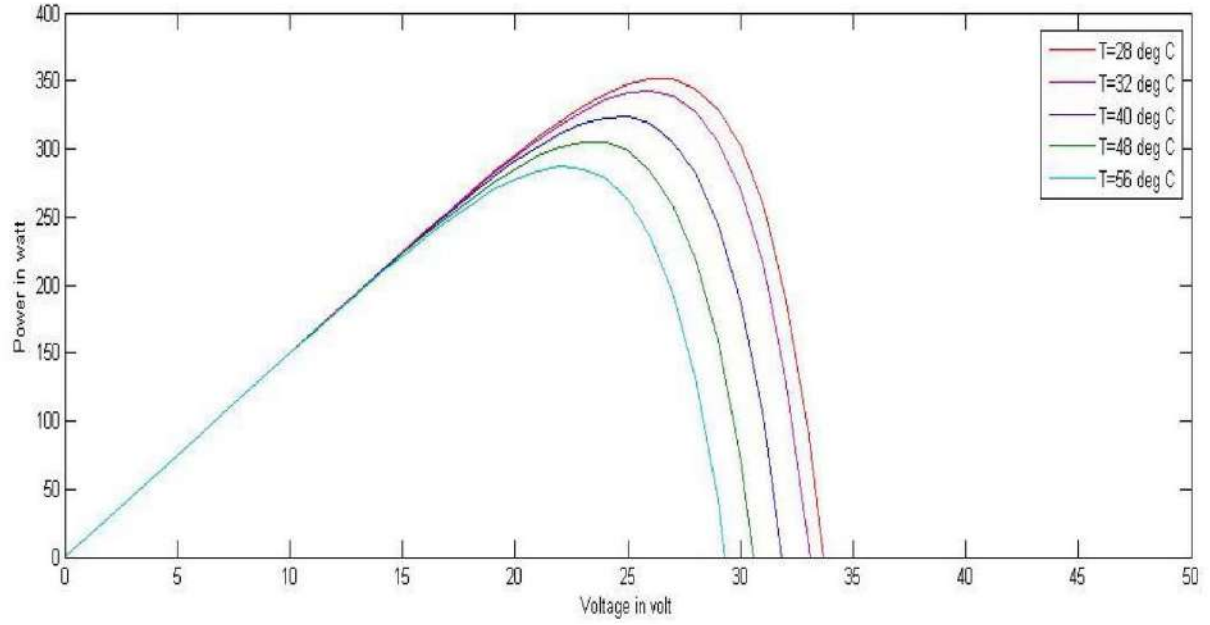



**Fig 5.14** P-V curves obtained at an irradiance of 100 mW/cm² various temperatures.

## V.6SIMULINK MODEL:

The Figure below shows the block diagram of the complete circuit. This includes the PV module, boost converter and control circuit. The modeling and simulation of the whole system has been done in MATLAB-SIMULINK environment.

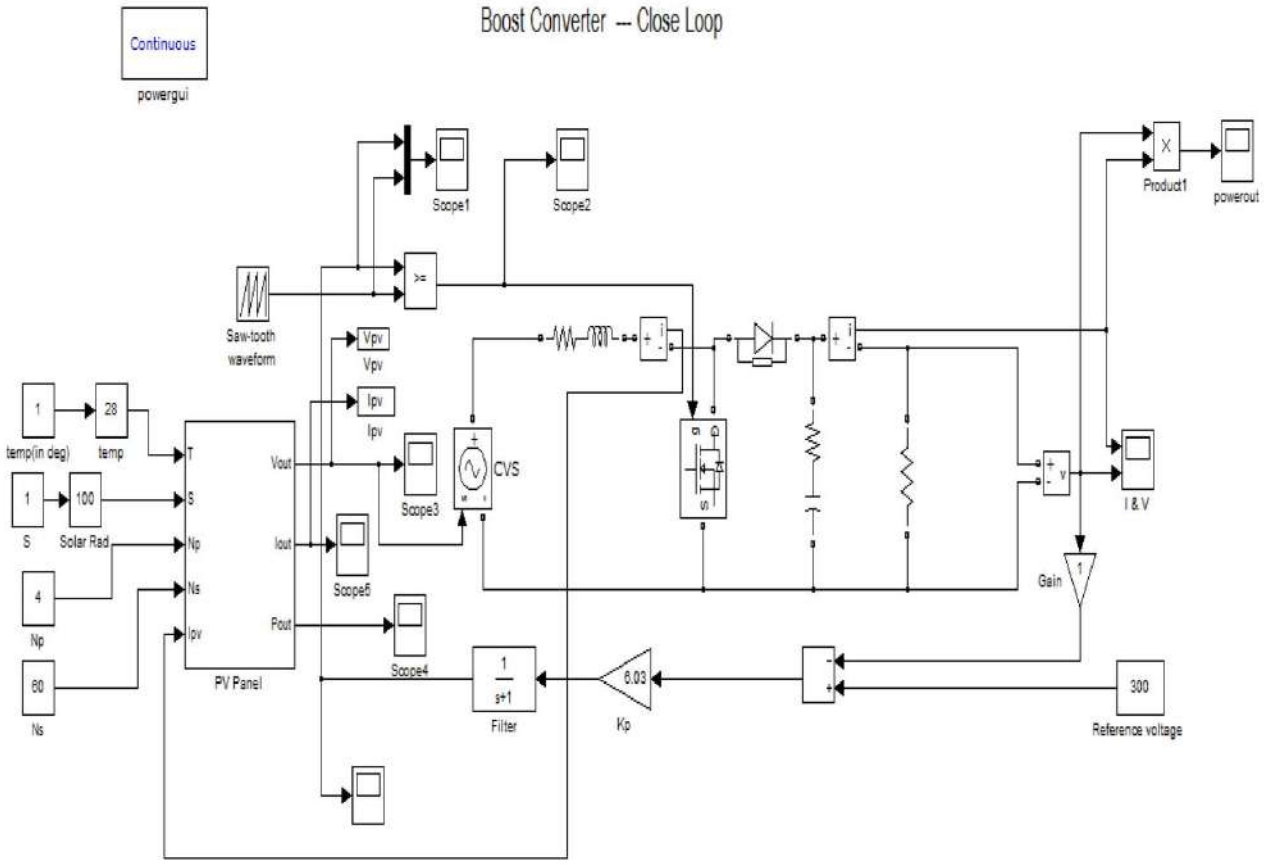



**Fig 5.15** The complete simulation model of the PV energy conversion system.

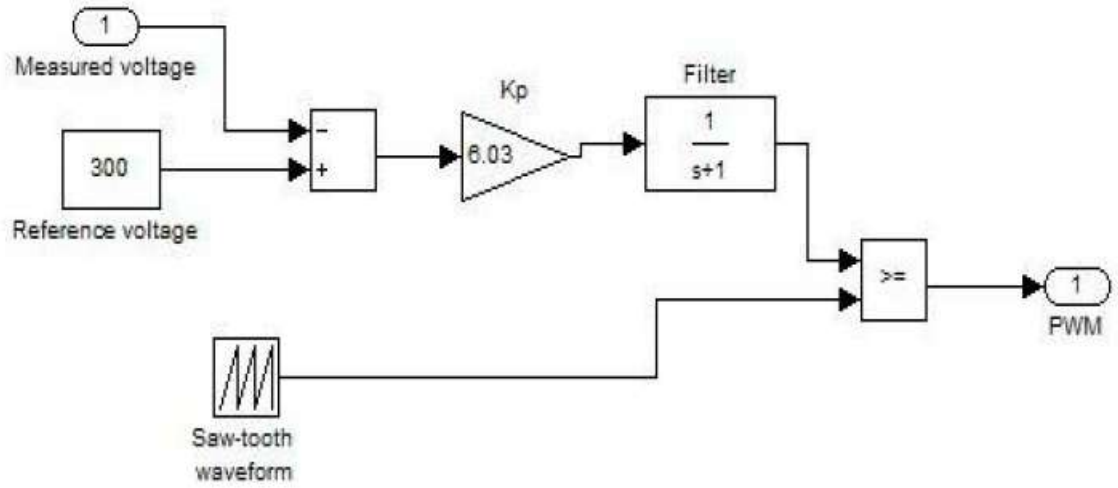



**Fig 5.16** Circuit diagram for PWM signal generation

The output of the filter which is the control signal is compared with the saw-tooth waveform having a peak voltage of 25V to generate the PWM signal which is fed as gate signal to the MOSFET. The simulation diagram showing the comparison of the saw-tooth waveform with thecontrol signal is shown below:

## V.7 SIMULINK Results :

The output I out and V out curves obtained across the load resistance of the boost converter of the simulink model as shown in above Figureis drawn below.

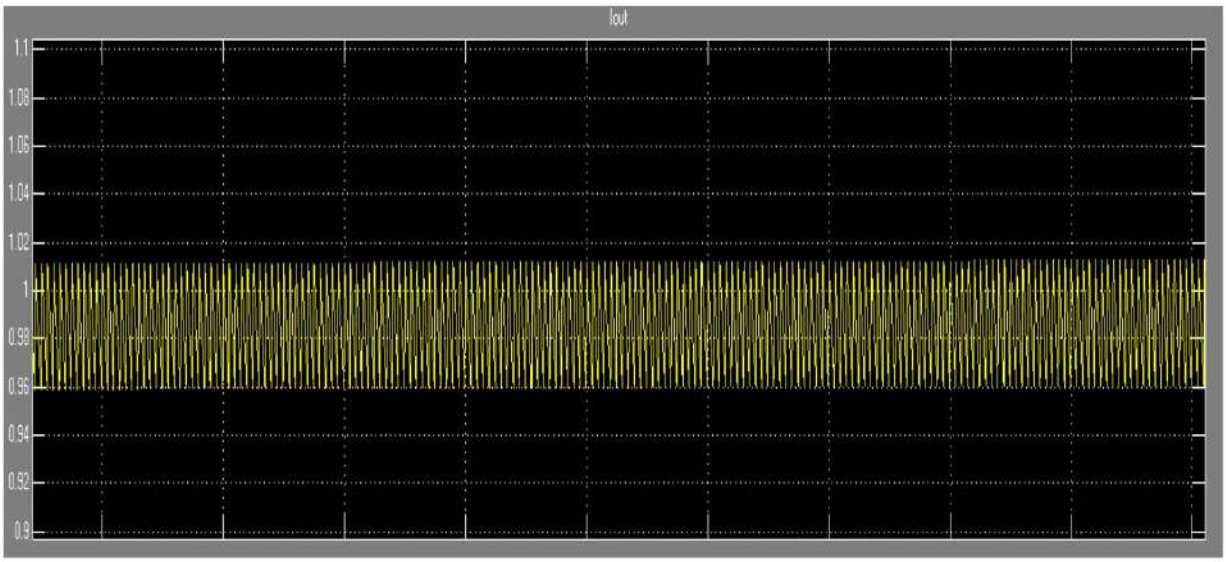



**Fig 5.17** The current output of the system

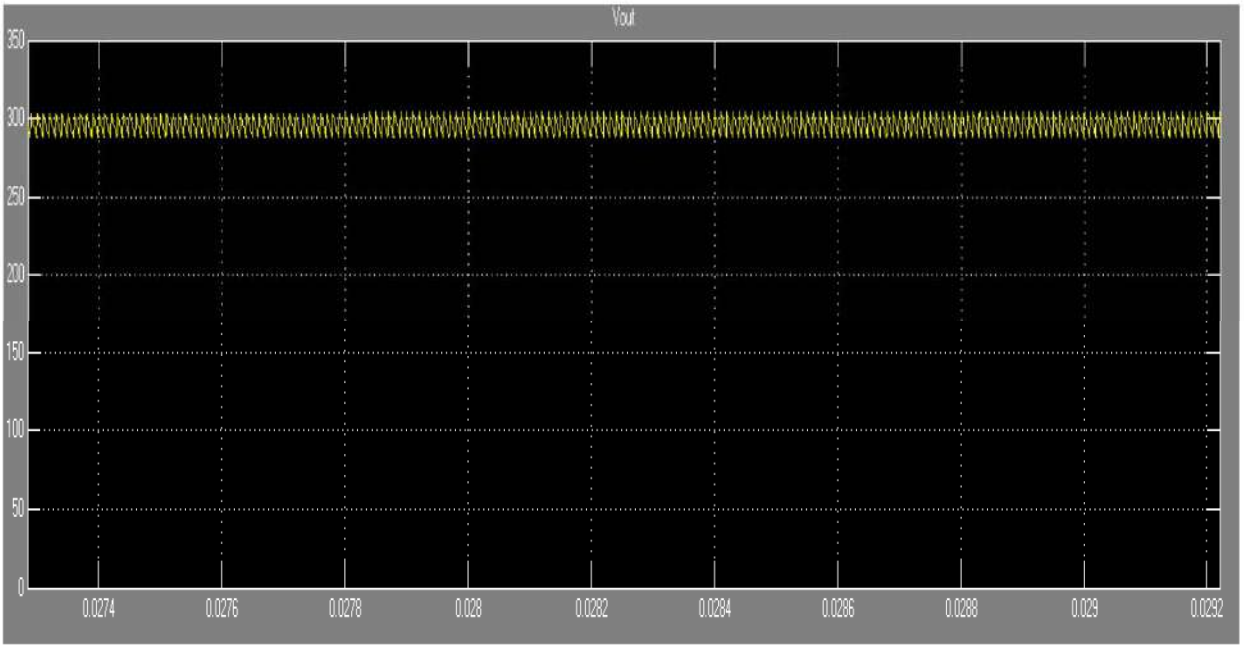



**Fig 5.18** The voltage output across the load resistance of the boost converter

## V.8 Conclusion

The open circuit P-V, P-I, I-V curves we obtained from the simulation of the PV arraydesigned

in MATLAB environment explains in detail its dependence on the irradiation levels and temperatures. The entire energy conversion system has been designed in MATLB-SIMULINK environment. The various values of the voltage and current obtained have been plotted in the open circuit I-V curves of the PV array at insolation levels of 100 $mW/cm^2$ and 80 $mW/cm^2$.

The voltage and current values lie on the curve showing that the coupling of the PV array with the boost converter is proper. However, the performance of the photovoltaic device depends on the spectral distribution of the solar radiation.

# General Conclusion

The memory has discussed methods for interconnection PV system with general contenets of its paramaters and the systematic using of its methods

The recent availability of high voltage band gap devices switching at very high frequencies make it possible to replace the power frequency transformer with a high switching frequency inverter of the conventional or possibly a novel type followed by a high frequency transformer, leading to a compact system.

The effect of PV penetration on grid stability has been investigated, and it was found that with the small relative ratings of the PV system, the threat to stability is minimal. How temperature and irradiance and amperage effects on our productivity with many different values,

However this high Technogym is very good to investigate more in this great field and to develop it to protect more our environment

# References

# References


1. http://energyprofessionalsymposium.com/?p=7446 [ 21-03-2019 14 :12 ]
2. https://energyeducation.ca/encyclopedia/Solar_energy_to_the_Earth [ 14-04-2019 19:00 ]
3. duffiebeckman - solar engineering of thermal processes edition 3
4. A. Einstein, Ann. Phys. (4) 322, 132 (1905).
5. A publication on .researchgate by A. Z. Hafez**Simulation and Estimation of a Daily Global Solar Radiation in Egypt**
6. EQUATION OF TIME — PROBLEM INASTRONOMYby M.M¨uller
7. https://www.sunearthtools.com/dp/tools/pos_sun.php?lang=en [22-05-2019 13 :02]
8. https://en.wikipedia.org/wiki/Electron_shell [16-06-2019]
9. http://hyperphysics.phy-astr.gsu.edu/hbase/Solids/dope.html [22-05-2019 19 :52]
10. United States Geological Survey, (2003), http://www.usgs.gov .[02-01-2019 02:56]
11. K. Jäger, On the Scalar Scattering Theory for Thin-Film Solar Cells, Ph.D. thesis, Delft University of Technology, Delft, the Netherlands (2012).
12. B. Mills, (2007), commons.wikimedia.org/wiki/File:
13. .**Proff. Dr. Alaa H. Shneishil 2018-2019. Ch.(3) Solar Photovoltaic** SystemO. Kluth, B.
14. https://doctiktak.com/a-student-introduction-to-solar-energy.html [12-05-2019 16:16]
15. https://www.solaris-shop.com/solar-components/ [12-05-2019 19:16]
16. https://www.qookka.com/en/blog/monocrystalline-polycrystalline-and-amorphous-solar-panels-n5 [19-06-2019 14:33]
17. https://www.ecmweb.com/green-building/highs-and-lows-photovoltaic-system- calculations [19-06-2019 15:23]
18. A publication on researchgate by Manuel S. Alvarez Alvarado
19. A publication on researchgate by **Miguel Alonso Abella**
20. http://www.imooc.co.kr/local/main/study_common_micro.php?id=2784&section=7990&module=27223 [20-06-2019 15:53
21. GeoModel Solar s.r.o., (2014), solargis.info/doc/71 .
22. https://www.pveducation.org/pvcdrom/solar-cell-operation/short-circuit-current[19-05-2019 18:26]
23. E. A. de la Breteque, Solar Energy 83, 1425 (2009).
24. C. Rigollier, O. Bauer, and L. Wald, Solar Energy 68, 33(2000).


Somebooks that I made them as reference but used them indirectly (just ideas)

- Photovoltaique_Etude2010_V14-Fr.pdf [it was on 2018]
- Soutnance de stage Gabriel Bousquet Analyse, conception et fabrication de cellulesphotovoltaïques à nano-fils
- Cours Energie Solaire Photovoltaïquede Dr. BELAID LALOUNI Sofia 2014
- Abouchabana Nabil, "Etude d'une nouvelle topologie buck-boost appliquée à un
- MPPT''. Mémoire de Magister, Université de Laghouat, 2009
- https://www.cder.dz/
- Jef Poortmans (Editor), **Vladimir Arkhipov** (Co-Editor) ... **Thin-film** solarcells